This Dissertation

entitled

CHANNEL ACCESS AND PACKET SCHEDULING IN WIRELESS MULTIHOP NETWORKS WITH QOS GUARANTEES

typeset with NDdiss2$_\varepsilon$ v3.0 (2005/07/27) on December 13, 2006 for

Min Xie

This LaTeX 2$_\varepsilon$ classfile conforms to the University of Notre Dame style guidelines established in Spring 2004. However it is still possible to generate a non-conformant document if the instructions in the class file documentation are not followed!

> Be sure to refer to the published Graduate School guidelines at `http://graduateschool.nd.edu` as well. Those guidelines override everything mentioned about formatting in the documentation for this NDdiss2$_\varepsilon$ class file.

It is YOUR responsibility to ensure that the Chapter titles and Table caption titles are put in CAPS LETTERS. This classfile does *NOT* do that!

This page can be disabled by specifying the "`noinfo`*" option to the class invocation.* (i.e.,\`documentclass[...,noinfo]{nddiss2e}`)

This page is *NOT* part of the dissertation/thesis, but MUST be turned in to the proofreader(s) or the reviwer(s)!

NDdiss2$_\varepsilon$ documentation can be found at these locations:

`http://www.gsu.nd.edu`
`http://graduateschool.nd.edu`

CHANNEL ACCESS AND PACKET SCHEDULING IN WIRELESS MULTIHOP NETWORKS WITH QOS GUARANTEES

A Dissertation

Submitted to the Graduate School
of the University of Notre Dame
in Partial Fulfillment of the Requirements
for the Degree of

Doctor of Philosophy

by

Min Xie, B.S., M.S.

Martin Haenggi, Director

Graduate Program in Electrical Engineering
Notre Dame, Indiana
December 2006

CHANNEL ACCESS AND PACKET SCHEDULING IN WIRELESS MULTIHOP NETWORKS WITH QOS GUARANTEES

Abstract

by

Min Xie

Wireless Multihop Networking (WMN) has emerged as a key and promising next-generation wireless technology. The ad hoc network formation and multihop communications incur more challenges than conventional wireless networks. This dissertation investigates channel access, medium access control (MAC), packet scheduling, and their interactions with the physical layer in WMNs. Existing wireless MAC and packet scheduling algorithms are briefly reviewed. Their analysis often does not consider the specific properties of WMNs, in particular in terms of the wireless channels, the traffic characteristics, and their interaction.

In this thesis, we apply queueing theory to analyze typical MAC and scheduling schemes in WMNs, including delay-balancing priority scheduling, TDMA and slotted ALOHA. Packet dropping strategies are employed to guarantee delay constraints and reduce unnecessary energy consumption. The Quality of Service (QoS) parameters under study include delay, packet loss rate, throughput, and capacity.

Our analysis quantitatively explains why TDMA outperforms slotted ALOHA not only in terms of throughput, but also of delay. An important feature caused by multihop communications is the *correlations*, which exist between the wireless

channels themselves, between the channels and traffic flows, between the traffic flows themselves, and between the delays of each node. Due to such correlations, the wireless channel performance is better than when all traffic flows are independent. Besides, the traffic correlation helps to form a natural spacing between simultaneously transmitting nodes, achieve efficient spacial reuse, and more importantly, avoid the overhead of establishing and maintaining the spacing. Furthermore, the correlation between the delays of each node substantially improve the end-to-end (e2e) delay variance. Therefore, taking advantage of these correlation could be helpful in the cross-layer design of efficient, distributed and cooperative protocols in WMNs.

CONTENTS

FIGURES

TABLES

ACKNOWLEDGMENTS

I am truly grateful to everyone who has directly or indirectly supported and helped me complete this Ph.D. dissertation. First of all, I would like to express my genuine gratitude to my advisor, Prof. Martin Haenggi, for his guidance, encouragement, and contributions in the development of my research. Without his vision, deep insight, advice and willingness to provide funding, this work would not have been possible. His extensive knowledge and commitment to the excellence of research and teaching are truly treasures to his students. He reviewed the drafts of papers and dissertation with amazing turn-around times and offered many insightful feedback on my research. I am very fortunate to have been able to tap his technical and professional advice.

I would also like to thank Professor Panos J. Antsaklis, Daniel J. Costello and Peter H. Bauer for serving on my dissertation committee and providing valuable advice on my research during the course of completing this dissertation. I thank Professor Francois Ledrappier for chairing my defense committee.

Finally, this dissertation is dedicated to my parents and sister for their love, sacrifice and support.

CHAPTER 1

INTRODUCTION TO WIRELESS MULTIHOP NETWORKS

1.1 Wireless Multihop Networks (WMNs)

Wireless multihop networking has emerged as a key and promising technology evolving into the next generation wireless to provide better and new services. WMNs are formed by a group of nodes that communicate with each other over wireless channels and operate in a dynamically self-organizing manner. Each node possesses at least memory, a processor, and a transceiver. If the destination node cannot be directly reached by the source node over a single hop, the intermediate nodes will assist the transmission by relaying the data over multiple hops.

WMNs are versatile. Their range of applications include broadband home networks, enterprise networks, transportation systems, health and medical systems, and distributed control systems [8, 42]. Multihop networking techniques also constitute the basis for wireless sensor networks (WSNs) [6] and wireless mesh networks (WMHNs) [8], and are evolving as an alternative to support inter-vehicle communications. Mobile ad hoc networks (MANETs) are expected to become an important part of the 4G architecture [25] since the introduction of Bluetooth, IEEE 802.11 (WiFi), IEEE 802.15.4 (ZigBee), and IEEE 802.16 (WiMAX) has been generating growing interest in research and development of ad hoc networks in commercial applications. In the future, WMNs will be seamlessly and ubiquitously integrated with other types of wireless networks and wire-line backbone

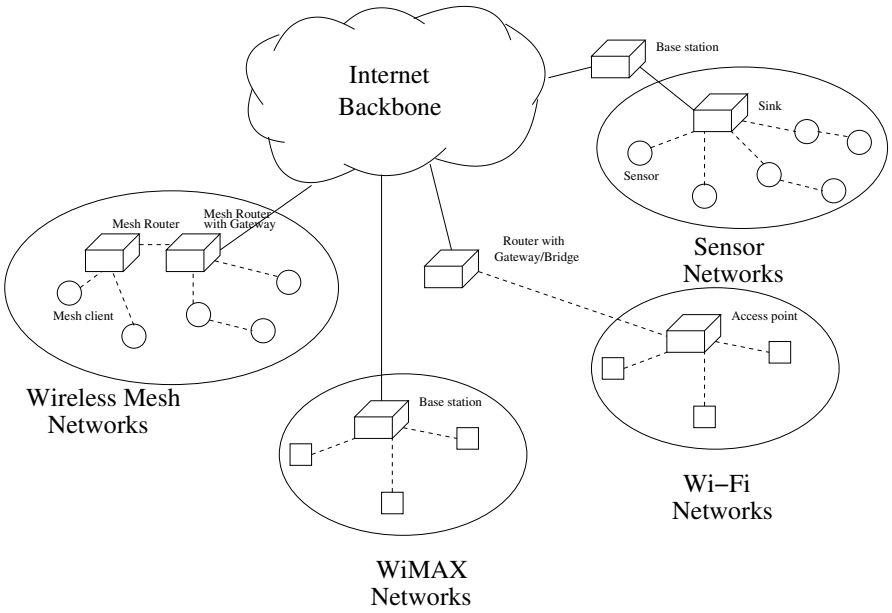

Figure 1.1. Next-generation networks

networks to converge data, voice, and multimedia traffic over a single packet-switched network (Fig. 1.1) [8, 25]. In other words, the next-generation networks are heterogeneous and seamless connectivity is required in the protocol stack, as shown in Fig. 1.2 [6, 22].

The network design is mainly investigated from two aspects, *computation* and *communication*, which address what data and how these data are communicated in the network. These two aspects turn out to be interdependent and conflicting. Savings in communication are achieved by increasing computation, and vice versa. Communication can be classified into *broadcasting/multicasting*, *unicasting*, and *convergecasting* [11, 133]. If using flooding, broadcasting is relatively simple to implement and immune to dynamic changes in the network topology. Convergecasting is a many-to-one communication mode and can be regarded as the dual to broadcasting. The data can be classified into *application data* and *infrastructure*

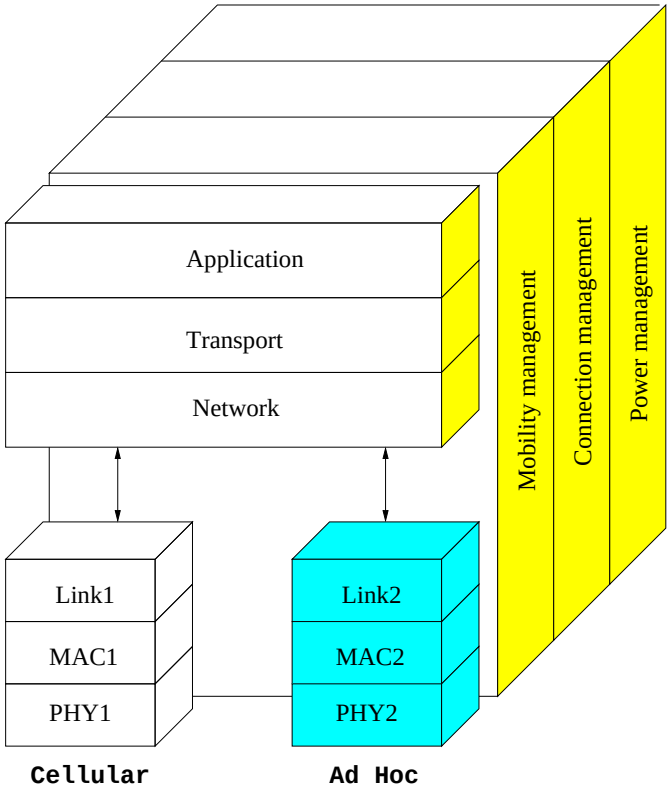

Figure 1.2. Protocol stack of next-generation networks in a heterogeneous environment [6, 22]

data [133]. The communication of application data could be cooperative in such a way that a cluster of nodes is coordinated to implement data aggregation and thus reduce the traffic load, at the expense of increased computational load. Infrastructure data refer to the information that is needed to configure, maintain and optimize the network. As infrastructure communication represents the protocol overhead, investing in this type of communication may result in a reduction in application data while optimizing the overall network performance. The amount of infrastructure data is highly influenced by the network protocols and dynamics. Therefore, their characteristics are hardly predictable. Application data, on the

other hand, can be controlled or regulated by the nodes even if they are generated randomly and unpredictably. We discuss only application data in this dissertation.

WMNs inherit the problems of wireless communications such as error-prone dynamic channels, sparse bandwidth, and hidden and exposed terminal phenomena [6, 8, 25]. On the other hand, the multihop transmission pattern and ad hoc network formation impose more challenges on WMNs [25, 65]:

- *Self-organization and lack of infrastructure.* The network is formed dynamically by an autonomous system of possibly mobile nodes that are connected via wireless links without using a fixed network infrastructure or centralized administration. Then, network management has to be distributed across the network, causing additional difficulties in fault detection and management.

- *Cooperation between nodes.* The multihop transmission requires intermediate nodes to relay packets hop by hop. Without centralized control, the relaying operations must be implemented cooperatively by all nodes [6, 7, 34, 52]. The cooperation should both guarantee the efficient resource utilization and avoid potential collision/interference.

- *Dynamically changing network topology.* The nodes are free to enter and/or leave and/or move in the network and organize themselves arbitrarily. The frequently changing network topology results in not only the change of connectivity and coverage, but also route changes, network partitions, and possibly data losses and long delay.

- *Variation in link and node capabilities.* Each node may be equipped with one or more radio interfaces that have varying transmit/receive capabilities and operate across different frequency bands. Typical examples include direc-

tional and smart antennas, MIMO systems, and multi-radio/multi-channel systems [8].

- *Energy constrained operation.* Since additional energy is consumed for packet forwarding, energy efficiency is crucial when energy is constrained like in wireless sensor networks.

- *Network scalability.* Some WMNs are large scale and dense (*e.g.*, sensor networks). Many problems remain unsolved such as addressing, routing, location management, configuration management, interoperability, security, capacity (*e.g.*, network transport capacity decreases to zero as the network size increases to infinity [47]), etc.

- *QoS guarantees.* The multihop communication pattern incurs correlations in the status of nodes and links in the network. More importantly, all QoS parameters should be measured over end-to-end (e2e) and thus need to take into account the impact of these correlations. In most cases, these correlations are interdependent and affected by many factors such as transmission rates, MAC schemes, and routing and packet scheduling protocols. It is difficult to tractably analyze the correlations and provide explicit QoS measurements.

The resulting challenges [6, 8, 25] are discussed from layer to layer in the following section.

1.2 Challenges in WMNs

1.2.1 The Physical Layer

The *physical layer* is responsible for frequency selection, carrier frequency generation, signal detection, and modulation. It is required to adapt rate, power, and coding to meet the requirements of the application given the current channel and network condition [72, 74, 75, 78, 79]. As RF and circuit design for wireless communications evolve, advanced physical layer techniques are enabled, such as Multiple-Input-Multiple-Output (MIMO), multiple radio, and software defined radio. But their complexity and cost are still too high to be implemented [8].

1.2.2 The Medium Access Control (MAC) Layer

The *MAC layer* is designed to adapt to the underlying link and interference conditions as well as delay constraints. MAC protocols must form the basic infrastructure needed for wireless communication hop by hop and share communication resources fairly and efficiently between all nodes involved. In addition, they must have built-in power conservation, mobility management and a failure recover strategy. Power control can make the access protocols more efficient [41]. The the peer-to-peer (P2P) nature and the lack of infrastructure in WMNs make random access protocols the natural choice for medium access control [7]. The dynamic multihop topology further requires MAC to be distributed, cooperative and adaptive. However, to guarantee Quality of Service (QoS), demand assignment or reservation-based access schemes are more suitable. It is challenging to design MAC schemes that achieves optimal balance between feasibility and QoS guarantees. Moreover, classical wireless MAC schemes such as IEEE 802.11 (CSMA/CA) have been designed for single-hop communications and are not op-

timized for multihop communications, in which there are more challenges, *e.g.*, inter-flow interference and spatial reuse.

1.2.3 The Network Layer

The *network layer* is aimed at using the one-hop transmission services provided by the enabling technologies like IEEE 802.11, Bluetooth, to construct reliable e2e delivery services from a sender to one or more receiver(s). The network layer protocols include a location service, routing and forwarding, scheduling, and clustering. The location service answers queries about the nodes' location. Traditional location services use centralized servers and are thus not applicable to WMNs.

The routing protocols are classified into unicast, geocast, multicast or broadcast forwarding. Unicast forwarding is a one-to-one communication while multicast and broadcast are one-to-many. Geocast is a special case of multicast when the group of destination nodes is situated inside a specified geographical area. The highly dynamic and unpredictable network topology and energy-constrained devices in WMNs incur more challenges on routing design in WMNs, *e.g.*, robustness, scalability, and energy efficiency. Energy-efficient and power-aware routing protocols generally select the route according to one of the parameters: *maximum available power (PA)*, *minimum energy (ME)*, *minimum hop (MH)*, or *maximum minimum PA node* [6]. If combined with the location service, routing can be location-aware in that a node selects the next hop based on the position of its one-hop neighbors and the destination node.

For large heterogeneous networks, there is a large amount of data to be processed and communicated. It is beneficial to use cluster-based routing that can

combine or aggregate the data of a cluster in an intelligent way to reduce routing overhead and the network load. For example, in dense sensor networks, there exist correlations among data generated by neighboring sensor nodes. A great gain is obtained by combining these correlated unreliable data measurements so that the common signal is enhanced, the uncorrelated noise is reduced, and the overall data load is decreased [34, 46, 52, 106]. Optimal data aggregation, also known as data fusion, enables load balancing, results in an increased SNR and induces an improvement in detection and classification. Localized data fusion schemes can achieve large energy savings and have significant robustness and scalability advantages. Clustering also enables efficient centralized scheduling locally, which is hard to implement with flat routing.

In wireless networks, packet scheduling needs to not only determine the transmission order of packets, but also alleviate the impact of error-prone wireless channels whether or not the channel state information (CSI) is known. The scheduler differentiates flows/nodes by their QoS requirements. For example, to guarantee a certain e2e delay, the packets that have been relayed over multiple hops and will expire soon should be given higher transmission priorities than those newly generated. Moreover, since the e2e delay depends on the path length, the design of optimal packet scheduling should be coupled with routing. With finite memory size or a hard delay bound, packet dropping will occur, and the scheduler needs to determine when and which packets are discarded.

1.2.4 Cross-Layer Design

In the layered approach, each layer in the protocol stack (Fig. 1.2) is designed and operated independently. Their interfaces are static and independent of the

individual network constraints and applications. Communication between layers is limited with a minimum set of primitives. This paradigm has greatly simplified the protocol design. However, in wireless networks, there is a direct coupling between the physical and the upper layers. Hence the layered approach is not efficient due to its inflexibility and suboptimality [121, 127]. For instance, the physical layer affects MAC and routing decisions by its choice of transmission power and rate. The MAC layer is responsible for allocating the wireless resources and will determine the available bandwidth and potential delay, both of which can affect the routing decision on how to select the link. On the other hand, the routing decision has a significant influence on the contention level at the MAC layer, which, in turn, accordingly changes the physical layer parameters. Moreover, in WMNs, data transmission and reception at a node may be affected by nodes within two or more hops away. However, in the layered approach, the MAC schemes are limited to one-hop communications and the routing protocols take care of multihop communications. In this sense, MAC and routing are closely connected.

In contrast to the layered approach, a cross-layer design principle [25, 42, 62, 111, 121, 127] aims at actively and dynamically exploiting the dependence between protocol layers to obtain performance gains. In Fig. 1.2, several management planes cover all layers to ensure energy/power efficiency, mobility control, and fair resource sharing in the network.

In cross-layer design, information must be exchanged across all layers such that the protocols adapt in a global manner to the application requirements and underlying network conditions [42]. It is fundamental to determine i) what and how information should be exchanged; and ii) how global constraints and characteris-

tics should be factored into the protocol design at each layer. Since communication is usually more energy consuming than computation, the primary concern is to minimize communication while achieving the desired network operation. In the following, we specify several problems that are considered in a cross-layer manner [25, 42, 62, 111, 121, 127].

1.2.4.1 Energy conservation

Mobile devices rely on batteries as energy supplies. Efficient energy management is vital to ensure that application demands are satisfied at minimum energy expenditure. For communications, the main sources of power consumption are the *transmit*, *receive*, *idle* and *sleep* states [58]. A wireless interface consumes nearly the same amount of power in the first three modes, but consumes much less in the sleep mode. In WMNs with cooperation efforts, additional energy is consumed to forward packets. Energy inefficiency mainly comes from [29, 150]

- *collision*, caused by the transmissions of multiple nodes to the same destination at the same time. If the received signal-to-noise-and-interference-ratio (SNIR) is too small, retransmissions become necessary;
- *overhearing and overemitting*, when a node receives packets that are not destined to itself or when the node is not ready yet;
- *idle listening*, listening to receive possible packets while no nearly node transmits.

It is not sufficient to minimize only the sum energy consumption of all the nodes since the network lifetime depends on the lifetime of the individual nodes, especially the bottleneck nodes. Therefore, energy saving is considered at two levels,

local strategies operating at the node level and *global strategies* at the network level [25]. Local strategies put the node in a power saving mode as aggressively as possible and are typically implemented at the physical and MAC layers. For example, at the physical or link layer, if CSI is available, unless a delay constraint forces a transmission, power control generally uses a "water-filling" approach that exploits good channels and prevents transmissions over bad channels to avoid useless transmissions. On the other hand, at the MAC layer, transmissions are withheld to avoid collision when the channel is congested [42]. Energy consumption is minimized if the network interface is tuned to the optimal channel utilization.

Global strategies dynamically decide which nodes should participate in packet forwarding to guarantee network connectivity and which nodes can remain in the sleep mode to save energy. Network connectivity can be guaranteed by increasing transmit power levels, which, however, increases energy consumption and interference. On the other hand, decreasing transmit power and covering the sender-to-receiver distance with a multihop path may require less energy from the transmission standpoint, but also may increase the e2e delay and the processing energy [49]. Therefore, minimizing the per-packet per-hop energy consumption does not necessarily maximize the network lifetime. Cross-layer energy/power control is desired to solve the tradeoff between energy consumption, delay, throughput, and connectivity.

1.2.4.2 Cooperation

The cooperation requirements of WMNs may conflict with the selfishness of each node. Sometimes the nodes do not cooperate because they are not willing to spend their own battery life, CPU cycles, or available bandwidth to forward

packets not of direct interest to them. Then they may intentionally drop relayed packets, which significantly damages the network functionalities like routing and forwarding. Cooperation enforcement schemes are needed to detect and isolate these misbehaving nodes through mechanisms based on watchdogs and reputation systems [87]. Watchdog-based mechanisms are related to the MAC layer in terms of collisions and the physical layer in terms of the transmission range. Game theory [89] is a natural way to model and analyze cooperation aspects.

1.2.4.3 Performance evaluation

QoS guarantees require evaluating system performance, which consists of two steps, defining the system model and solving it with analytical and/or simulation techniques. The selection of the system model affects multiple layers. For example, the channel model and mobility model not only characterize the physical channel properties, but also determine the design of the MAC layer and routing schemes. The performance metrics of each layer are coupled with each other. For example, the physical layer techniques determine the network throughput, a fundamental parameter for the MAC layer; while the MAC schemes affect interference, which, in turn, changes the throughput. Therefore, the network performance should be evaluated over all layers.

1.2.5 QoS in WMNs

QoS is the performance level of a service offered by the network to the user. The goal of QoS provisioning is to deliver information in a timely and reliable fashion while efficiently utilizing network resources [111, 153]. A service can be characterized by a set of measurements such as minimum bandwidth, maximum

delay and delay variance (jitter), maximum packet loss rate, and maximum energy consumption. The desired QoS parameters differ from application to application, but are usually interdependent. Some of them are even conflicting, *e.g.*, latency *vs.* reliability.

A QoS framework mainly consists of QoS routing, QoS signaling for resource reservation, QoS MAC, call admission control, and packet scheduling (Fig. 1.3). QoS can be provided through several ways, *e.g.*, per flow, per link, per class or per node. For example, the IEEE 802.11e MAC supports best-effort traffic by the distributed coordination function (DCF) and real-time traffic by the point coordination function (PCF) (in infrastructure-based configurations) [15]. QoS per class is provided by differentiating the DCF access to the wireless medium, which is reflected through the backoff time [115].

In WMNs, the QoS framework could be cross-layer, *e.g.* Proactive Real-Time MAC (PRTMAC, see Fig. 1.3) [111] that combines an on-demand QoS extension of DSR routing protocol at the network layer with a real-time MAC protocol. Depending on the requested QoS parameters, more modules can be added to the framework such as traffic shaping/traffic rate control and mobility control.

It is challenging to guarantee QoS in WMNs [111]. For example, lack of central coordination complicates the implementation of QoS provisioning. Due to the dynamic network topology and channel characteristics, the admitted QoS flows may suffer from frequent path breaks and thereby are required to be re-established, which may incur delay violations. Moreover, the resulting imprecise state information may lead to inaccurate MAC, scheduling and routing decisions. Also, error-prone shared radio channels suffer from several impairments such as attenuation, multi-path propagation, inter-flow and intra-flow interference. The inherent

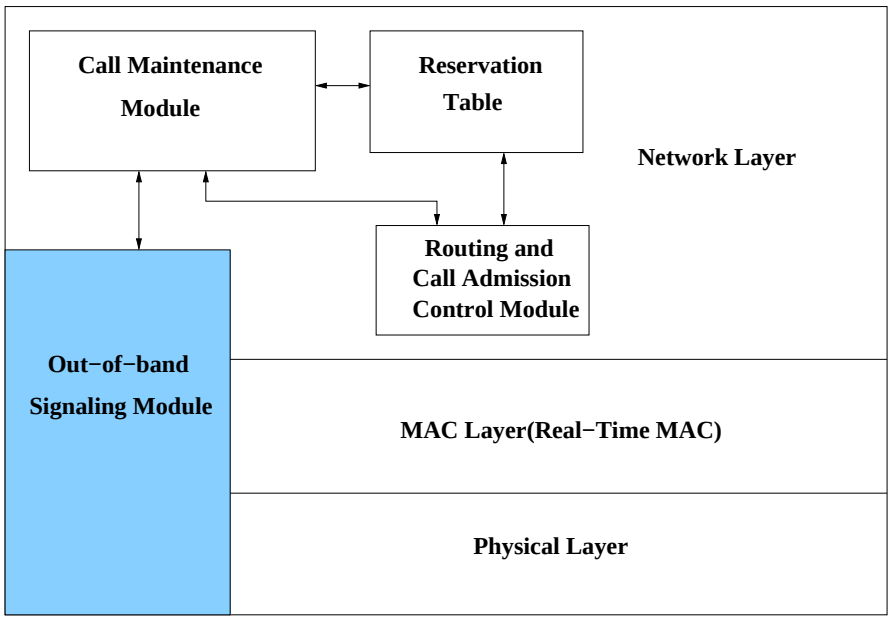

Figure 1.3. Modules in a QoS framework

hidden terminal phenomenon incurs energy waste, while the exposed terminal phenomenon wastes time. Therefore, QoS is a critical issue in WMNs.

1.3 Versatile WMNs

1.3.1 Mobile Ad Hoc Networks (MANET)

MANETs represent complex distributed systems that comprise wireless *mobile* nodes. Based on the coverage area, they can be classified into Body (BAN), Personal (PAN), Local (LAN), Metropolitan (MAN) and Wide (WAN) area networks. The key feature of MANETs is the "ad-hoc" network topology. MANETs are not limited to multihop communications. Ad hoc single-hop BAN, PAN and LAN wireless technologies are already common on the market [25]. Currently, two main standards have emerged for ad hoc wireless networks: the IEEE 802.11

standard for WLANs and the Bluetooth or IEEE 802.15.1 specifications for short-range wireless communications. These technologies constitute the building blocks for constructing small, multihop ad hoc networks to extend their range over multiple radio hops.

The highly dynamic nature of a MANET results in frequent and unpredictable changes of the network topology. The resulting challenges and complexities, coupled with the critical importance of the routing protocol in establishing communications among mobile nodes, make routing the most active research area within the MANET domain. MANET routing are typically subdivided into two main categories: *proactive table-driven* and *reactive on-demand* [113]. Proactive routing protocols are derived from legacy Internet distance-vector and link-state protocols. They attempt to maintain consistent and updated routing information for every pair of network nodes. They require each node to maintain one or more tables to store routing information, and they respond to changes in network topology by propagating updates throughout the network in order to maintain a consistent network view. They differ in the number of necessary routing-related tables and the methods by which changes in network structure are broadcast. Existing table-driven ad-hoc routing protocols include Destination-Sequenced Distance-Vector Routing (DSDV), Wireless Routing Protocol (WRP), and Clusterhead Gateway Switch Routing (CGSR).

On the other hand, reactive on-demand routing (RODR) is source-initiated and establishes routes only when requested by the source node. Once a route has been established, it is maintained by a route maintenance procedure until either the destination becomes inaccessible along every path from the source or the route is no longer desired. Typical on-demand routing protocols include Ad-hoc

On-Demand Distance Vector Routing (AODV), Dynamic Source Routing (DSR), and Temporally-Ordered Routing Algorithm (TORA).

In general, the proactive routing approach is similar to the connectionless approach of forwarding packets since a route to every other node in the network is always available regardless of whether it is needed or not. This feature provides better QoS but also incurs substantial signaling overhead and power consumption to maintain the routing tables. The reactive routing approach takes time to establish the route before nodes can be served but routing information stored is actually needed. Therefore, the reactive approach is more efficient than the proactive approach though it is hard to guarantee QoS.

The other challenge brought up by mobility is security. Mobility makes the network more vulnerable to information and physical security threats than fixed wired or wireless networks. Note that security is a cross-layer issue involved with the data link, network, presentation and application layers.

Since mobility affects the ability of network protocols to behave correctly, the selection of an accurate mobility model is important in MANET. Due to the resulting system complexity, the impact of mobility models is usually studied through simulations. Popular network simulators used in ad hoc networks include OPNET [98], ns-2 [3], Qual-Net [1], and GloMoSim [151].

1.3.2 Wireless Sensor Networks (WSNs)

The development of low-cost, low-power WSNs is inspired by improvements in MEMS-based sensor technology, low-power analog and digital electronics, wireless communications, computer networking, and countless applications. WSNs are a subclass of WMNs, but the the unique characteristics of sensing devices and

the application requirements make many of the solutions designed for WMNs not suitable for WSNs. Sensor nodes are untethered and deployed in an ad hoc fashion and communicate over *short* distances. Given that individual sensors are neither reliable nor accurate, cooperation efforts are especially desirable in order to construct high quality and fault-tolerant sensing networks. To cover the target area successfully, sensor networks usually consist of a large number of nodes. Since it is generally difficult or impractical to charge/replace the exhausted batteries in sensor networks, the primary objective is to maximize node/network lifetime [105].

A WSN is usually composed of three components (Fig. 1.4) [133]: sensor nodes that sense environmental phenomena and report their measurements; an observer (or observers) that is interested in obtaining information disseminated by the sensor nodes about the phenomenon; and the phenomenon, the entity to be sensed. The sensed information is potentially analyzed or filtered by the sensor network. All components can be either static or mobile. Unlike in ad hoc networks where all nodes are assumed to choose their destination randomly, in WSNs, the observer is the unique destination of all sensor nodes. Therefore, a special feature of WMNs is "convergecasting" (many-to-one) communication [11]. In contrast to convergecasting, broadcasting (one-to-many) communication is the way that the observer broadcasts data (infrastructure or application) to all sensor nodes. For example, in the reprogramming application, the new programs are loaded to each sensor node in a broadcasting way.

Fig. 1.4 shows a WSN with a single observer at which all sensed information converges. The closer a sensor node to the observer, the more data flows converge. The area in proximity to the observer is referred to as *critical area* (dark nodes in Fig. 1.4) and the nodes in the critical area are referred to as *critical nodes*

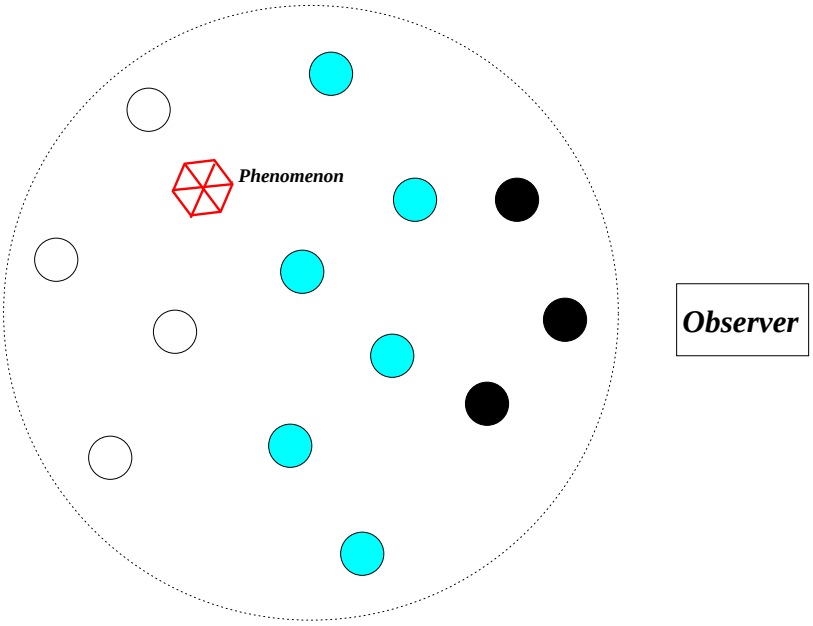

Figure 1.4. A network of randomly deployed sensor nodes

[48]. The critical area delivers a large fraction of accumulated data. The critical nodes consume more energy than non-critical nodes, which will create a cascading effect that shortens system lifetime. Energy-balancing strategies can be used to balance the energy consumption of the nodes and thus increase the network lifetime substantially [48].

In practice, sensed data is often bursty and of very low rate when the sensor nodes are driven by events and/or observer requests. Global *Directed Diffusion* [34] and *reactive routing* appears better suited in this case. The sensed raw data can be processed before being communicated, for example, *compressed*, to be more succinct and/or accurate. WSN applications require accuracy and short latency. The data generation pattern, along with the large scale, convergecasting communication and application requirements, impose more challenges on the design of WSNs than general WMNs [6, 7, 34]. Correspondingly, *localization* and

combination of routing and data aggregation [34] are proposed to deal with node cooperations. Node addressing maps the observer interest into a set of sensor nodes instead of a single sensor so that data is decoupled from the sensor that generates it [133]. Delay-balancing and load-balancing principles are developed to support real-time applications and meet energy constraints.

1.3.3 Wireless Mesh Networks (WMHNs)

WMHNs consist of a mix of fixed and mobile nodes interconnected via wireless links to form a multihop ad hoc network [8, 19]. They inherit many properties from MANETs but have civilian applications as the main target. More importantly, mesh networks have already shown great potential in the wireless market [8, 19].

WMHNs are composed of two types of nodes, *mesh routers* and *mesh clients*. Other than the routing capability for gateway/repeater functions as in a conventional wireless router, a wireless mesh router contains additional routing functions to support mesh networking, including multiple wireless interfaces, much lower transmission power or higher rates through multihop communications, and scalable MAC protocols in a multihop mesh environment. Mesh clients can also work as routers but without gateway or bridge functions. Since mesh clients have only one wireless interface, their hardware platform and software can be much simpler than those for mesh routers.

The architecture of wireless mesh networks is not necessarily infrastructure-less. For example, in *infrastructure/backbone wireless mesh networks* [8], mesh routers form an infrastructure for clients connecting to them. This infrastructure mesh networking is the most commonly used type since it provides a backbone for conventional clients and enables integration of WMHNs with existing wireless

networks through gateways/bridges functionalities in mesh routers. The other architecture includes *client wireless mesh network* and *hybrid wireless mesh network*. In the former, clients communicate to each other in a P2P manner without routers. This type is more infrastructure-less ad hoc and thus increases the requirements on mesh clients that must perform additional functions such as routing and self-configuration. In the latter, clients can access the network through mesh routers or directly communicate with other clients. This type is a combination of infrastructure and client meshing and will be more applicable in the future.

WMHNs distinguish themselves from other WMNs by:

- *Broadband services*: most mesh applications are broadband with various QoS requirements. Thus, additional performance metrics such as delay jitter, aggregate and per-node throughput, and packet loss rate, must be considered, as well as delay and fairness.

- *Heterogeneity*: the presence of powerful and static or slowly moving mesh routers and wireless backbone provides different coverage, connectivity, topology change and robustness than ad hoc networks, in which the individual contributions of end devices are almost equivalent (homogeneous networks). The separation of functions between mesh routers and mesh clients significantly decreases the load and energy consumption on end devices (clients).

- *Multiple radios*: mesh routers can be equipped with multiple radios to perform routing and access functionalities. Then infrastructure and application data can be separated and the network capacity will be improved. In ad hoc networks, there is usually only a single radio.

So, the additional challenges imposed on mesh networks include

- *compatibility and inter-operability.* WMHNs are expected to support network access for both conventional and mesh clients. Integration of WMHNs with other wireless networks require certain mesh routers to have the capability of inter-operation among heterogeneous wireless networks.

- *mesh connectivity.* Mesh routers and clients move and function differently. Network connectivity is different from ad hoc networks in which all nodes are assumed to move randomly.

Currently, IEEE 802.11s, IEEE 802.15.4 and IEEE 802.16 standards provide support for mesh networks [8].

1.4 Wireless Channels

The performance of wireless communications systems is fundamentally limited by wireless channels. Radio signals generally propagate according to four mechanisms: *reflection*, *diffraction*, *scattering*, and *regular electro-magnetic propagation*. As a result of these mechanisms, radio propagation can be roughly characterized by three nearly independent phenomena [129]: *path loss* variation with distance, large-scale log-normal *shadowing*, and small-scale *multipath fading*. The propagation models focus on predicting the average received signal strength at a given distance from the transmitter (T-R separation), as well as the variability of the signal strength at a particular location [110].

1.4.1 Path Loss Propagation Model

The path loss model predicts the received signal strength when the transmitter and the receiver have a clear, unobstructed line-of-sight (LOS) path between them.

In free space, the received power P_r decays with the square of the T-R separation distance d, given by the Friis free space equation [110]:

$$P_r(d) = \frac{P_t G_t G_r \lambda^2}{(4\pi)^2 d^2 L} \tag{1.1}$$

where P_t is the transmit power, λ is the wavelength, G_t and G_r are the gains of the transmitter and receiver antenna, respectively. L is the system loss factor not related to propagation ($L \geq 1$).

The Friis free space model is valid only for values of d in the far-field of the transmitting antenna. A refined predictor is

$$\begin{aligned} P_r(d) &= P_r(d_0)(\frac{d_0}{d})^{\alpha} \\ P_r(d)\ [\text{dB}] &= P_r(d_0)\ [\text{dB}] + 10\alpha \log_{10}(\frac{d_0}{d}), \end{aligned} \tag{1.2}$$

where d_0 is the close-in distance for a reference point such that $d > d_0$. Note that the value of d_0 depends on the frequency, antenna heights and gains, and other factors. The *path loss exponent* α is a key parameter that affects the spatial reuse of a wireless system. α usually ranges from 2 to 5.

This log-distance path loss model does not consider the fact that the surrounding environmental clutter may be vastly different at two different locations that have the same T-R separation. A random variable is introduced to capture this effect, *shadowing*.

1.4.2 Log-Normal Shadowing

Random shadowing effects occur over a large number of measurement locations which have the same T-R separation, but have different levels of clutter on the

propagation path. Measurements have shown that this shadowing follows a log-normal distribution. Measured signal levels (in dB) at a specific T-R separation have a Gaussian (normal) distribution about the distance-dependent mean of (1.2):

$$P_r(d) = P_r(d_0) + 10\alpha \log_{10}(\frac{d_0}{d}) + X_\sigma, \tag{1.3}$$

where $P_r(d_0)$ is the received signal power (in dBm) at a known reference distance d_0, and X_σ is a zero-mean Gaussian distributed random variable (in dB) with standard deviation σ_Ω (in dB). The value of σ_Ω ranges from 5 to 12dB and increases slightly with frequency, but is nearly independent of the T-R separation. A more accurate path loss model leads to a smaller σ_Ω.

More specifically, the received signal power (in dBm) at the distance d is a random variable of a probability density function (pdf) [110, 129]

$$p_r(x) = \frac{1}{\sqrt{2\pi}\sigma_\Omega} \exp\big\{ - \frac{(x - \mu_\Omega(d))^2}{2\sigma_\Omega^2}\big\}, \tag{1.4}$$

where

$$\mu_\Omega(d) = \mu_\Omega(d_0) + 10\alpha \log_{10}(\frac{d_0}{d}) \text{ dBm}$$

and $\mu_\Omega = E[P_r]$.

The normal distribution of $P_r(d)$ allows the use of Q-function or error function (erf) to calculate the reception probability or outage probability, *i.e.*, the probability that the received signal level exceeds or falls below a particular level.

1.4.3 Multipath Fading

As a consequence of reflections, scattering and diffraction, multiple copies of a signal may arrive at the receiver and add up constructively or destructively. This

is called multipath propagation, resulting in *multipath fading*. Multipath fading possibly results in rapid variations in the received signal over a short distance, approximately half a wavelength. The other possible effect caused by multipath propagation is intersymbol interference (ISI) due to the interference overlap of the delayed version of the previous symbol and the current symbol.

Fading effects can be classified into *flat* or *frequency-selective* [128] based on the signal bandwidth with respect to the channel bandwidth. The frequency-selective fading channel induces ISI, and thus the received signal is distorted. Or, depending on how rapidly the transmitted signal changes as compared to the symbol rate, the channel fading can be classified either as *fast* or *slow*. Coherence time T_C is a statistical measure of the time duration over which the channel is essentially invariant [110]. If the baseband symbol duration is smaller than the coherence time of the channel, then the channel may be assumed to be static over one or several symbol transmissions. This is denoted as slow fading (block fading). Note that all current wireless systems are subject to slow fading only.

Additive White Gaussian Noise (AWGN) is a simple channel model that can be used to characterize space communication and some wire transmission. More complex and accurate fading channel models, like Ricean and Rayleigh fading [110, 128], are desired for terrestrial wireless communication,

1. *Rayleigh Fading* occurs when there are multiple indirect paths between transmitter and receiver and no distinct dominant path, such as an LOS path. This represent the worst-case scenario in terms of channel fluctuations. Specifically, at any time t, the received complex envelope has a pdf

$$f(x) = \frac{x}{\sigma^2} \exp\Big\{ -\frac{x^2}{2\sigma^2}\Big\}, \quad x \geq 0 \tag{1.5}$$

where σ^2 is the time-average power of the received signal before envelope detection. The squared-envelope or the received power is exponentially distributed with pdf

$$f(x) = \frac{1}{2\sigma^2} \exp\{ - \frac{x}{2\sigma^2}\}. \tag{1.6}$$

Like log-normal shadowing, the exponential distribution of the received power allows a simple expression of the reception probability and outage probability in Rayleigh fading, *e.g.*, given a received power threshold R, the outage probability is

$$p_{out} = \Pr\{x \leq R\} = 1 - \exp\big(- \frac{R}{2\sigma^2}\big). \tag{1.7}$$

2. *Ricean Fading* occurs when there is a direct LOS path in addition to a number of indirect multipath signals. The Ricean distribution is given by

$$f(x) = \frac{x}{\sigma^2} \exp\{ - \frac{x^2 + A^2}{2\sigma^2}\} I_0\big(\frac{xA}{\sigma^2}\big), \tag{1.8}$$

where A denotes the peak amplitude of the dominant signal and $I_0(\cdot)$ is the modified Bessel function of the first kind and zero order. The Ricean distribution can be completely specified by a parameter K, which is defined as

$$K = \frac{\text{power in the dominant path}}{\text{power in the scattered paths}} = 10 \log_{10} \frac{A^2}{2\sigma^2} \text{ (dB)}. \tag{1.9}$$

When $K = 0$, the dominant component fades away and the Ricean distribution degenerates to a Rayleigh distribution. When $K = \infty$, no indirect multipath signals exist, and the channel is AWGN.

The Ricean model is often applicable in an indoor environment whereas the

Rayleigh fading model characterizes outdoor settings. Both characterize the flat fading channels [128].

Multipath fading results in correlated and bursty errors. Markov models have been proposed to deal with correlated errors. In [139] it is confirmed that the first-order continuous Markov channel provides a mathematically tractable and accurate model for time-varying Rayleigh fading channels and uses only the received SNR value immediately preceding the current one. In the sequel paper, a finite-state Markov chain was proved to be accurate enough to approximate the channel characteristics. The two-state model dates back to the early work by Gilbert [40]. For this Gilbert-Elliott channel model, it is possible to find exact expressions for the block-error rate. It was found in [154] that the block-error process can be reasonably well modeled as Markov, which can be used to measure delay, throughput, packet dropping probability, and packet transmission errors. Throughout this dissertation, the error process of blocking fading channels is modeled as a first-order two-state Markov chain. That is, let 0 and 1 denote successful (or "good" state) and erroneous (or "bad" state) transmission in a given time slot. The transition matrix for the packet-error process is

$$\mathbf{C} = \begin{bmatrix} c_{00} & c_{01} \\ c_{10} & c_{11} \end{bmatrix}, \tag{1.10}$$

and the average packet error rate is

$$\varepsilon = \frac{c_{01}}{c_{10} + c_{01}}. \tag{1.11}$$

Note that if $c_{01} + c_{10} = 1$, this Markov chain is reduced to a Bernoulli process, in which all channel errors are independent. We will use this reduced version (*i.e.*,

Bernoulli process) to characterize the channel errors in Chapter 4 to 7.

1.4.4 Composite Shadowing-Fading Distribution

For slow moving or stationary wireless devices, the receiver is unable to average over the effects of fading. Then a composite distribution is necessary for performance evaluation to account for both shadowing and multipath fading. Two different approaches have been suggested in the literature to obtain the composite distribution [129]. In the first one, the envelope (or square-envelope) is expressed as a conditional density on the average envelope strength V, and then integrate over the density of V to obtain the composition distribution. For example, in a composite log-normal shadowing and Rayleigh fading channel, the mean of the Rayleigh distribution obeys a log-normal distribution. In the second one, the composite received signal is expressed as the product of the small scale multipath fading and the large scale shadow fading. As stated in [100], a mobile radio signal composed of log-normal shadowing and Rayleigh fading can be approximated by a log-normal distribution in terms of the received SNR as follows

$$f(x) = \frac{1}{s\sigma\sqrt{2\pi}} \exp\Big\{ - \frac{(-\ln x - \mu)^2}{2\sigma^2} \Big\}, \tag{1.12}$$

i.e., ln(SNR) is normally distributed with mean μ and variance σ^2. If the fading and shadowing processes are independent, these two approaches lead to identical results.

1.5 Our Contributions

In the previous sections we discussed the features and challenges of WMNs. Our contributions lie in the investigation of MAC schemes, packet scheduling,

and their interactions with other components of WMNs. First, we review current MAC and packet scheduling protocols in wireless networks in Chapter 2. Second, we propose a priority scheduling protocol that can achieve delay balancing in the critical area of WSNs (Chapter 3). Combined with packet dropping strategies, a hard delay bound is guaranteed. Discrete-time queueing theory is used to derive the corresponding packet loss rates.

Third, we focus on the cross-layer analysis of the physical channel and MAC schemes in one-dimensional (1-D) WMNs. The analysis starts with a single node controlled by TDMA and fed with CBR traffic (Chapter 4). In wireless networks, assuming the channel errors are independent, a node controlled by TDMA is modeled as a G/Geom/1 system but the interarrival times are not integer as conventionally. We use probability generating functions (pgf) and eigenvalue approach to derive the distributions of the queue length and delay, and the output characteristics. Then, we extend the analysis from the single node scenario to the multihop scenario. Two typical MAC schemes, m-phase TDMA and slotted ALOHA are studied in Chapter 5. Specifically, for Rayleigh fading channel, the interaction between the physical channel, the MAC schemes and the traffic statistics is investigated (Chapter 6). These analyses provide insight on the design of multihop MAC schemes.

Finally, an energy-efficient and delay-constrained scheduling protocol is developed for networked control systems. For real-time applications, it is critical to guarantee delay bounds with a small amount of packet loss. Therefore, scheduling and MAC schemes are designed to be associated with packet dropping strategies to reduce unnecessary energy consumption on obsolete packets and guarantee the on-time transmission of useful packets (Chapter 7). Our conclusions are presented

in Chapter 8.

CHAPTER 2

WIRELESS MEDIUM ACCESS CONTROL AND PACKET SCHEDULING

The scarce bandwidth and contention-based multiple access of wireless networks motivate the need of effective scheduling algorithms. Scheduling can be investigated at two levels. Medium Access Control (MAC) is system-level scheduling that determines the transmission orders over multiple nodes in the network, while packet scheduling is node-level scheduling that allocates the transmission opportunities among multiple flows within a node. The packet scheduler is positioned between the routing agent and the MAC layer. *Multi-hop* scheduling is quite complex because of connectivity and spatial reuse. The schemes can be implemented in a *centralized* or *distributed* way or as a hybrid of both. In general, centralized scheduling outperforms distributed scheduling in terms of throughput and reliability because the latter is non-work-conserving (*i.e.*, the server or channel is kept idle even though there are users waiting for service) and always incurs collisions, but distributed scheduling is more practical in the multihop environment. In this chapter, we review the wireless scheduling principles and their implementations at the system level and node level, respectively.

2.1 Wireless Scheduling

Like wired scheduling, wireless scheduling is expected to support different levels of service, like *guaranteed* and *best-effort* service, but its design and implementa-

tion are more complex. For instance, the fluctuation in the link rate necessitates a distinction between *effort* and *outcome* [20, 30, 78]. *Effort* is the resource allocated to a user, whereas *outcome* is the service obtained by the user. In wired networks, these two terms are equivalent. In wireless networks, some designated resource is wasted due to channel errors and collision, and thus *outcome* is usually smaller than *effort*. Performance metrics and criteria should be specified with *effort* or *outcome*. For instance, *effort/temporal fairness* and *outcome/throughput fairness* [30, 78] need different fair scheduling schemes. There are some uncertain factors complicating the design of wireless scheduling [35, 92, 109]:

- *Time- and location-dependent link errors*, caused by interference, fading, and path loss. The link errors are bursty in nature. *Node failures*, together with link errors, lead to changes in the network topology and connectivity. The scheduler should be aware of and keep track of these changes to adjust the allocation scheme. Fairly accurate channel prediction can be achieved using n-state Markov models [92].

- *Contention* for the shared wireless medium among all nodes. In the distributed environment, the contention possibly results in collision and *hidden* and *exposed* terminal problems.

- *Information collection and sharing*, including the channel state, the number of flows, their reserved rates and queue length. Most wireless schedulers need this information to adjust the transmission order for better performance. The more distributed the information, the more accurate and efficient the scheduling algorithm. But the accuracy of such information cannot be guaranteed in distributed and wireless networks.

- *Energy efficiency and fairness.* Energy and power conservation should be supported across all the layers, including MAC and packet scheduling. Throughput and energy efficiency are maximized by transmitting each packet over a very long period of time [42]. Allowing one node/flow to maximize its throughput in this energy efficient way certainly causes other nodes/flows to starve. They have less time to spend and thus consume more energy to transmit their data within the delay bound. Unfair resource allocation incurs unbalanced energy consumption and may shorten the network lifetime.

Based on the implementation, wireless scheduling algorithms can be classified as follows [35]:

- *Non-work-conserving vs. work-conserving.* In order to avoid collisions, many distributed scheduling algorithms require nodes to wait backoff period before transmission even though the channel is idle. The resulting scheduler is thus non-work-conserving.

- *Timestamped vs. round robin (RR).* In timestamped schedulers, each packet is tagged with a timestamp the moment when it arrives in the system, and all packets are transmitted according to their stamps. RR schedulers serve packets simply based on their flow index. Timestamped scheduling usually guarantees better QoS but is more complex than RR scheduling.

- *Sorted-priority-based vs. frame-based.* In sorted-priority-based scheduling, each flow is assigned a priority level and served by priority scheduling. In contrast, in frame-based scheduling, each flow reserves a portion of the frame for transmission. The reservation mechanism is less flexible than the priority schemes but can guarantee a minimum individual throughput for each flow.

The scheduling algorithms are evaluated from the following parameters [35, 92]:

- *Energy efficiency* ξ, defined in [158] as

$$\xi = \frac{\text{Total number of packets delivered successfully}}{\text{Total energy consumed}}, \tag{2.1}$$

  which provides two ways to achieve high energy efficiency, *i.e.*, maximizing the throughput given a fixed energy constraint, or minimizing consumed energy to transmit a certain amount of packets.

- *Efficient link utilization.* In a single-hop network, the scheduler attempts to assign transmission slots to nodes/flows with good channels. In a multihop network, due to signal attenuation with distance, the exploration of spatial reuse can improve the link utilization.

- *Delay.* Delay-sensitive applications require hard delay bounds. If the channel errors are bounded in duration, so is the packet delay. Hence the delay performance is channel-dependent.

- *Fairness*, defined in either the time-domain or the throughput-domain. In a network supported by rate control, *temporal/effort fairness* is more suitable than *throughput/outcome fairness.* In order to achieve throughput fairness, the flows experiencing bad channels need to capture the medium for such a long time that the throughput gains available due to a multi-rate physical layer will be offset. Temporal fairness requires that the difference between the time shares allocated to flow i and j, denoted by $T_i(t_1, t_2)$ and $T_j(t_1, t_2)$, is bounded, *i.e.*,

$$| T_i(t_1, t_2) - T_j(t_1, t_2) | \leq T_f \tag{2.2}$$

Effort fairness cannot guarantee outcome fairness while outcome fairness always implies effort unfairness. In addition, fairness guarantee also should be specified in terms of the time scale, *i.e.*, *long-term* or *short-term*. Short-term fairness is more constrained, even in wireline networks. Energy efficiency is sometimes traded off for high throughput fairness.

- *Throughput*, defined as

$$\omega = \frac{\text{Total number of packets delivered successfully}}{\text{Total time spent in delivery}}, \tag{2.3}$$

  can be optimized by either maximizing the overall throughput or maximizing the minimum throughput of each user. Generally, a good scheduling algorithm should maximize both. Simply maximizing the network throughput leads to unfairness and cannot guarantee the individual throughput of each flow.

- *Implementation complexity*. In wireless networks, if the scheduling algorithms are distributed and implemented by nodes with limited memory, energy, and processing capability, low complexity is certainly more desirable. Centralized scheduling allows algorithms of moderate complexity for performance improvement.

- *Isolation*. The algorithm should isolate a node/flow from the effects of misbehaving nodes/flows. Isolation is usually coupled with fairness.

- *Delay/bandwidth decoupling*. For most rate-based schedulers, the delay is tightly coupled with the reserved rate; that is, a higher reserved rate provides a lower delay, and vice versa. However, many applications are of low rate

and small delay bound. Scheduling then should be able to decouple delay from the reserved rate.

- *Support for latency and reliability.* Delay-sensitive applications usually can tolerate a small amount of packet loss, while error-sensitive applications could allow larger delays. It is not efficient to treat them identically. The connection-level packet management policies should be decoupled from link-level packet scheduling policies. This can be achieved by assigning additional slot queues to each flow [92].

- *Scalability.* As the number of nodes/flows contending for transmission increases, the algorithms should preserve their efficiency.

- *Packet loss rate.* Packet loss may be caused by channel errors, congestions and/or a packet dropping strategy that is intentionally implemented by the nodes.

Among these parameters, *energy efficiency*, *fairness*, *delay*, and *throughput* are the most important ones. But they are conflicting, and it is almost impossible to optimize them at the same time. The objective is to optimize few parameters under the constraints of other parameters.

There are two approaches to deal with the channel errors and the resulting incapability to transmit packets at a constant rate. One is to *defer* the transmission and *compensate* later. The other one is to insist transmitting, but to reduce the transmission rate until reliable communication is achieved. These two approaches can be used separately or jointly. For example, fair scheduling exploits the deferring and compensating scheme, whereas energy-efficient scheduling takes advantage of the low transmission rate to save energy.

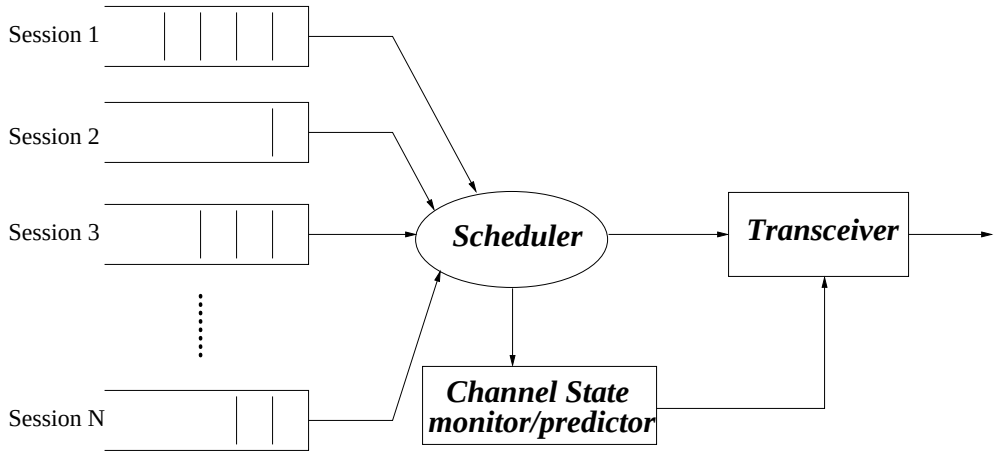

Figure 2.1. A typical wireless scheduler

2.1.1 Wireless Fair Scheduling

Since wireline scheduling algorithms have been well developed to address the fairness problem, it is natural to extend them to wireless fair scheduling. The unfairness problem caused by wireless channel errors is usually solved by the deferring and compensating approach. First, the channel state monitor/predictor estimates the channel status, as shown in Fig. 2.1. Then, the compensation model determines how the flows/nodes are compensated if these flows/nodes are not served as allocated because of channel errors. Typically, a wireless fair scheduler is composed of five components [35, 92]:

- An *error-free service model*, which emulates the service evolution in an error-free scheduling system. Wireline scheduling schemes can be directly used in this model, *e.g.*, Weighted Fair Queueing (WFQ), Virtual Clock (VC), Self-Clocked Fair Queueing (SCFQ), and Start Time Fair Queueing (STFQ).

- A *lead/lag model*, which compares the service received by each flow/node

in reality to that allocated by the error-free service model. The lead/lag counter indicates whether the flow/node is leading, is in sync with, or is lagging its error-free service model and by how much. Obviously, a flow/node is lagging if the channel is too bad to ensure a successful transmission. For efficient resource utilization, other flows in sync or leading may replace the lagging flow to transmit and become leading. The counter records the service difference, *e.g.*, the number of slots that are allocated to the lagging flow but used by leading flows.

- A *compensation model*, which specifies how the lagging flows are compensated once their channels become good. The compensation is either complete or partial. In the complete compensation model, a lagging flow with a good channel captures the medium until all its lags are compensated for or its channel becomes bad again. All other flows will be prevented from transmitting even they are in-sync and suffer starvation. On the other hand, the partial compensation model punishes only the leading flows that replace the lagging flows to transmit in the slots assigned to the lagging flows.

- *Separate slot queues and packets queues.* To drop Head of Line (HOL) packets will incur a decrease of precedence of the flow. Slot queues are added to maintain the precedence of the flows. This component is used to support for both delay-sensitive and error-sensitive data.

- A *channel monitor/predictor.*

The following are several instances of the above architecture.

- *Channel State-Dependent Packet Scheduling (CSDPS)* [14] may be the simplest instance because it does not include the lead/lag and compensation

models. The error-free service model can use any wireline service disciplines such as RR, WFQ, Feasible Earlier Due Date (FEDD) [122], and Longest Connected Queue (LCQ) [131]). If the channel is bad, the packet transmissions are simply deferred without further compensation. Apparently, fairness and throughput are traded off for simplicity.

An enhanced CSDPS is proposed in [126] that uses a priority-based link sharing mechanism *Class Based Queueing* (CBQ) to improve fairness and throughput. CBQ provides a lead/lag and a compensation model. The lead/lag model counts the percentage of the outcome instead of the service difference. The performance is thus sensitive to the statistically reserved fraction. CSDPS-based scheduling does not provide short-term guarantees for fairness and throughput.

- *Idealized Wireless Fair Queueing (IWFQ)* [81] uses WFQ or WF^{2}Q (Worst-case Fair WFQ) as the error-free service model. Lagging flows are completely compensated to guarantee long-term fairness and throughput though the short-term fairness is violated and in-sync and leading flows may be starved. In [81], a frame-based *Wireless Packet Scheduling (WPS)* algorithm is developed that uses a WRR with spreading slots as its error-free service. The flow experiencing channel errors first attempts to swap its assigned slot with flows behind it in the frame. If this fails, the flow is tagged as lagging and partially compensated in the subsequent frames by increasing its weight according to its lag counter. This approach limits the access capability of the lagging flows and attenuates the starvation problem of IWFQ.

  The other enhanced IWFQ is *Wireless Fair Service (WFS)* [80], in which both the lead/lag counter and the compensation are partial. The punished

leading flows give away only a dynamic fraction of their service, which is fairly distributed among all lagging flows, rather than being solely captured by a single lagging flow with the minimum service tag. To decouple bandwidth and delay, each flows is assigned two parameters, a *rate weight* and a *delay weight*. In general, WFS achieves almost all desired properties of a wireless fair service.

- *Channel-Condition-Independent Fair Queueing (CIF-Q)* [96] is similar to WFS in the lead/lag and compensation model. The major distinction from WFS is its using Start Time Fair Queueing (STFQ) as the error-free service model. With location-dependent channel errors, it is easier to schedule packets based on their start time rather than the finish time. Therefore, CIF-Q achieves the same performance as WFS but is simpler to implement.

- *Server-Based Fairness Approach (SBFA)* [109] reserves a fraction of bandwidth, referred to as Long-Term Fairness Server (LTFS), for lagging flows to guarantee long-term fairness and throughput. Within the LTFS, the lagging flows are served in a WRR fashion. Like CBQ-CSDPS, the performance is sensitive to the statistically reserved fraction of bandwidth.

- *Effort-Limited Fair Scheduling (ELF)* [30] follows a different compensation principle. Both leading and in sync flows are required to yield to lagging flows. The error-free service model is WFQ with dynamic flow weights that vary with channel error rates. The compensation is partial by bounding the flow weight with an "limited effort" so that one flow experiencing long bursty channel errors cannot capture the medium for a long time. The performance is tightly coupled with the weight bounds.

- *Wireless Credit-based Fair Queueing (WCFQ)* [73] uses Credit-Based Fair Queueing (CBFQ) as its error-free service model, which does not need service tags as other fair scheduling algorithms. The channel condition is reflected through a cost parameter, which, in combination with the flow credit, determines the transmission order. The lead/lag counter and compensation are implicitly expressed by the *credit* and *cost* parameters. Fairness and throughput are balanced.

The distributed version of fair scheduling [138] provides an implementation approach for wireless MAC if broadcasting is allowed. For example, in IEEE 802.11, the service tag of each packet can be calculated individually, piggybacked onto the handshaking packets RTS and CTS, and then broadcast to all neighboring nodes. Or, in a CSMA-based scheme, the node sets its backoff timer in proportion to the service tag of the HOL packet [138]. Distributed fair scheduling can be applied to both single-hop and multi-hop networks.

Note that above fair scheduling schemes aim at guaranteeing outcome/throughput fairness. With modifications, they can achieve effort/temporal fairness.

2.1.2 Energy-Efficient Wireless Scheduling

Based on the definition of energy efficiency, high energy/power efficiency can be obtained by maximizing the amount of information transmitted for a given average power/energy constraint, or by minimizing the power/energy consumption per specified amount of information being transmitted successfully [137]. Accordingly, energy-efficient scheduling can be classified into *opportunistic* scheduling [78] and *lazy* scheduling [103].

2.1.2.1 Opportunistic scheduling

Opportunistic scheduling [72, 74, 75, 78, 79], as its name implies, schedules the flows with the best transmission opportunity, which indicates the channel condition from the perspective of energy/power conservation. The rate and power are adaptively allocated to take advantage of favorable channel conditions. Basically, a constant signal-to-noise ratio E_b/N_0 (in terms of the ratio of the signal energy per bit to noise power spectral density) is maintained for reliable communication but the transmit power level, symbol transmission rate, constellation size, coding rate/scheme, space diversity, or any combination of these parameters can be varied [41]. Fig. 2.2 illustrates the theoretical relationship between the bit error rate (BER) and the E_b/N_0 for several different modulation schemes and data rates. For each modulation scheme, the BER decreases with better channel conditions and increasing E_b/N_0. For a given E_b/N_0, an increase in data rate results in an increase in BER. For a given BER, a decrease in data rate permits a decrease in E_b/N_0 that is proportional to energy consumption. Opportunistic schedulers select the maximum data rate available under the specific channel condition (E_b/N_0) and reliable communication constraint (BER) to achieve the best throughput performance [53, 72, 74, 75, 78, 79, 116, 140]. This technique aims at compensating for random channel variations due to multipath fading, reducing the transmit power required for reliable communication and thus reducing the resulting interference, minimizing the probability of link outage, satisfying delay constraints, preventing buffer overflow, achieving high network performance (*e.g.*, throughput), and controlling the level of QoS among all nodes [72, 74, 75, 78, 79].

The design of opportunistic scheduling usually consists of two steps [78]. First, define a channel-dependent function, called *utility* function or *channel condition*

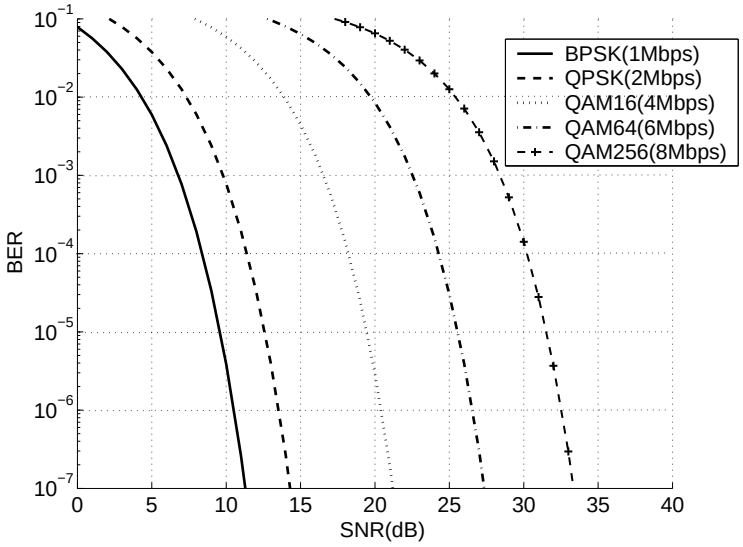

Figure 2.2. Theoretical BER *vs.* E_b/N_0 for several modulation schemes and data rates

function [72, 74, 75, 78]. Second, translate the problem of maximizing the average network performance subject to some constraints (*e.g.*, delay, fairness, or minimum throughput of each flow) into an optimization problem that can be solved using conventional optimization tools. Additional parameters can be added into the optimization formulation to further compensate for the capacity loss caused by wireless channel errors and may achieve the same fairness as wireless fair scheduling described in Section 2.1.1. Then, the obtained scheduler is good at both fairness and throughput.

From the perspective of throughput optimization, [9, 10, 14, 67, 120, 130] concluded that *Longest Queue First (LQF)* or *Largest Delay First (LDF)* based scheduling is throughput-optimal even in the wireless environment. Compared to their wireline counterparts, this class of wireless scheduling algorithms enhances the performance by weighing the queue length or delay according to the channel

condition and taking advantage of the multiuser diversity. Therefore, the scheduler can select user i to transmit based on the link rate or queue length as follows [99], where $R_i(t)$ denote the maximum available rate under the channel condition at time t, $i^*(t)$ the user selected at time t, $T_i(t)$ the average throughput of user i till slot t, $D_i(t)$ the delay, and $Q_i(t)$ the queue length,

- The *Maximum Rate (MR)* algorithm [136] simply selects the user with the maximum rate:

$$i^*(t) = \arg\max_i R_i(t); \tag{2.4}$$

- The *Proportional Fairness (PF)* algorithm [57] selects the user with the maximum normalized rate:

$$i^*(t) = \arg\max_i \frac{R_i(t)}{T_i(t)}; \tag{2.5}$$

- [78] favors the user of the maximum compensated rate, where v_i is a compensation factor that dynamically changes with the received performance,

$$i^*(t) = \arg\max_i (R_i(t) + v_i) \tag{2.6}$$

- [17] determines the scheduling order based on the weighted data rate, scaled by a weight w_i

$$i^*(t) = \arg\max_i w_i R_i(t) \tag{2.7}$$

- $0-1$ *indicator* [14],

$$\begin{aligned} i^*(t) &= \arg\max_i D_i(t)\mathbf{1}_{\{\mathrm{SNR}\geq\mathrm{SNR}_T\}}, \\ i^*(t) &= \arg\max_i Q_i(t)\mathbf{1}_{\{\mathrm{SNR}\geq\mathrm{SNR}_T\}}. \end{aligned} \tag{2.8}$$

  where SNR_T is a threshold for a reliable reception. Since the condition $\{\mathrm{SNR} \geq \mathrm{SNR}_T\}$ essentially indicates the probability of successful reception, or the probability that the link exists, this scheme is akin to CSDPS (introduced in Section 2.1.1). In other words, the scheduler chooses the user with the longest queue length or largest delay among all backlogged users experiencing a good channel.

- *Logarithmically weighing* [67],

$$i^*(t) = \arg\max_i w_i(t)Q_i(t), \tag{2.9}$$

  where the weight $w_i(t)$ can be determined by the channel error rate $\varepsilon_i(t)$ (note that here we modify the set of w_i in [67] in order to make it suitable for the wireless system), $w_i(t) = -\ln \varepsilon_i(t)/B_i$, in which B_i is the maximum queue length.

- *Multiplicatively weighing* [9],

$$i^*(t) = \arg\max_i \gamma_i R_i(t)(Q_i(t))^\beta, \tag{2.10}$$

  where γ_i and β are constants. The channel condition is reflected through the maximum available rate $R_i(t)$.

- *Exponentially weighing* [120],

$$i^*(t) = \arg\max_i \gamma_i R_i(t) \exp\Big(\frac{a_i Q_i(t)}{\beta + (\bar{Q}(n))^\eta}\Big), \tag{2.11}$$

where β, η, and a_i are positive constants. $\bar{Q}(t)$ is the average weighted queue length over all sessions, *i.e.*,

$$\bar{Q}(n) = \frac{1}{N}\sum_{i=1}^{N} a_i Q_i(t). \tag{2.12}$$

2.1.2.2 Lazy scheduling

Lazy scheduling saves energy by prolonging the transmission time. As observed in [38], with many coding schemes, the energy needed to transmit a given amount of information is strictly decreasing and convex in the transmission duration. This observation becomes an important guideline to design energy-efficient scheduling algorithms [39, 43, 64, 103, 108, 119, 137].

Lazy Scheduling was first proposed in [103] for a single flow. A batch of packets arriving during a time period of T will be sent out in next T slots. Their transmission times are assigned as evenly as possible within the T slots. In other words, with appropriate coding and modulation techniques, the scheduler attempts to transmit each packet as long as allowed by the delay constraint. Several mechanisms are involved, including the *calculation* of the optimal transmission time, *online implementation*, and *discretization* of the transmission rates. [39, 64, 103, 137] generalize single-flow Lazy Scheduling to multiple flows, but they treat the multiple flow scenario as a special single-flow case. Each flow independently calculates the transmission times of its queued packets, and the scheduler serves them using conventional wireline scheduling, but with different transmission times. This gen-

eralization is not feasible. With a deterministic delay bound, allowing one flow to dominate channel access (particularly in TDMA systems) will preclude other flows from transmitting. In order to guarantee QoS metrics such as like delay, other flows must complete transmitting backlogged packets in a short time and thus consume more energy.

The other disadvantage of Lazy Scheduling is its requirement on the knowledge of the arrival pattern. Since the calculation of the optimal transmission time is based on the packet arrivals in a frame, the on-line scheduler needs to estimate or predict the real arrival pattern, which is not realistic in WMNs. Moreover, such calculation is complex and energy-inefficient.

2.1.2.3 Comparison

In summary, wireless fair scheduling uses compensation techniques to guarantee *fairness* without power and rate control. Each node transmits at a constant rate when the channel is good. At the system level, throughput is normally balanced among all nodes, but energy consumption is not constrained. On the other hand, energy-efficient scheduling takes advantage of good channels and allocates low transmission rates with power and rate control. Lazy scheduling saves energy at the cost of low link utilization and throughput and lack of fairness. Opportunistic scheduling can be combined with partial compensation mechanisms to guarantee fairness constraints. With appropriately selected parameters, this scheduling can better balance throughput, fairness, and energy efficiency.

2.1.3 Telatar Model for the Analysis of Wireless Scheduling Algorithms

Energy-efficient scheduling algorithms involve rate control, which is supported by dynamic modulation schemes. Modulation is the process of translating an outgoing data stream into a form suitable for transmission on the physical medium. For digital modulation, this involves translating the data stream into a sequence of *symbols*. Each symbol may encode a certain number of bits, the number depending on the modulation scheme. The symbol sequence is then transmitted at a certain rate, the *symbol rate*. So for a given symbol rate, the data rate is determined by the number of encoded bits per symbol [53].

Conventionally, the issue of reliably communicating data over a fading channel falls mainly within the province of information theory, at the physical layer. Queueing is usually considered a network layer issue and divorced from physical layer consideration. Cross-layer design abandons the separation of physical layer coding and network layer queueing in wireless networks [13, 132].

Consider a discrete-time model. Assume that both the transmitter and the receiver have perfect knowledge about channel state information (CSI). Then transmitters are capable of adaptively adjusting their transmission rate $R_i(t)$ for reliable communication. In [13, 132], a Telatar model is presented to combine the issue of reliable communication with queueing theory.

In the Telatar model, the buffer occupancy corresponds to the *reliability* required by the data in the buffer plus the remaining reliability. Here the reliability is denoted by the maximal allowable error probability η_i. We assume that each time slot is divided into M subslots. A packet is encoded into L subslots if for any $\rho \in (0, 1)$:

$$\sum_{n=1}^{L} E_0(\rho, \mathrm{SNR}_i^n(t)) \geq \rho \ln K - \ln \eta_i, \tag{2.13}$$

where K is the number of codewords and

$$E_0(\rho, \mathrm{SNR}_i^n(t)) \triangleq \rho \ln(1 + \frac{\mathrm{SNR}_i^n(t)}{1+\rho}). \tag{2.14}$$

The above inequality guarantees the error probability η_i. From the perspective of queueing theory, $(\rho \ln M - \ln \eta)$ can be considered the demand of a packet once it enters the encoder and $E_0(\rho, \mathrm{SNR}_i^n(t))$ is the number of bits reliably transmitted in the n-th subslot of the t-th slot given the channel state $H_i^n(t)$. $L \geq 1$ is the number of subslots required to transmit the current packet with an error probability less than η_i. Then the number of packets reliably transmitted in slot t, $R_i(t)$ is

$$R_i(t) = \lfloor \frac{M}{L} \rfloor. \tag{2.15}$$

Note that if L is too large and exceed M, then $R_i(t) = 0$ and the scheduler decides that node i does not transmit. In a block fading channel, the channel condition is assumed to hold during the whole time slot, *i.e.*, $\mathrm{SNR}_i^n(t) = \mathrm{SNR}_i(t)$. Then the channel-condition-dependent random variable L is reduced to

$$L = \lceil \frac{\rho \ln K - \ln \eta_i}{\rho \ln(1 + \frac{\mathrm{SNR}_i(t))}{1+\rho})} \rceil. \tag{2.16}$$

This number L is now dependent only on the channel condition at time t. Then, queueing theory can be used to analyze energy efficient scheduling algorithms in a cross-layer manner.

2.2 Wireless MAC

Wireless MAC schemes can be implemented by applying wireless scheduling algorithms in a distributed way over all nodes in the network. However, the distributed implementation not only requires global information exchange that adds overhead, but also results in performance degradation, especially in the wireless environment. Therefore, many wireless MAC algorithms do not follow the wireless scheduling principles.

2.2.1 Classifications of Wireless MAC

Wireless MAC schemes can be classified into contention-free and contention-based, as shown in Fig. 2.3 [66]. Contention-free schemes (*e.g.*, TDMA, FDMA and CDMA) are more applicable to single-hop networks with centralized control like cellular networks. When they are applied to multihop networks with spatial reuse, they are no longer fully contention-free. In WMNs, contention-based schemes are more practical but they suffer from collisions.

Random access schemes are distinguished by whether carrier sensing occurs prior to data transmissions or not. Compared to ALOHA, the CSMA-based schemes reduce the possibility of packet collisions and thus improve the throughput. In the multihop environment, random access schemes result in hidden and exposed terminal problems. Reservation-based schemes are proposed to solve these problems [66]. The channel is reserved before the nodes are allowed to transmit data. Resource reservation can be implemented by exchanging control packets (*e.g.*, Request-to-Send/Clear-To-Send (RTS/CTS) in MACA, MACAW, FAMA) or by broadcasting busy tones through control channels (DBTMA).

There are several guidelines for power conservation [66]. First, collisions are a

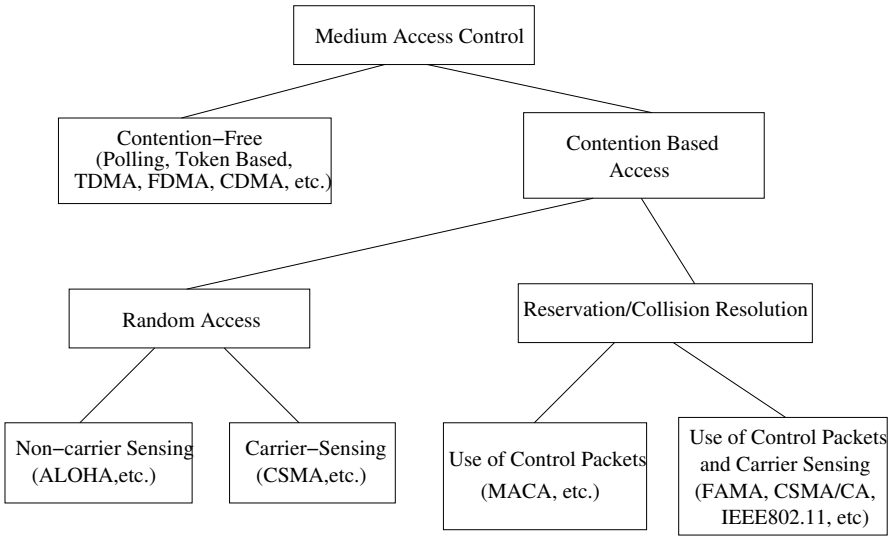

Figure 2.3. Classifications of Wireless MAC Schemes

major cause of expensive retransmissions. Second, the transceiver should remain in *sleep* mode whenever possible. Third, the transmitter should switch to a lower power mode that is sufficient for the destination node to receive the data. Therefore, energy-efficient and power-aware MAC protocols can be classified into *power management* and *power control* protocols. Power management MAC protocols aim at alternating sleep and wake cycles (*e.g.*, Power Aware Medium Access Control with Signaling (PAMAS) and Dynamic Power Saving Mechanism (DPSM)), while power control MAC protocols use a variation in the transmission power (*e.g.*, Power Control Medium Access Control (PCM) and Power Controlled Multiple Access (PCMA)) [66].

The probability of packet collision can be reduced by using multiple channels. For example, some reservation-based MAC protocols use a dedicated channel for control packets or signaling and another channel for data transmissions (*e.g.*, Dual Busy Tone Multiple Access (DBTMA)). It is also possible to use multiple channels

for data transmissions like Multi-Channel CSMA MAC, Hop-Reservation Multiple Access (HRMA), Multi-Channel Medium Access Control (MMAC). One advantage of the multi-channel MAC approaches is their capability to support QoS.

It is difficult to provide effective QoS in multihop networks because of the lack of centralized control, limited bandwidth, error-prone wireless channels, node mobility, and power and computational constraints. Most QoS aware MAC protocols in the literature are designed to distinguish between real-time and non-real-time traffic flows. In general, real-time flows are given high priorities, which leads to short waiting time and/or backoff contention window (*e.g.*, Enhanced DCF, Black Burst contention). However, such prioritization cannot fully guarantee packet delays. Some deadline-based MAC protocols are proposed, like Real-Time MAC, Elimination by Serving DCF, Deadline Bursting DCF, and Distributed Fair Scheduling [66]. They use the packet deadlines to determine the transmitter's waiting time and backoff value. The disadvantage of these MAC schemes is that they may not provide fair sharing between real-time and non-real-time flows. The lower priority flows often suffer from starvation in the presence of heavy real-time flows.

2.2.2 Modeling and Analysis of MAC Schemes

Most of the proposed MAC schemes, if not all, were analyzed based on an overly-simplified circular step-function model, often referred to as "disk model" [124]. The transmission range of each node is assumed to be an identical constant, and the transmission success purely depends on the distance between the transmitter and receiver. If there is more than one transmission within the range to the same receiver at the same time, the transmission is regarded to be failed.

Although this model simplifies protocol design and theoretical analyses, it may provide vastly inaccurate information. In practice, i) the transmission range is time- and location-varying; ii) with a high signal-to-noise-and-interference (SNIR), the node can recover the data even if there are overlapped transmissions. These properties are characterized by the more practical "physical" or "capture model" [88, 155]. In the capture model, the transmission success is determined by SNIR, a function of multiple access interference (MAI), which accounts for not only the distance and MAC, but also traffic statistics. Therefore, MAI should be considered in the design and analysis of wireless MAC.

2.3 Wireless Multihop Scheduling

A simple way to design multihop scheduling is to apply current wireless scheduling principles to the multihop environment [60, 61, 83–86, 107]. For example, in CSMA/CA, the backoff timer is controlled by the service tag of the HOL packet. Opportunistic scheduling can be implemented in slotted ALOHA in a way that each node determines its transmission probability according to the information on both its own channel and other nodes [107]. The difference from single-hop scheduling is that as soon as the topology changes, the updated information should be quickly broadcast through the network. However, most of the current wireless scheduling approaches neither result in optimum transmission pattern nor provide maximum network utilization in WMNs [66, 147, 148]. The main difficulties are [148]:

- The hidden terminal problem still exists and its impact on WMNs is more severe than in single-hop networks.
- The exposed terminal problem is not solved in WMNs and will cause resource

waste, which is more harmful in multihop networks.

- The rapidly varying network topology incurs heavy overhead. Moreover, the exchanged information on network topology cannot be ensured to be timely and accurate. Then the information of the entire network is usually unknown and/or erroneous, which results in performance degradation.

The challenge for scheduling in WMNs is to use limited local information to allocate the nodes to transmit in an orderly and effective manner.

In order to simplify the problem, current multi-hop scheduling often assumes that the channels are noise-free and unsuccessful receptions are due to collisions [35]. For fair scheduling, the objective is to ensure fair channel allocation among spatially contending packet flows, as well as to maximize channel reuse [83–86].

Conflicts in multi-hop networks may occur in two ways [35]. A *primary conflict* occurs when two or more nodes simultaneously transmit to a common destination node. A *secondary conflict* occurs when a node receiving a transmission intended for it is interfered with by another transmission not intended for it. In the disk model, two nodes can transmit simultaneously without mutual interference if they do not have a common node as either transmitter or receiver. Scheduling should be able to avoid conflicts while maximizing spatial reuse at the same time.

With little infrastructure support, a multihop scheduler is desired to possess *topology transparency* and *low connectivity information requirement*, because both topology and connectivity information incur substantial overhead with frequently changing topology. Since this information belongs to the infrastructure data and is determined by the routing protocol, scheduling and routing should be designed jointly for optimization.

There are numerous open issues to be investigated in multihop scheduling. We are interested in the following:

- *Spatial reuse.* In the multihop environment, if two node pairs are far away from each other, their simultaneous transmissions will not interfere or collide with each other. To improve network throughput, some nodes should be allocated to transmit at the same time. Previous work usually uses the "disk model" with fixed transmission range and assume that nodes interfere if they lie within the ranges of each other. Therefore, it is very popular in the study of spatial reuse to assume that in a chain network, single nodes *three* hops away can transmit simultaneously with no possibility of interference [23, 124]. However, this assumption does not hold if the "capture model" is used to measure interference. For fading channels, the "capture model" is more accurate, and it is essential to investigate spatial reuse using this model.

- *Correlations.* The performance of WMNs is measured not only individually at a node but also e2e. Each node along the path contributes to the e2e performance. Note that their contributions will be correlated. For example, if a packet flow experiences longer delay than expected at the upstream nodes and its delay bound may be violated soon, then the downstream nodes can make up for it by increasing the priority of this flow to give it more transmission opportunities [59, 70]. Moreover, there exist so close correlations between neighboring nodes that the upstream nodes can predict the transmission patterns of downstream nodes. Specifically, after the upstream nodes successfully deliver packets to its neighboring downstream nodes, it is certain that the downstream nodes will immediately join to contend for

the medium even if their buffer status is unknown. To avoid conflict, either the upstream nodes or the downstream nodes should withhold their transmission. Taking advantage of such correlations is helpful to design more efficient and cooperative scheduling algorithms in WMNs.

2.4 Design Objectives of Scheduling in WMNs

In terms of fairness, if treating all flow identically, the MAC-layer fairness (or node fairness) implicitly indicates network-layer unfairness (or flow unfairness). Node-level scheduling is required to achieve both node-level and flow-level fairness. That is why we study the scheduling problem of WMNs in two levels, the *system level* and the *node level*.

Packet scheduling can be location-dependent and is not necessarily distributed in the entire network. For example, in sensor networks, because the observer is more powerful in terms of signal processing capabilities, memory, and energy supply, a complex scheduling scheme is feasible in the proximity to the observer. Therefore, in contrast to general WMNs, the critical area of sensor networks can employ centralized scheduling algorithms, which are more energy-efficient [58] since most decisions can be made by the observer. Besides, with central control, collisions can be avoided and retransmission energy will be saved. On the other hand, in the non-critical area that is composed of multihop paths, simple distributed MAC schemes are required. In summary, a hybrid scheduling principle is more desirable for heterogeneous WMNs.

Besides, in the non-critical area, node competition is not severe and the impact of interference is light. Then the noise power is dominant in terms of SNIR (Signal-to-Noise and Interference Ratio) and the SNIR is reduced to SNR. Hence

the non-critical area can also be called *noise-limited area*. Correspondingly, in the critical area, the interference power is dominant and the SNIR is reduced to SIR. The critical area can thus be called *interference-limited area*. Efficient scheduling can allocate transmissions in an intelligent way to mitigate interference.

Routing and scheduling are interdependent. So the node-level scheduler needs to take into account the overhead generated by routing, *i.e.*, infrastructure data. It may be necessary for the scheduler to assign different priorities to infrastructure data and application data to support real-time updates of the routing information. Furthermore, giving higher weight to application data packets with a shorter path length reduces the average delay significantly and improves the average throughput. However, in multihop networks, simply favoring short path packets, *i.e.*, giving high priority to locally generated packets over relayed packets at the critical nodes, will make the relayed packets expire soon because they have already experienced a longer delay before arriving at this critical node.

In general, the scheduler first distinguishes infrastructure data from application data. Then, application data are dealt with based on both their QoS requirements and "distances" to the destination. In this sense, the scheduler needs to know certain routing information, *e.g.*, the remaining distance of a packet to its destination. A simple scheduler is a weighted scheduler as described in [27], in which the weight is determined by the remaining distance. The fewer hops a packet needs to traverse, the more potential it has to reach its destination quickly, and the smaller queueing delay it incurs in the network. The principle behind this shortest remaining processing time (SRPT) scheduling algorithm is to minimize the mean response time. For WMNs, as mentioned before, this approach may increase the packet loss rate. If applications require both accuracy and small la-

tency, then, more balanced schemes are needed to guarantee both delay and packet loss rate. Therefore, the design of MAC and scheduling should be tightly coupled with physical layer, routing and other protocols to achieve optimal performance.

CHAPTER 3

A DELAY-BALANCING PRIORITY SCHEDULING ALGORITHM IN WIRELESS SENSOR NETWORKS (WSN)s

In sensor networks, packet scheduling is most desired in the critical area, which has to carry all the traffic generated in the network and becomes a bottleneck. When the traffic load at a critical node exceeds the transmission capability of the link (at least temporarily), queueing is unavoidable. In order to provide delay guarantees for delay-sensitive applications in multihop communications, we first consider a delay-balancing packet scheduling algorithm.

As mentioned in Section 2.4, scheduling in the critical area can be centralized. Assume there is a powerful BS (*e.g.*, the observer in Fig. 1.4). To better design scheduling algorithms, first of all, we need to know the request of the observer. Two scenarios are investigated. First, all data sensed at the same time are of the same importance, in which case the algorithms are expected to uniformly balance the delay such that all these data can reach the destination with approximately the same delay. Since the packets with a long path usually experience a longer delay than packets with a short path and all packets have the same destination, delay-balancing is achieved by giving high priority to relayed packets. Second, new data are preferred. Then, the scheduling algorithms need to cooperate with the routing protocols such that both the transmission path (routing) and transmission order (scheduling) are adapted to favor the newer data. Since the locally generated

packets are usually newer than the relayed packets, high priority will be given to local packets. In both scenarios, stale data should be discarded to empty buffer space and reduce queueing. Then, delay and packet loss probability are the primary concerns. Both scenarios can be implemented through priority scheduling.

In the first scenario, *i.e.*, to uniformly balance the delay among all packets, the scheduling algorithm is in essence delay balancing. Without priority scheduling, the more distant the node from the destination, the longer the delay its packets experience. To balance delays, the scheduler cleverly favors the relayed packets over the local packets. In contrast, in the second scenario, the locally generated packets have a short path and experience short delay. Then the scheduler favors them over the relayed packets for better average delay and throughput.

The performance of wireline priority scheduling algorithms has been well analyzed [28, 37]. However, in the wireless environment, due to unavoidable channel errors, the resulting priority queueing system should be analyzed with a service model that captures the fragility of the wireless channel. In [141], we proposed and analyzed a wireless priority queueing system for Rayleigh fading channels.

3.1 System Model

We consider a wireless link subject to bursty errors with time divided into equal-sized slots. A two-state Markov chain, given in (1.10), is used to model such a wireless channel. Channel state transitions and packet arrivals occur at the end and the beginning of each slot, respectively. The arrival process is independent of the transmission errors.

In a slot, at most one packet can be transmitted, and each transmission may fail because of channel errors. The feedback is assumed to be error-free such that the

transmitter knows whether the transmission is successful before the next time slot and then determines to transmit the new packet or retransmit the failed packet. The failed packets will be discarded based on the specified dropping strategy.

For simplicity, we first study a two-queue priority system to deal with two priorities, a high priority (HP) queue and a low priority (LP) queue. Each priority queue contains one or several flows of the same priority. In sensor networks, this system is adequate to distinguish relayed traffic from local traffic. In a multimedia system, it can distinguish guaranteed traffic from best-effort served traffic and provide differentiated service. For delay-balancing scheduling, HP is assigned to relayed traffic, which is aggregated from all upstream nodes. Without loss of generality, we assume that the HP arrival process has a much higher average rate than the LP arrival process.

Considering a Bernoulli arrival process of rate λ_i, *i.e.*, at each time slot, flow i has a packet arriving with probability λ_i ($i = 1, 2$ for HP and LP, respectively). We assume $\lambda_1 \gg \lambda_2$. The HP packets are transmitted immediately if the HP queue is not empty, whereas the LP packets have to wait until the HP queue becomes empty. The single queue complies with FIFO.

3.2 Decomposition Approach

The non-preemptive priority scheduling exhibits a property that the HP queue is exclusively served and independent of the LP queue, while the LP queue is served only when the HP queue does not need to occupy the channel. The wired and continuous counterpart of our wireless priority queueing system is given in [32] using fluid flow models. Following a similar principle, we decouple the two-queue system into two single-queue systems to simplify the analysis.

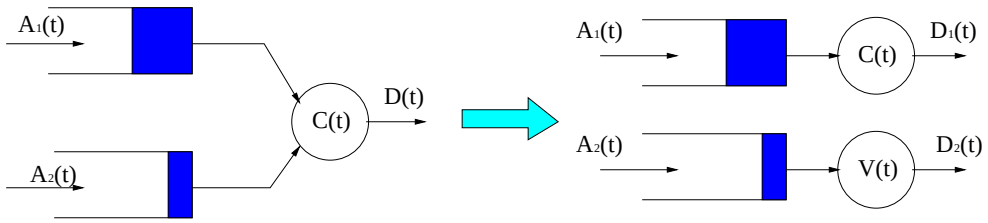

Figure 3.1. Decomposition of a two-queue system into two single-queue systems

In Fig. 3.1, the arrival process of each queue is denoted by $A_i(t)$. The channel error process $C(t)$ is modulated by a two-state Markov chain, *i.e.*, $C(t) \in \{0, 1\}$ and the transitions between 0 and 1 follow the transition matrix in (1.10). Two queues share this channel according to priority scheduling. After decomposition, each queue is served by an individual server with the channel error process $C_1(t)$ and $C_2(t)$, respectively. The output process $D(t)$ is an addition of two individual output processes $D_1(t)$ and $D_2(t)$.

Since the HP queue is exclusively served by the channel, as if no LP queue existed, its service rate process $C_1(t)$ is exactly the channel error process $C(t)$. The LP queue is in fact served by the remaining service, expressed as $C_2(t) = C(t) - D_1(t)$. The state space of the output processes $D(t)$ and $D_i(t)$ is $\{0, 1\}$, in which 1 represents a packet departure event, and 0 otherwise. To guarantee a state space $\{0, 1\}$ for $C_2(t)$, we have

$$C_2(t) = (C(t) - D_1(t)) \bmod 2 = C(t) + D_1(t). \tag{3.1}$$

Note that $C(t)D_1(t) \equiv 0$, because it is impossible that a packet departs the system as the channel is bad. Fig. 3.2 shows a sample path of each process. $C_2(t) = 0$ if $C(t) = 0$ and $D_1(t) = 0$, *i.e.*, the channel is good and no HP packet is waiting

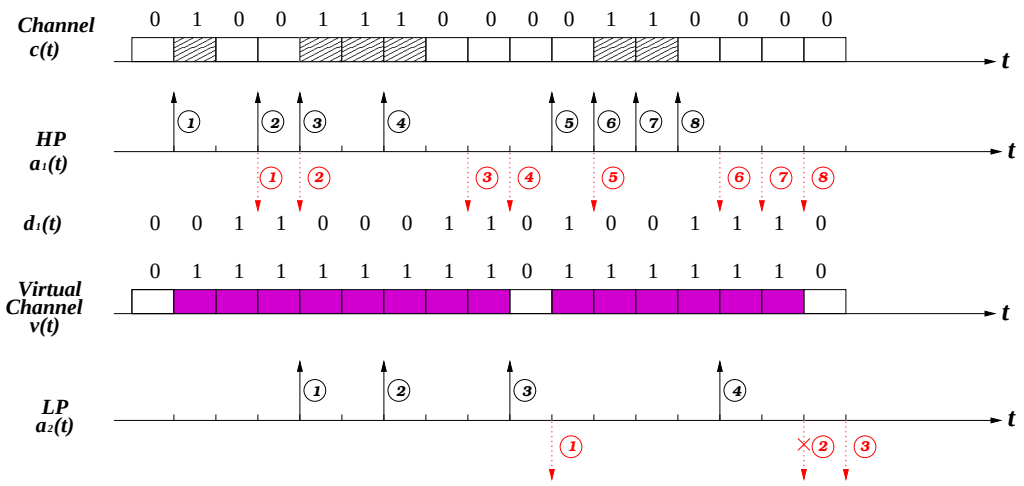

Figure 3.2. Sample path of the two-priority system

for service. Then the LP packets will be transmitted successfully. Similarly, as $C_2(t) = 1$, either the channel is bad, or the HP queue is not empty, then the LP packet transmission is either failed or blocked. In any case, no successful LP packet transmission occurs. Therefore, the LP is served as if there is a virtual channel with service process $C_2(t)$. As long as $C_2(t)$ is determined, the HP and LP queue can be analyzed as two independent queues.

3.3 A Single Wireless Queue with a Bounded Delay Strategy

Reliable data communication can be provided either by increasing the transmit power or reducing the transmission rate. There are two error control models in wireless networks, *Forward Error Correction (FEC)* and *Automatic Repeat request (ARQ)*. FEC requires greater decoding complexity and reduced effective transmission rate to build in error correction capabilities, while ARQ introduces additional retransmission energy cost. Combining ARQ and FEC is a way to achieve energy efficiency. There are hybrid ARQ schemes too. But they are

beyond the scope of this thesis. For a tractable analysis, we consider ARQ in this section.

100% reliability is provided by retransmitting the failed packets until they are successfully received, which, however, may cause long delay, especially in multihop networks. A simple approach to improve packet delays is to drop packets with long delay or when the buffer is full. In [156], three dropping strategies are presented:

- *Finite Buffer (FB)* that drops the newly arriving packet if the buffer is full. This strategy is applied to the system with a finite buffer of size B.
- *Limited Attempts (LA)* that drops the packets, which has experienced L unsuccessful attempts. The system can have an infinite queue.
- *Bounded Delay (BD)* that drops the packets of delay more than D_B. The system can an infinite buffer.

Considering the delay-sensitive property of sensor network applications, we use the BD model to drop packets. A two-dimensional Markov chain has been proposed in [68] to describe the BD dropping system. The state space $\{(i,j)| -\infty < i \leq D, \quad j = 0,1\}$ contains two components. The first entry i keeps track of the delay of the packet at the head of the line, and the second models the channel error process. When $i < 0$ (negative delay), the queue is empty and $|i|$ represents the remaining time before a new packet arrives at the empty queue.

In the HP system, let $X(n)$ denote the system state at time t and $D_{B,1}$ the

HP delay bound. Define $P_{(i,j),(k,l)}$ as the one-step system transition probability

$$
\begin{aligned}
P_{(i,j),(k,l)} &= \Pr\{X(t+1)=(k,l) \quad | \quad X(t)=(i,j)\} \\
&= \begin{cases}
c_{jl} & i<0,\ k=i+1 \\
a_1^{i-k+1}c_{0l} & 0\le i\le D_{B,1},\ k\le i,\ j=0 \\
c_{1l} & 0\le i<D_{B,1}, k=i+1,\ j=1 \\
a_1^{D_{B,1}-k+1}c_{1l} & i=D_{B,1},\ k\le D_{B,1},\ j=1 \\
0 & \text{otherwise,}
\end{cases}
\end{aligned} \tag{3.2}
$$

where c_{ij} is the transition probability of the channel error process given by (1.10) and

$$
a_1^t := \lambda_1(1-\lambda_1)^{t-1} \quad ; \quad (\text{ note that } \quad \sum_{t=1}^{\infty} a_1^t = 1\ ). \tag{3.3}
$$

The resulting Markov chain is of infinite length. The steady-state probabilities $\pi(i,j)$, solved by using the balance equations of the Markov chain, are

$$
\pi(i,j) = \begin{cases}
\frac{c_{10}}{\omega}x^{D_{B,1}-i}\pi(D_{B,1},1) & i>0,\ j=0 \\
(1-\lambda_1)^{D_{B,1}-i}\Big[1+\frac{c_{10}(1-\omega)^{D_{B,1}-i}}{(1-\omega)\omega^{D_{B,1}-i}}\Big]\pi(D_{B,1},1) & i\ge 0,\ j=1 \\
\frac{c_{10}}{c_{01}}x^{D_{B,1}}\pi(D_{B,1},1) & i=0,\ j=0 \\
(1-\lambda_1)^{-i}\frac{c_{10}}{c_{01}}x^{D_{B,1}}\pi(D_{B,1},1) & i<0,\ j=0 \\
(1-\lambda_1)^{D_{B,1}-i}(1+c_{10}\omega_{D_{B,1}})\pi(D_{B,1},1) & i<0,\ j=1,
\end{cases} \tag{3.4}
$$

where

$$\begin{cases} \omega & = & 1-\lambda_1(1-c_{01})-c_{10}(1-\lambda_1) \\ x & = & \dfrac{1-\lambda_1}{\omega} \\ \omega_{D_{B,1}} & = & \dfrac{1-\omega^{D_{B,1}}}{\omega^{D_{B,1}}(1-\omega)}. \end{cases}$$

Note that the first three expressions in (3.4) have been derived in [68], and the last two equations are obtained after we apply the condition of *infinite interarrival time* ($A_1 = \infty$) to $\{\pi(i,j) \mid i < 0\}$.

The dropping probability $\pi(D_{B,1}, 1)$ is calculated by using

$$\sum_{i=-\infty}^{D_{B,1}} \sum_{j=0}^{1} \pi(i,j) = 1 \quad ; \quad \text{therefore} \quad \pi(D_{B,1}, 1) = \frac{1}{k_{sum}}, \tag{3.5}$$

where

$$\begin{aligned} k_{sum} = {} & \frac{c_{10}x^{D_{B,1}}}{c_{01}\lambda_1} + (1 + c_{10}\omega_{D_{B,1}})\frac{(1-\lambda_1)^{D_{B,1}+1}}{\lambda_1} + \frac{\left[1-(1-\lambda_1)^{D_{B,1}+1}\right](1-\omega-c_{10})}{\lambda_1(1-\omega)} \\ & + \frac{c_{10}(1-x^{D_{B,1}})}{\omega(1-x)} + \frac{c_{10}(1-x^{D_{B,1}+1})}{(1-\omega)(1-x)}. \end{aligned} \tag{3.6}$$

3.4 Characterization of the Virtual Channel Error Process $C_2(t)$

We find that as $i < 0$ ($\Leftrightarrow D_1(t) = 0$) and $j = 0$ ($\Leftrightarrow C(t) = 0$), there is no packet in the HP queue (thus no packet departure) and the channel is good, which corresponds to $C_2(t) = 0$; the remaining states correspond to $C_2(t) = 1$. Since the virtual channel cares only about the transition between 0 and 1, not how the HP system evolves, it is sensible to divide the HP state space into two subsets $\mathcal{I}$ and $\mathcal{B}$, defined as $\mathcal{I} = \{(i,j) \mid i < 0 \text{ and } j = 0\}$, $\mathcal{B} = \mathcal{I}^C$. The subset $\mathcal{I}$ and $\mathcal{B}$ correspond to 0 and 1 of $C_2(t)$, respectively. Now, we compute the transition probabilities between these two subsets. (Note that we use $\sim$, as in $\tilde{c}_{10}$ and $\tilde{\varepsilon}$, to

denote the parameters associated with the virtual channel error process $C_2(t)$).

$$\begin{aligned}\tilde{c}_{01} = \Pr\{X(t+1) \in \mathcal{B} | X(t) \in \mathcal{I}\} &= \frac{\Pr\{X(n+1) \in \mathcal{B}, X(n) \in \mathcal{I}\}}{\Pr\{X(n) \in \mathcal{I}\}} \\ &= \frac{\sum_{i<0} \pi(i,0) \Big(\sum_{k=-\infty}^{D_{B,1}} P_{(i,0),(k,1)} + \sum_{k=0}^{D_{B,1}} P_{(i,0),(k,0)} \Big)}{\sum_{i<0} \pi(i,0)} \\ &= c_{01} + \frac{\pi(-1,0)}{\sum_{i<0} \pi(i,0)} (1 - c_{01}) = c_{01} + \lambda_1 (1 - c_{01}); \end{aligned} \tag{3.7}$$

$$\begin{aligned}\tilde{c}_{10} = \Pr\{X(t+1) \in \mathcal{I} | X(t) \in \mathcal{B}\} &= \frac{\Pr\{X(n+1) \in \mathcal{I}, X(n) \in \mathcal{B}\}}{\Pr\{X(n) \in \mathcal{B}\}} \\ &= \frac{\sum_{i=-\infty}^{D_{B,1}} \sum_{k<0} \pi(i,1) P_{(i,1),(k,0)} + \sum_{i=0}^{D_{B,1}} \sum_{k<0} \pi(i,0) P_{(i,0),(k,0)}}{\sum_{i=-\infty}^{D_{B,1}} \pi(i,1) + \sum_{i=0}^{D_{B,1}} \pi(i,0)} = \frac{k_{10}}{k_1}, \end{aligned} \tag{3.8}$$

where

$$k_{10} = c_{10}(1-\lambda_1)^{D_{B,1}+1} \Big[(1 - c_{01} - c_{10}) \omega_{D_{B,1}} + \frac{1 + c_{10}\omega_{D_{B,1}}}{\lambda_1} + \frac{1 - c_{01}}{c_{01}\omega^{D_{B,1}}} \Big] \pi(D_{B,1}, 1)$$

$$k_1 = 1 - \frac{c_{10}}{c_{01}} \frac{1-\lambda_1}{\lambda_1} x^{D_{B,1}} \pi(D_{B,1}, 1).$$

$\tilde{c}_{01}$ in (3.7) is consistent with our intuition. There is a transition from $C_2 = 0$ to $C_2 = 1$ if either the channel becomes bad (*i.e.*, $j : 0 \to 1$ with probability c_{01}) or a packet arrives but the channel remains good (*i.e.*, $i : -1 \to 0, j = 0$ with probability $\lambda_1 c_{00}$).

Furthermore, the average error rate $\tilde{\varepsilon}$ is obtained in a straightforward way:

$$\begin{aligned}\tilde{\varepsilon} &= \frac{\tilde{c}_{01}}{\tilde{c}_{01}+\tilde{c}_{10}} = 1 - \frac{c_{10}}{p_{01}}\frac{1-\lambda_1}{\lambda_1}x^{D_{B,1}}\pi(D_{B,1},1) \\ &= \sum_{i=0}^{D_{B,1}}\pi(i,0) + \sum_{i=-\infty}^{D_{B,1}}\pi(i,1) = \Pr\{X \in \mathcal{B}\}. \end{aligned} \tag{3.9}$$

The computed error rate $\tilde{\varepsilon}$ is identical to the sum probability of all bad states in $\mathcal{B}$, which proves that our approach of state aggregation is reasonable. In summary, we aggregate all the good states of the HP queueing system into one state 0 of the virtual channel error process $C_2(t)$ and all the bad states into 1. Thus we have another two-state Markov model $\{\tilde{c}_{ij}|i,j=0,1\}$ for $C_2(t)$.

3.5 The Two-Queue Priority System

In Section 3.2, the two-priority queueing system is decomposed into two single-queue systems whose channel processes are $C(t)$ and $C_2(t)$, which can be modulated by two-state Markov chains with transition probabilities $\{c_{ij} \mid i,j=0,1\}$ and $\{\tilde{c}_{ij} \mid i,j=0,1\}$, respectively. Each class has its own delay bound $D_{B,k}$ $(k=1,2)$. A reasonable assumption is that $D_{B,2} > D_{B,1}$ because the locally generated packets can tolerate a longer delay than the relayed packets if they have the same e2e delay constraint.

Naturally, the packet delay $d_j^{(k)}$ and packet loss probability $p_L^{(k)}$ for queue k are calculated as in the single-queue system (given in [68]):

$$d_j^{(k)} = \frac{\pi^{(k)}(j,0)}{\sum_{i=0}^{D_k}\pi^{(k)}(i,0)} \quad \text{and} \quad p_L^{(k)} = \frac{\pi^{(k)}(D_k,1)}{\lambda_k}, \tag{3.10}$$

where $\pi^{(1)}(i,j) = \pi(i,j)$ in (3.4), and $\pi^{(2)}(i,j)$ is calculated in the same way as in (3.4), but with different parameters λ_2 and $\{\tilde{c}_{ij}|i,j=0,1\}$ given by (3.7) and (3.8).

With this decomposed system, it is not difficult to approximate the output process $D(t)$. The arrival processes are Bernoulli. However, due to the correlations in the channel errors and the two queues, the output process does not preserve the memoryless property. For the e2e analysis, it is desired that the output process has the same probabilistic properties as the input process. A natural idea is to introduce some approximations and make the output process memoryless. The key in the Bernoulli process is the probability λ of an event occurring. In terms of the output process, the desired probability is the average departure probability.

As pointed out before, the output process $D(t)$ is the sum of two individual processes $D_1(t)$ and $D_2(t)$. Denote the departure probability of queue k by $p_d^{(k)}$. By means of the decomposition principle, the overall departure probability is:

$$p_d = p_d^{(1)} + p_d^{(2)}(1-\tilde{\varepsilon}). \tag{3.11}$$

Similar to the calculation of $\tilde{\varepsilon}$, $p_d^{(k)}$ can be calculated by dividing the system space into two subsets. For instance, in the HP system, a packet departs when $i \geq 0$ and $j = 0$. Consequently, we denote the subset $\mathcal{D} = \{(i,j) \mid i \geq 0 \text{ and } j = 0\}$ as the set of all states in which a packet departure occurs, and $\mathcal{N} = \mathcal{D}^C$ is the set of remaining states. Therefore, the departure probability for the HP queue is given by the equation

$$p_d^{(1)} \;=\; \Pr\{X \in \mathcal{D}\} \;=\; \sum_{i=0}^{D_{B,1}} \pi(i,0) \;=\; \frac{c_{10}}{c_{01}} x^{D_{B,1}} \big(1 + \frac{c_{01}}{\omega} \frac{1-x^{D_{B,1}}}{1-x}\big) \pi(D_{B,1},1). \tag{3.12}$$

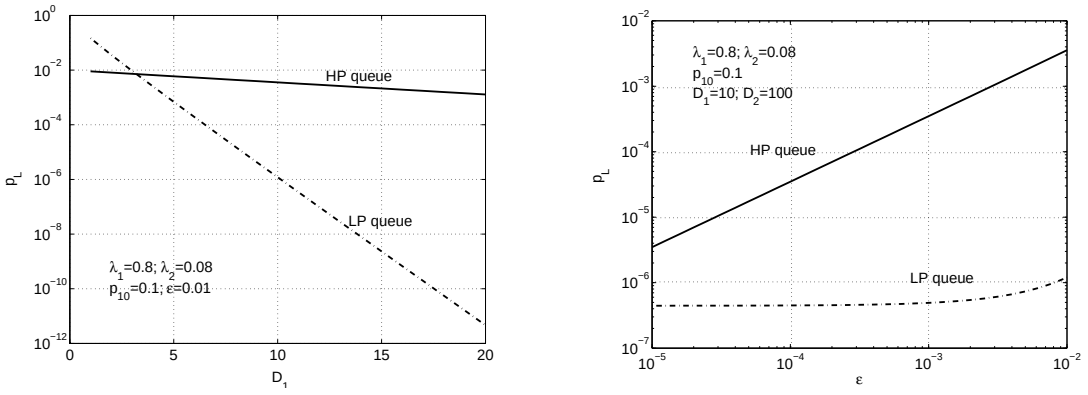

(a) Impact of $D_{B,1}$

(b) Impact of channel error rate ε

Figure 3.3. Packet loss rate p_L in a two-queue priority system

$p_d^{(2)}$ can be computed the same way as $p_d^{(1)}$.

3.6 Numerical Results

In this section, we present some example results obtained based on the analysis described above. Since the focus is on the critical nodes, the exported traffic load λ_1 is assumed to be heavy, and $\lambda_2 \ll \lambda_1$. As mentioned in Section 3.5, $D_{B,2} > D_{B,1}$. Specifically, we set $D_{B,2} = 10D_{B,1}$.

We first display the impact of the delay bound on the packet loss probability. The arrival rates are $\lambda_1 = 0.8$ and $\lambda_2 = 0.08$, respectively; the mean burst error length is $\frac{1}{c_{10}} = 10$, and the average error rate $\varepsilon = 10^{-2}$. This setting implies a heavy traffic load and highly correlated errors, which is the worst case system. Fig. 3.3(a) exhibits the dropping probabilities p_L of the two queues. Besides the part where the delay bound is very small ($D_{B,1} \leq 4$ which is not practical — in fact, we usually have $D_{B,1} \geq 10$), the packet loss probability of the local traffic is

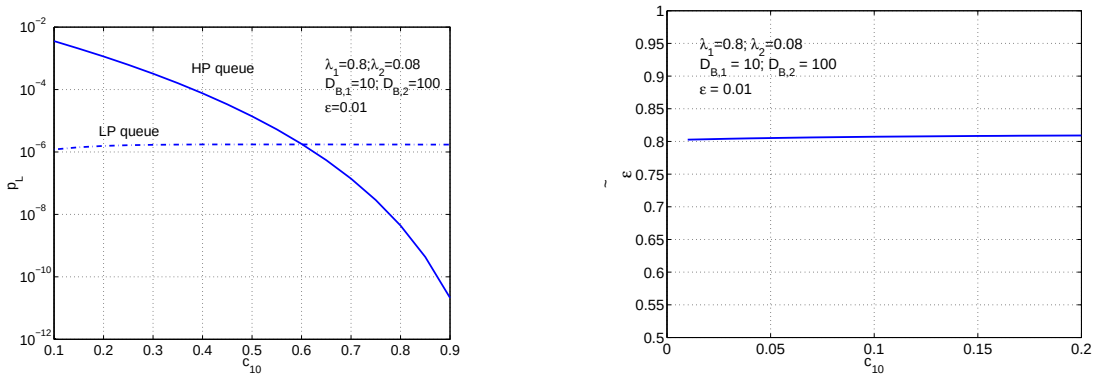

(a) Packet loss probability *vs.* channel transition probability c_{10}

(b) Error rate of the virtual channel *vs.* channel transition probability c_{10}

Figure 3.4. The impact of the channel transition probability c_{10}

much smaller than that of the relayed traffic (can be ignored when $D_{B,1} \geq 20$). This is consistent with our expectation. Even though the relayed traffic exclusively occupies the channel, most local packets are still sent out successfully, with a fairly small loss. Therefore, the delay-balancing scheme improves the delay of the long-path packets at a small price on the short-path packets. Moreover, as proved by [68], the packet loss probability (log scale) is linear in the delay bound.

Next, we investigate the impact of the channel. First consider the channel error rate ε. The delay bounds are fixed at $D_{B,1} = 10$ and $D_{B,2} = 100$, and other parameters remain unchanged. Fig. 3.3(b) displays the two queues' packet loss probability versus the channel error rate ε. The HP queue is like a single queue with a server $C(t)$, and its $p_L^{(1)}$ (log scale) is near-linear to $\log(\varepsilon)$ (which is identical to the result of [68]). On the other hand, for LP packets, when ε is small ($< 10^{-3}$), the packet loss probability is almost independent of ε. Even as ε increases (to 10^{-2}), the change of $p_L^{(2)}$ is still very small.

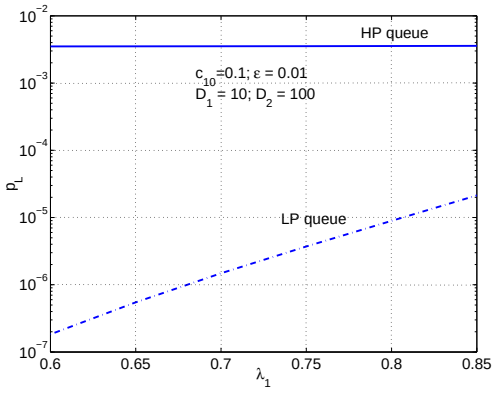

(a) Packet loss probability *vs.* arrival rate λ with $\lambda_1 + \lambda_2 = 0.9$

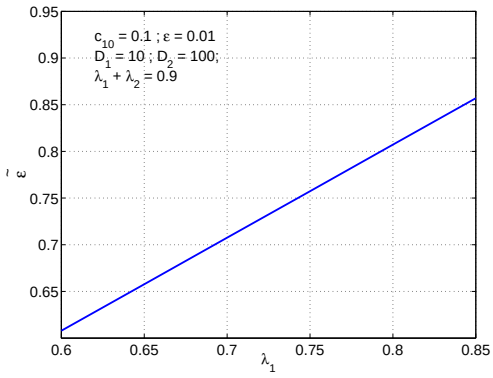

(b) Error rate of the virtual channel $\tilde{\varepsilon}$ *vs.* arrival rate λ

Figure 3.5. The impact of the HP flow's arrival rate λ_1

c_{10} is another channel parameter considered. Fig. 3.4(a) shows that, like ε, c_{10} does not play a significant role in $p_L^{(2)}$. Fig. 3.4(b) shows how the error rate $\tilde{\varepsilon}$ of the virtual channel changes with c_{10}. No apparent change in $\tilde{\varepsilon}$ happens when the channel error correlation decreases (c_{10} increases). That explains why $p_L^{(2)}$ does not greatly change with c_{10}.

Fig. 3.5(a) and Fig. 3.5(b) show the influence of the arrival rates λ_i given that $\lambda_1 + \lambda_2 = 0.9$. The virtual channel error rate $\tilde{\varepsilon}$ linearly increases with λ_1, which results in the increase of the LP queue's packet loss probability $p_L^{(2)}$ (Fig. 3.5(a)).

In summary, the LP queue's performance is determined by the virtual channel, which, in turn, is a combination of the HP queue and the real channel. Our numerical results show that the HP flow is more important for the LP queue than the channel $C(t)$. This is reasonable, since the channel is good on average (given the assumption of small error rate ε), and the bad period of the virtual channel is highly possibly caused by the arrival of HP packets. Therefore, small changes in

the arrival rate of the HP flow will lead to a bigger improvement of the LP packet loss probability, compared to the channel statistics.

3.7 Conclusions

A priority algorithm with BD dropping can provide balanced delay guarantees for sensor networks. We use a decomposition approach to solve the queueing problems in such a priority queueing system, in which the channel errors are correlated. The numerical results show that when the wireless channel is not bad on average (small error rate), which is reasonable in practice, the queueing performance of flows with low priorities is mainly determined by that of the high priorities, rather than the channel itself. Moreover, if the delay bounds are chosen appropriately (*e.g.* $D_{B,2} = 10D_{B,1}$) and the LP traffic load is light, the loss rate in the LP packets is small. This decomposition approach can be easily generalized to a k-priority system ($k > 2$) in an iterative way by constructing a virtual channel for each lower priority class i ($i > 1$).

CHAPTER 4

QUEUEING ANALYSIS OF TDMA AT A SINGLE NODE

One challenge for the design of MAC schemes in WMNs is spatial reuse. A simple but effective scheme is spatial TDMA [23] in which a node is served only once in m time slots but nodes m hops away can transmit simultaneously in line networks. Such TDMA systems look very simple but their delay performance is difficult to statistically analyze even at a single node because of the involvement of both MAC and packet queueing. From the perspective of discrete-time queueing theory, the TDMA system at a single node can be modeled a G/G/1 systems with non-integer interarrival time. Specifically, denote m time slots as one frame. Service is available at the frame boundaries but packet arrivals may happen at every time slot. So interarrival times are non-integers. Consider deterministic packet arrivals, *i.e.*, CBR traffic. For tractable analysis, the wireless channel errors are assumed to be independent and the system is reduced to D/Geom/1 [145]. Conventional G/Geom/1 systems with integer interarrival times have been studied extensively [24, 55]. However, the system with non-integer interarrival times, to the best of our knowledge, has not been investigated.

4.1 System Model

Assume the outage rate of the wireless channel is $\varepsilon = 1 - \mu \leq 1$, where ε can be obtained from (1.11) even if the channel is modeled as a two-state Markov

chain. Then the served packet will depart the node with probability μ and stay with probability ε. The overall service time is geometric with μ. The unit time is denoted as a frame of m slots. The arrival process is deterministic with a constant interarrival time of r slots. In terms of frames, the interarrival time is $r/m > 1$. Both m and r are integers, and $m/r < \mu$ for stability. The system is modeled as a D/Geom/1 with an irreducible fractional rational interarrival time of r/m. Define $\Delta \triangleq r - m$ as the arrival silence time and $\delta = \Delta/m$ as the relative arrival silence time. If $\delta < 1$, the server cannot be idle for more than one frame, the average arrival rate is $m/r = 1/(1+\delta) > 0.5$ and traffic is said to be heavy.

Fig. 4.1(a) illustrates such a TDMA system with $m = 3, r = 4$. Obviously, the packet arrival pattern is repeated in every r frames, which is denoted as "cycle" in the figure. The number of arrivals in one frame depends on the arrival pattern of all previous $r-1$ frames and is shown in Fig. 4.1(b), where $i(j)$ $(i \leq 1, |j| < r)$ indicates that i packets arrive during the current frame, and the next packet will arrive in the $|j|$th slot of the next frame. Since $r > m$, $i \leq 1$. The transition of j is: (i) if $|j| \geq m$, then $|j| \xrightarrow{1} |j| - m$; (ii) if $|j| < m$, then $|j| \xrightarrow{1} |j| + \Delta$. This arrival pattern cannot be characterized by a random process, but its repetitive property can be used to keep track of the system evolution.

The system states at the beginning of frame t are represented by a two-dimensional Markov chain $\{Q(t), Y(t)\}$, where $Q(t) \geq 0$ is the queue length and $Y(t) = 1, 2, \ldots, r$ is the number of *slots* to the next packet arrival. The arrival process is characterized by $A(t)$, the number of arrivals *during* frame t. Naturally, if $1 \leq Y(t) \leq m$, a packet will arrive during frame t and $A(t) = 1$. Otherwise, no packet arrives and $A(t) = 0$. Then, we can divide $\{1, 2, \ldots, r\}$ into two subsets $\mathbb{Y}_1 = \{1, 2, \ldots, m\}$ and $\mathbb{Y}_0 = \{m+1, \ldots, r\}$. Assume that the service starts at

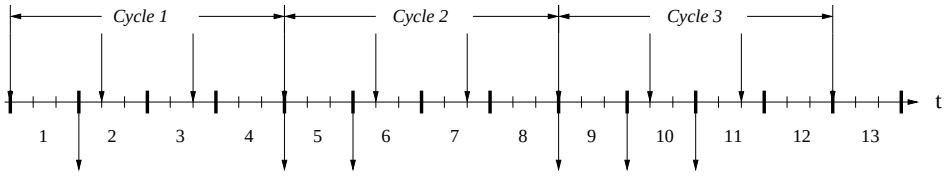

(a) Packet arrivals and departures represented by the downward arrows. The frames are delimited by the bold line and indexed by numbers. The slots are delimited by the thin lines. Packet departures occur at the frame boundaries while packet arrivals can occur during the frames. System states transit at the frame boundaries. The arrival pattern is repeated after one cycle of r frames.

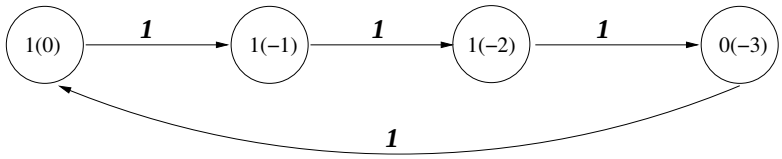

(b) Arrival pattern in one cycle. Denote the number of arrivals in one frame by $i(j)$, where $i \geq 0$ indicates the number of packet arrivals in one frame while $j < 0$ and $|j|$ is the number of slots till the next packet arrival.

Figure 4.1. D/Geom/1 queueing systems with non-integer interarrivals $(m = 3, r = 4)$

the beginning of a frame. So, system states transit at the frame boundaries,

$$Q(t+1) = (Q(t) + A(t) - S(t))^+, \quad Y(t+1) = \begin{cases} Y(t) + \Delta, \ A(t) = 1 \\ Y(t) - m, \ A(t) = 0, \end{cases} \tag{4.1}$$

where the service process $S(t) = 1$ with probability μ and $S(t) = 0$ with probability $1 - \mu$. Note that if $A(t) = 1$, $Y(t+1) \in \{\Delta + 1, \ldots, r\} \triangleq \mathbb{Y}_1'$, and if $A(t) = 0$, $Y(t+1) \in \{1, \ldots, \Delta\} \triangleq \mathbb{Y}_0'$. Both $\mathbb{Y}_1$ and $\mathbb{Y}_1'$ indicates the occurrence of an arrival event. The difference is in the former, this event occurs *during* a frame while in the latter, the event has occurred *prior to* the beginning of a frame.

Denote the steady-state system probability by $Q(n, y) := \lim_{t \to \infty} \Pr\{Q(t) = n, Y(t) = y\}$. The equilibrium state transitions are as follows

$$\begin{aligned} y \in \mathbb{Y}_0' : Q(n,y) &= \begin{cases} (1-\mu)Q(n, y+m) + \mu Q(n+1, y+m) & n > 0 \\ Q(0, y+m) + \mu Q(1, y+m) & n = 0 \end{cases} \\ y \in \mathbb{Y}_1' : Q(n,y) &= \begin{cases} (1-\mu)Q(n-1, y-\Delta) + \mu Q(n, y-\Delta) & n > 1 \\ Q(0, y-\Delta) + \mu Q(1, y-\Delta) & n = 1 \end{cases} \end{aligned} \tag{4.2}$$

Note that if $Y(t+1) \in \mathbb{Y}_1'$ (or $A(t) = 1$), a new packet has arrived but is not served yet at the beginning of frame $t + 1$. Then $Q(t + 1) > 0$. Therefore, $Q(0, y) = 0$ for $y \in \mathbb{Y}_1'$. Once the probabilities $Q(n, y)$ are known, various performance measures of interest can be obtained straightforwardly. We first use the probability generating function (pgf) of $Q(n, y)$ to obtain the system idle and busy probability, then solve $Q(n, y)$ with an eigenvalue approach.

4.2 Probability Generating Functions (pgf)

The queue length probability distribution is

$$\pi_n = \sum_{y=1}^{r} Q(n, y). \tag{4.3}$$

Define the pgf of $Q(n, y)$ and π_n as follows

$$\begin{aligned}
Q_n(z) &\triangleq \sum_{y=1}^{r} Q(n, y) z^y \triangleq Q_{n,0}(z) + Q_{n,1}(z), \\
G(s, z) &\triangleq \sum_{n=0}^{\infty} \sum_{y=1}^{r} \pi(n, y) z^y s^n = \sum_{n=0}^{\infty} Q_n(z) s^n \triangleq G_0(s, z) + G_1(s, z) \\
G(s) &= \sum_{n=0}^{\infty} \pi_n s^n = G(s, 1) \triangleq G_0(s) + G_1(s),
\end{aligned}$$

where

$$Q_{n,i}(z) \triangleq \sum_{y \in \mathbb{Y}_i} Q(n, y) z^y, \quad G_i(s, z) \triangleq \sum_{n=0}^{\infty} \sum_{y \in \mathbb{Y}_i} Q(n, y) z^y, \quad i = 0, 1$$

Then, $\pi_n = Q_n(1) = Q_{n,0}(1) + Q_{n,1}(1)$. Here $Q_{n,i}(z)$ and $G_i(s, z)$ are distinguished by $\mathbb{Y}_1$ and $\mathbb{Y}_0$ to indicate the impact of the potential arrivals. Multiplying (4.2) with z^y, we obtain

$$\begin{aligned}
Q_0(z) &= \mu z^{-m} Q_{1,0}(z) + z^{-m} Q_{0,0}(z) \\
Q_1(z) &= \mu z^{-m} Q_{2,0}(z) + (1 - \mu) z^{-m} Q_{1,0}(z) + \mu z^{\Delta} Q_{1,1}(z) + z^{\Delta} Q_{0,1}(z) \\
Q_n(z) &= \mu z^{-m} Q_{n+1,0}(z) + (1 - \mu) z^{-m} Q_{n,0}(z) + \mu z^{\Delta} Q_{n,1}(z) + (1 - \mu) z^{\Delta} Q_{n-1,1}(z).
\end{aligned} \tag{4.4}$$

Then, multiplying both sides of (4.4) by s^n yields

$$G(s,z)z^m = (1-\mu+\mu s^{-1})\Big[G_0(s,z)+sz^rG_1(s,z)\Big]+\mu(1-s^{-1})\Big[Q_{0,0}(z)+sz^rQ_{0,1}(z)\Big], \tag{4.5}$$

which is followed by the pgf of π_n,

$$\begin{aligned} G(s) &= (1-\mu+\mu s^{-1})\mu^{-1}sG_1(s)+Q_{0,1}s+Q_{0,0} \\ &= G_1(s)+\frac{1-\mu}{\mu}G_1(s)s+Q_{0,1}s+Q_{0,0} \quad \Longrightarrow \\ G_0(s) &= \frac{1-\mu}{\mu}G_1(s)s+Q_{0,1}s+Q_{0,0}, \end{aligned} \tag{4.6}$$

where $Q_{n,i} = Q_{n,i}(1)$. Summing (4.4) up yields

$$\begin{aligned} \sum_{n=0}^{\infty}Q_n(z) &= z^{-m}\sum_{n=0}^{\infty}Q_{n,0}(z)+z^{\Delta}\sum_{n=0}^{\infty}Q_{n,1}(z) \\ \Longrightarrow \sum_{n=0}^{\infty}Q_{n,1}(z) &= \frac{1-z^{-m}}{z^{\Delta}-z^{-m}}\sum_{n=0}^{\infty}Q_n(z) \\ \Longrightarrow \sum_{n=0}^{\infty}Q_{n,1} &= \frac{1-z^{-m}}{z^{\Delta}-z^{-m}}\Big|_{z=1} = \frac{m}{r}, \end{aligned} \tag{4.7}$$

which confirms that the arrival rate is m/r. In terms of $\mathbb{Y}_1'$ and $\mathbb{Y}_0'$,

$$\frac{\sum_{y\in\mathbb{Y}_1'}Q(n,y)}{\sum_{y\in\mathbb{Y}_0'}Q(n,y)} \triangleq \frac{Q_{n,1}'}{Q_{n,0}'} = \frac{\mu}{1-\mu}, \quad n\geq 1. \tag{4.8}$$

Although $Q_{n,1} \neq Q_{n,1}'$, the average arrival rate m/r can be obtained in a similar way

$$\sum_{n=0}^{\infty}Q_{n,1}' = \frac{m}{r}, \tag{4.9}$$

where $Q'_{0,1} = 0$. Setting $z = 1$ in (4.4), we obtain

$$\begin{aligned} \pi_0 &= \mu Q_{1,0} + Q_{0,0} \\ (1-\mu)\pi_n &= (1-\mu)Q_{n,0} + \mu Q_{n+1,0},\ n \geq 1. \end{aligned} \tag{4.10}$$

Summing up (4.10) gives the system idle probability $\pi_0 = 1 - m/(r\mu) = 1 - \rho$, where $\rho \triangleq m/(r\mu)$ is the normalized traffic intensity at the frame level. Recall that $Q(0, y) = 0$ for $y > m$. Therefore, $Q_{0,0} = Q'_{0,0} = 0$ and $\pi_0 = Q_{0,1}$ for $\Delta < m$. From (4.10), $Q_{n,1}$ and $Q_{n+1,0}$ are related by

$$\begin{aligned} Q_{0,1} &= \mu Q_{1,0} \\ (1-\mu)Q_{n,1} &= \mu Q_{n+1,0},\ n \geq 1, \end{aligned} \tag{4.11}$$

which leads to

$$\frac{Q_{n,1}}{Q_{n+1,0}} = \frac{\mu}{1-\mu}, \quad n \geq 1. \tag{4.12}$$

Note the difference between (4.12) and (4.8). $Q_n(z)$ and $G(s)$ are mainly used to confirm $\pi_0 = 1-\rho$, which is consistent with the results of conventional D/Geom/1 systems. The probabilities $Q(n, y)$ are solved by an eigenvalue approach.

4.3 Eigenvalue Approach

Define the row vector $\boldsymbol{v}_n := \{Q(n,1), Q(n,2), \ldots, Q(n,r)\}$ $(n \geq 0)$. For $n \geq 1$, the transition equations (4.2) are of a special structure that can be rewritten as a set of balance equations in a matrix form,

$$\boldsymbol{v}_n \mathbf{M}_0 + \boldsymbol{v}_{n+1}\mathbf{M}_1 + \boldsymbol{v}_{n+2}\mathbf{M}_2 = 0, \tag{4.13}$$

where

$$\mathbf{M_0} = \begin{bmatrix} \mathbf{0}_{m\times\Delta} & (1-\mu)\mathbf{I}_m \\ \mathbf{0}_{\Delta\times\Delta} & \mathbf{0}_{\Delta\times m} \end{bmatrix},$$

$$\mathbf{M_1} = \begin{bmatrix} \mathbf{0}_{m\times\Delta} & \mu\mathbf{I}_m \\ (1-\mu)\mathbf{I}_\Delta & \mathbf{0}_{\Delta\times m} \end{bmatrix} - \mathbf{I},$$

$$\mathbf{M_2} = \begin{bmatrix} \mathbf{0}_{m\times\Delta} & \mathbf{0}_{m\times m} \\ \mu\mathbf{I}_\Delta & \mathbf{0}_{\Delta\times m} \end{bmatrix}.$$

This is a homogeneous vector difference equation of order 2 with constant coefficients. Associated with it is the characteristic matrix polynomial, $\mathbf{Q}(\lambda)$, defined as

$$\mathbf{Q}(\lambda) = \mathbf{M_0} + \mathbf{M_1}\lambda + \mathbf{M_2}\lambda^2. \tag{4.14}$$

According to [95], using the method of spectral analysis, or eigenvalue method [44, 90], $\boldsymbol{v}_n$ can be expressed in an eigenvalue/eigenvector form

$$\boldsymbol{v}_n = \mathbf{C}\boldsymbol{\Lambda}^n\boldsymbol{\Phi}, \tag{4.15}$$

where the diagonal matrix $\boldsymbol{\Lambda} = \text{diag}(\lambda_i)$ and the matrix $\boldsymbol{\Phi} = [\boldsymbol{\phi}_i]^T$ are composed of the eigenvalues $\{\lambda_i\}$ and eigenvectors $\{\boldsymbol{\phi}_i\}$ of $\mathbf{Q}(\lambda)$ in the form of $\boldsymbol{\phi}\mathbf{Q}(\lambda) = 0$, where $\boldsymbol{\phi} = \{\phi(1), \phi(2), \ldots, \phi(r)\}$. The eigenvalues are solutions to

$$\det|\mathbf{Q}(\lambda)| = -\lambda^r + \lambda^\Delta(1-\mu+\mu\lambda)^r = 0, \tag{4.16}$$

which leads to the characteristic polynomial

$$\lambda^m = (1-\mu+\mu\lambda)^r, \quad \text{or} \quad \lambda = (1-\mu+\mu\lambda)^{r/m}. \tag{4.17}$$

The eigenvalues λ can be found by setting $x = \lambda^{1/r}$ and rewriting the polynomial (4.17) as

$$f(x) = \mu x^r - x^m + 1 - \mu. \tag{4.18}$$

This polynomial has M distinct roots [90], where $M = \text{degree}\{\det[\mathbf{Q}(\lambda)]\}$ and m of which are inside the unit circle. The corresponding m eigenvalues are defined as *effective eigenvalues*. Based on Descartes' Sign Rule, among the m effective eigenvalues, there is one positive real, denoted by $\lambda_0 < 1$ and all others are either negative real or complex, denoted by $|\lambda_i| < 1$ $(i = 1, \ldots, m-1)$. In order for $\boldsymbol{v}_n$ to form a vector of probabilities, (4.15) should include only eigenvalues inside the unit circle, *i.e.*, the effective eigenvalues. Therefore, $\boldsymbol{v}_n$ is a sum of m linearly independent vectors

$$\boldsymbol{v}_n = \sum_{i=0}^{m-1} C_i \boldsymbol{\phi}_i \lambda_i^n, \quad |\lambda_i| < 1, \tag{4.19}$$

where C_i is any constant such that the sum of all $Q(n, y)$ equals to 1. Since (4.18) is a polynomial with real coefficients, the complex eigenvalues appear in conjugate pairs. To guarantee that (4.19) is real, the corresponding C_i must be paired as well.

Recall that in the conventional D/Geom/1 system with integer interarrival times [24, 31, 55], *i.e.*, $m = 1$, the queue length distribution is

$$\pi_n = \begin{cases} 1 - \rho & n = 0 \\ \rho(1-\lambda)\lambda^{n-1} & n \geq 1, \end{cases} \tag{4.20}$$

where λ is a *unique* root of $\lambda = (1 - \mu + \mu\lambda)^r$. Based on (4.17), for $m = 1$, there is only one effective eigenvalue λ_0, which is positive real. Then, $Q(n, y)$ and the resulting π_n $(n \geq 1)$ are composed of a single exponential term λ_0^n, which is

consistent with (4.20). In other words, our analysis generalizes the conventional D/Geom/1 queueing analysis to the cases $m > 1$.

The eigenvectors can be derived from the eigenvalues. Given $\mathbf{M}_0$, $\mathbf{M}_1$, and $\mathbf{M}_2$, $\boldsymbol{\phi}\mathbf{Q}(\lambda) = 0$ expands to give

$$\phi(y) = \begin{cases} (1 - \mu + \mu\lambda)\phi(y + m) & y \leq \Delta \\ \dfrac{1 - \mu + \mu\lambda}{\lambda}\phi_(y - \Delta) & y > \Delta. \end{cases} \tag{4.21}$$

Let $\beta = 1 - \mu + \mu\lambda$. From (4.17), it is trivial to obtain $\lambda^m = \beta^r$. Given the definition $x^r = \lambda$, the relationships between x, λ and β are as follows

$$x^r = \lambda, \quad x^m = \beta, \quad x^\Delta = \frac{\lambda}{\beta}. \tag{4.22}$$

Then, (4.21) leads to

$$\phi(y) = x\phi(y + 1) \quad \Longrightarrow \quad \phi(y) = x^{-(y-1)}\phi(1), \quad y \geq 1, \tag{4.23}$$

i.e., the eigenvectors can be expressed exponentially with the r-th root of the associated eigenvalues. By normalizing the eigenvectors, we obtain

$$\phi_i(1) = \frac{1 - x_i^{-1}}{1 - x_i^{-r}} = \frac{\lambda_i}{1 - \lambda_i} \cdot \frac{1 - x_i}{x_i}. \tag{4.24}$$

Then, the system steady-state probabilities $Q(n, y)$ are

$$Q(n, y) = \sum_{i=0}^{m-1} C_i \lambda_i^{n-1} \phi_i(y) = \sum_{i=0}^{m-1} \frac{C_i(1 - x_i)x_i^{-y}\lambda_i^n}{1 - \lambda_i}, \quad n \geq 1. \tag{4.25}$$

$Q(0, y)$ are calculated from $Q(1, y)$ based on (4.2).

4.4 Queue Length Distributions

Based on (4.3) and (4.25), the queue length probabilities π_n ($n \geq 1$) are

$$\pi_n = \sum_{y=1}^{r} Q(n,y) = \sum_{y=1}^{r} \sum_{i=0}^{m-1} \frac{C_i(1-x_i)x_i^{-y}\lambda_i^n}{1-\lambda_i} = \sum_{i=0}^{m-1} C_i \lambda_i^{n-1}. \tag{4.26}$$

$\pi_0 = 1-\rho$ has been shown in (4.10). Unlike conventional D/Geom/1 systems with integer interarrival times, here π_n is a sum of m exponential terms. Specially,

$$\begin{aligned} Q_{n,1} &= \sum_{y=1}^{m} Q(n,y) \quad = \mu \sum_{i=0}^{m-1} \frac{C_i \lambda_i^n}{\beta_i} \\ Q_{n,0} &= \sum_{y=m+1}^{r} Q(n,y) = (1-\mu) \sum_{i=0}^{m-1} \frac{C_i \lambda_i^{n-1}}{\beta_i}, \end{aligned} \tag{4.27}$$

which verifies $Q_{n,1}/Q_{n+1,0} = \mu/(1-\mu)$ (4.12). Let $\nu_n = Q_{n,1}/\pi_n$. Since $Q_{n,1}$ is the sum of all $Q(n,y)$ for $y \in \mathbb{Y}_1$, which indicates a packet arrival, ν_n can be regarded as the arrival rate when there are n packets in the system. From (4.27) and $|\lambda_i| < 1$,

$$\frac{\nu_n}{1-\nu_n} == \frac{\mu}{1-\mu} \cdot \frac{\sum_{i=0}^{m-1} \frac{C_i \lambda_i^n}{\beta_i}}{\sum_{i=0}^{m-1} \frac{C_i \lambda_i^{n-1}}{\beta_i}} < \frac{\mu}{1-\mu} \quad \Longrightarrow \quad \nu_n < \mu, \tag{4.28}$$

i.e., stability is guaranteed that the arrival rate ν_n is smaller than the service rate μ. Apparently, ν_n is state-dependent while the average arrival rate is $\sum_{n\geq 0} \nu_n \pi_n = m/r$. Then, (4.11) can be rewritten as a set of balance equations

$$\begin{aligned} \nu_0 \pi_0 &= \mu(1-\nu_1)\pi_1 \\ (1-\mu)\nu_n \pi_n &= \mu(1-\nu_{n+1})\pi_{n+1}, \end{aligned} \tag{4.29}$$

and the transition diagram of the queue length n can be modeled by a birth-death process with state-dependent arrival rates as shown in (Fig. 4.2). The queue length probabilities are

$$\pi_n = \frac{\pi_0}{1-\mu}\Big(\frac{1-\mu}{\mu}\Big)^n \prod_{i=0}^{n-1} \frac{\nu_i}{1-\nu_{i+1}}, \quad n \geq 1. \tag{4.30}$$

Specially, if $m = 1$, $\nu_n = \mu\lambda/(1-\mu+\mu\lambda) \equiv \nu$ becomes state-independent and the system evolution follows the birth-death process with an arrival rate ν and service rate μ (just like Geom/Geom/1).

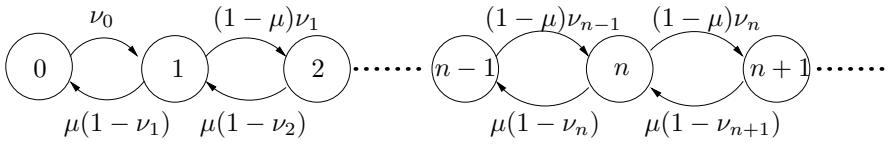

Figure 4.2. State transition diagram of the queue length in the D/Geom/1 system

4.5 Delay Distributions

4.5.1 General Analysis

If Δ is any positive integer greater than 1, the delay distribution are directly derived from the steady-state system probabilities $Q(n, y)$. In terms of slots, the packet delay D is composed of three parts, the access delay $D_A \in \{0, \ldots, m-1\}$, the queueing delay D_Q, and the service time D_S. If a packet arrives during frame

t, its access delay is $d_A = m - Y(t)$, where $Y(t) < m$. Then $Y(t+1) = Y(t) + \Delta = m - d_A + \Delta = r - d_A \in \mathbb{Y}_1'$. Note that this new arriving packet is accounted for by $Q(t+1) = n$, *i.e.*, $n-1$ packets have been buffered upon the arrival of the new packet. Given the access delay d_A, the conditional probability $Q(n|d_A)$ that the new packet sees $n-1$ packets in the system is

$$Q(n|d_A) \triangleq \frac{Q(n, r-d_A)}{\sum_{n=1}^{\infty} \sum_{y \in \mathbb{Y}_1'} \pi(n,y)} = \frac{r}{m} Q(n, r-d_A) = \frac{r}{m} \sum_{i=0}^{m-1} \frac{C_i (1-x_i) \lambda_i^{n-1} x_i^{d_A}}{1-\lambda_i}. \quad (4.31)$$

The packet queueing delay D_Q is the sum of service times D_{S_0} of the $n-1$ buffered packets. D_{S_0} is geometric with μ at the frame level. At the slot level, it is

$$\Pr\{D_{S_0} = n\} = \begin{cases} \mu(1-\mu)^{k-1}, \; n = km, & k \geq 1 \\ 0, & \text{otherwise.} \end{cases} \quad (4.32)$$

Its pgf is thus

$$G_{D_{S_0}}(z) = \sum_{k=1}^{\infty} \mu(1-\mu)^{k-1} z^{km} = \frac{\mu z^m}{1-(1-\mu)z^m}. \quad (4.33)$$

Since the service times are independent, the pgf of D_Q is $G_{D_Q}(z) = (G_{D_{S0}}(z))^{n-1}$. The service time of the packet under consideration is studied in two cases: (1) if the packet departs at the end of the frame. Then, its service time D_S has the same distribution as D_{S_0}; (2) if the packet departs at the end of the first slot of the frame (which happens in communications networks using TDMA), its service

time distribution is

$$\Pr\{D_S = n\} = \begin{cases} \mu(1-\mu)^k, \, n = km+1, \quad k \geq 0 \\ 0, \qquad\qquad \text{otherwise.} \end{cases} \tag{4.34}$$

Correspondingly, the pgf of D_S is

$$G_{D_S}(z) = \sum_{k=0}^{\infty} \mu(1-\mu)^k z^{km+1} = \frac{\mu z}{1-(1-\mu)z^m}, \tag{4.35}$$

which is different from $G_{D_{S_0}}(z)$ by a factor z^{m-1}. The subsequent analysis is focused on the second case, whose results can be extended to the first case by scaling z^{m-1}.

Since D_A, D_Q, and D_S are all independent, the pgf of the total delay $D = D_A + D_Q + D_S$ is calculated as follows,

$$\begin{aligned} G_D(z) &= \sum_{n=1}^{\infty} \sum_{d_A=0}^{m-1} G_{D_Q}(z) G_{D_S}(z) \pi(n|d_A) z^{d_A} \\ &= \sum_{n=1}^{\infty} \sum_{y_a=0}^{m-1} \Big(\frac{\mu z^m}{1-(1-\mu)z^m} \Big)^{n-1} \frac{\mu z}{1-(1-\mu)z^m} \pi(n|d_A) z^{d_A} \\ &= \frac{1}{\rho} \sum_{i=0}^{m-1} \frac{C_i(1-x_i)z}{x_i(1-\lambda_i)(1-x_i z)}. \end{aligned} \tag{4.36}$$

Apparently, $G_D(z)$ is the sum of m geometric series with parameters x_i. The zeros of $G_D(z)$ are $z = x^{-1}$. Plugging $x = z^{-1}$ into (4.18), the zeros of $G_D(z)$ are the roots of the following polynomial

$$g(z) = (1-\mu)z^r - z^{\Delta} + \mu. \tag{4.37}$$

The delay distribution follows immediately

$$\Pr\{D = n\} = \frac{1}{\rho} \sum_{i=0}^{m-1} \frac{C_i}{1-\lambda_i} \cdot (1-x_i) x_i^{n-1}, \quad n \geq 1, \tag{4.38}$$

which leads to the delay mean and variance as follows

$$\overline{D} = \frac{1}{\rho} \sum_{i=0}^{m-1} \frac{C_i x_i}{(1-\lambda_i)(1-x_i)}, \tag{4.39}$$

$$\sigma^2 = \frac{1}{\rho} \sum_{i=0}^{m-1} \frac{C_i x_i (1+x_i)}{(1-\lambda_i)(1-x_i)^2} - \left(\overline{D}\right)^2. \tag{4.40}$$

The delay distributions depend on x_i and λ_i, which are solved from the characteristic polynomial $\lambda^m = (1-\mu+\mu\lambda)^r$. If either m or r are large, x_i and λ_i are obtained only numerically.

4.5.2 Special Case $\Delta = 1$

For a special case $\Delta = 1$ or $r = m+1$, the calculation of x_i and λ_i can be avoided in the derivation of the delay distribution by using a delay model [69]. Unlike traditional queueing analysis that usually sets the queue length as the system state, in the delay model, the system state is represented by the delay of the HOL (Head of Line) packet. To be consistent with previous sections, the delay is measured in terms of slots, but state transitions occur at the frame boundaries. The transition probabilities P_{ij} are

$$P_{ij} = \begin{cases} \mu & i \geq 0, \quad j = i-1, \\ 1-\mu & i \geq 0, \quad j = i+m, \\ 1 & i = -1, \; j = m-1, \end{cases} \tag{4.41}$$

The negative state -1 implies that the buffer is empty and thus the server is idle. Besides, the remaining time prior to the next arrival is one slot. For example, in Fig. 4.1(a), at the beginning of frame 2, the last packet has departed but the next packet has not arrived yet. Hence, the system is at state -1 and will jump to state $m-1$ at frame 3 since the newly arriving packet, also the HOL packet, has already been buffered for $m-1$ slots before it is served at the beginning of frame 3. Since $r = m+1$, this arrival event occurs with probability 1.

At frame t, let the HOL packet be indexed by k and its delay be $w_k(t)$. With probability μ, packet k will depart the system (either at the end of frame t or at the end of the first slot of frame t), and packet $k+1$ (if it has arrived) will become the HOL packet at frame $t+1$. The delay of packet $k+1$ at frame t is $w_{k+1}(t) = w_k(t) - r$ and increases by m up to $w_{k+1}(t+1) = w_k(t) - r + m = w_k(t) - 1$ at frame $t+1$. In other words, the system state transits from $w_k(t)$ to $w_k(t) - \Delta$. On the other hand, with probability $1-\mu$, packet k remains in the buffer and will be retransmitted after one frame. Its delay thus increases by m to $w_k(t+1) = w_k(t) + m$.

Let the steady-state probabilities be $\{\pi_i | -1 \leq i < \infty\}$ and the probability mass function (pmf) of the delay be $\{D_n | i \geq 1\}$. Then,

$$D_n = \frac{\mu\pi_{n-1}}{\sum_{i\geq 0} \mu\pi_i} = \frac{\pi_{n-1}}{\sum_{i\geq 0} \pi_i}, \tag{4.42}$$

where $\sum_{i\geq 0} \mu\pi_i$ is the normalization constant, and μ accounts for the fact that the packet departs the system with probability μ. The pgf and mean and variance of the local delay are given in Theorem 4.5.1.

Theorem 4.5.1 *Consider a discrete-time queueing system with a geometric server*

$\mathcal{G}_\mu$ and a constant interarrival time r/m, where $r = m + 1$. Then, the pgf, mean and variance of the delay are

$$G_D(z) = \frac{1-\rho}{\rho} \cdot \frac{(1-z^m)z}{(1-\mu)z^r - z + \mu} \tag{4.43}$$

$$\overline{D} = \frac{1}{2(1-\rho)}, \tag{4.44}$$

$$\sigma^2 = \frac{1}{4(1-\rho)^2} - \frac{m+2}{6(1-\rho)}. \tag{4.45}$$

where $\rho = m/(r\mu)$ is the traffic intensity.

Proof Based on (7.1) and (4.42), we obtain the following balance equations:

$$D_n = \begin{cases} \mu D_{n+1} & 1 \le n < m \\ \mu D_{n+1} + D_0 = \mu D_{n+1} + \mu D_1 & n = m \\ \mu D_{n+1} + (1-\mu) D_{n-m} & n > m \end{cases} \tag{4.46}$$

Manipulating (4.46), we have the pgf $G_D(z)$,

$$\begin{aligned} G_D(z) &= \mu(G_D(z)z^{-1} - D_1) + \mu D_1 z^m + (1-\mu)z^m G_D(z) \\ \Longrightarrow &= \frac{(1-z^m)z\mu}{(1-\mu)z^{m+1} - z + \mu} D_1. \end{aligned} \tag{4.47}$$

The only unknown parameter D_1 can be deduced from $G_D(1) = 1$,

$$D_1 = \frac{1-(m+1)(1-\mu)}{m\mu} = \frac{r\mu - m}{m\mu}. \tag{4.48}$$

The delay mean (5.9) and variance (5.10) can be calculated through the first two derivatives of $G_D(z)$ at $z = 1$.

(4.46) is applied to any $\Delta \ge 1$. However, since $G_D(z)$ contains Δ unknown

parameters D_n $(n = 1, \ldots, \Delta)$, $G_D(z)$ is solvable only for $\Delta = 1$, in which D_1 can be obtained from $G_D(1) = 1$.

Remarks:

- For general $\Delta \geq 1$, the delay distributions (4.38) are composed of m effective eigenvalues and the other $r - m = \Delta$ eigenvalues are ignored because they are outside the unit circle. Since the characteristic polynomial (4.18) determines that one eigenvalue must be 1, $\Delta = r - m = 1$ implies that the only eigenvalue to be ignored is 1. Then, if rewriting (4.36) in a single fraction form and multiplying both denominator and numerator by $(1 - z)$, the denominator becomes $g(z)$ (4.37) and (4.36) is consistent with (5.8).

- Unlike (4.36) for general $\Delta \geq 1$, the delay pgf (5.8) is a function of (m, r, μ) and does not require the eigenvalues obtained from the characteristic polynomial (4.18). Then, the impact of the arrival rate m/r and service rate μ on the system performance can be directly investigated.

In practice, we are usually most concerned how the network or system performs under heavy traffic. The closer m to r, the heavier the traffic load. For stability, $r > m$. Then, $r = m + 1$ (or $\Delta = 1$) represents the extreme case and its study is highly relevant from the perspective of practical applications.

4.6 Output Process Characterization

The output process characterization is based on the departure event. So in this section, we consider only the steady-state system probability at the moment

when a packet departs. $Q^D(n,y)$ can be derived from $Q(n,y)$ as follows

$$\begin{aligned} y \in \mathbb{Y}_0' &: Q^D(n,y) = \mu Q(n+1, y+m),\ n \geq 0 \\ y \in \mathbb{Y}_1' &: Q^D(n,y) = \mu Q(n, y-\Delta), \qquad n \geq 1. \end{aligned}$$

Then, the queue length probability π_n^D is

$$\begin{aligned} \pi_n^D &= \frac{\sum_{y=1}^{r} Q^D(n,y)}{\sum_{n=0}^{\infty}\sum_{y=1}^{r} Q^D(n,y)} \\ &= \begin{cases} \dfrac{1}{\rho}\displaystyle\sum_{y=m+1}^{r} Q(1,y) = \frac{Q_{1,0}}{\rho} & n = 0 \\ \dfrac{1}{\rho}\displaystyle\sum_{y=1}^{m} Q(n,y) + \mu \sum_{y=m+1}^{r} Q(n+1,y) = \frac{Q_{n,1}+Q_{n+1,0}}{\rho} & n > 0 \end{cases} \end{aligned} \tag{4.49}$$

Combining with (4.11), we obtain $\pi_n^D = Q_{n,1}/(\mu\rho)$. For a special case $\Delta < m$, it is proved in Section 4.2 that $Q_{0,0} = 0$ and $Q_{0,1} = \pi_0 = 1-\rho$. Then the system idle and busy probabilities at the packet departure instant are

$$\pi_I = \pi_0^D = \frac{Q_{0,1}}{\mu\rho} = \frac{1-\rho}{\mu\rho}, \quad \pi_B = \sum_{n\geq 1}\pi_n^D = 1 - \pi_I. \tag{4.50}$$

If $\Delta > m$, then $Q_{0,0} \neq 0$ has to be calculated iteratively from $Q_{0,1}$, $Q_{1,0}$ and $Q_{1,1}$. There is no closed-form solution for π_0^D. Besides, $\Delta < m$ implies $m/r > 0.5$ and represents medium-to-heavy traffic cases, which are more interesting than light-traffic case with $\Delta > m$. So, we focus on $\Delta < m$, in which the system idle time does not exceed one frame and the interdeparture time T is

$$T = \begin{cases} 1 + D_S, & \text{with probability } \pi_I \\ D_S & \text{with probability } \pi_B, \end{cases} \tag{4.51}$$

where D_S is the service time in terms of frames and is geometric with parameter μ. The pgf of D_S is $G_{D_S}(z) = \mu z/(1-(1-\mu)z)$. Then, the pgf of T is

$$G_T(z) = (\pi_B + \pi_I z)G_{D_S}(z) = \mu\pi_B z + \sum_{i=2}^{\infty} \mu(1-\mu)^{i-2}(1-\mu\pi_B)z^i, \qquad (4.52)$$

which leads to the closed-form pmf $\{t_i | i \geq 1\}$,

$$t_n = \begin{cases} \mu\pi_B & n = 1 \\ \mu(1-\mu)^{i-2}(1-\mu\pi_B) & n > 1. \end{cases} \qquad (4.53)$$

The pmf (4.53) corresponds to a correlated on-off process [69, Eqns.(1),(2)] with transition probabilities $a_{10} = 1 - \mu\pi_B = \frac{\Delta\mu}{m}$ and $a_{01} = \mu$, respectively. The conclusion is summarized in Theorem 5.3.5.

Theorem 4.6.1 *Consider a D/Geom/1 queueing system with a geometric server of rate μ and constant interarrival time r/m ($m < r < 2m$). Then the output process is a correlated on-off process with transition matrix*

$$\mathbf{A} = \begin{bmatrix} 1-\mu & \mu \\ \\ \dfrac{\Delta\mu}{m} & 1-\dfrac{\Delta\mu}{m} \end{bmatrix}, \quad \textit{where} \quad \Delta = r - m. \qquad (4.54)$$

The conditions $r < 2m$ and $\mu > m/r$ guarantee $\pi_B < 1$. Therefore, the smooth arrival process with constant interarrival times is transformed to bursty on-off traffic in the D/Geom/1 system.

4.7 Approximations

As stated before, $Q(n, y)$ (4.25) involves m effective eigenvalues, $m-1$ of which are complex and/or negative. For large m and r, the eigenvalue calculation is only numerically feasible. In communication networks, we are interested in heavy traffic, *i.e.*, $m/r > 0.5$, which implies $\rho > 0.5$. For $\rho > 0.5$, some approximations can be made to avoid the eigenvalue calculation and thus simplify the expression of $Q(n, y)$.

Based on Descartes' Sign Rule, the polynomial (4.18) has two real positive zeros, one of which is 1 and the other one is between 0 and 1 (Fig. 4.3). In other words, there is only one real positive root inside the unit circle, denoted as x_0 with corresponding eigenvalue λ_0. Numerical results show that λ_0 is the largest effective eigenvalue and is the dominant one if $0.5 < \rho \leq 1$. Since $Q(n, y)$ is composed of exponential series, it is reasonable to approximate $Q(n, y)$ by a single exponential with the dominant eigenvalue λ_0 as follows

$$\begin{aligned} Q(n, y) &\approx C_0 \phi_0(1) \lambda_0^{n-1} x_0^{-(y-1)} \\ &= \rho(1 - x_0) x_0^{-y} \lambda_0^n, \qquad n \geq 1. \end{aligned} \tag{4.55}$$

where $C_0 = \rho(1 - \lambda_0)$ comes from $\sum_{n \geq 1} \pi_n = \rho$. The queue length distribution (4.26) is thus reduced to a single geometric distribution,

$$\pi_n \approx \begin{cases} \rho(1 - \lambda_0)\lambda_0^{n-1} & n > 0 \\ 1 - \rho & n = 0. \end{cases} \tag{4.56}$$

Note that for $m = 1$ (integer interarrivals), there is only one effective eigenvalue λ_0, and (4.56) is an accurate expression for the queue length distribution [24, 31, 55].

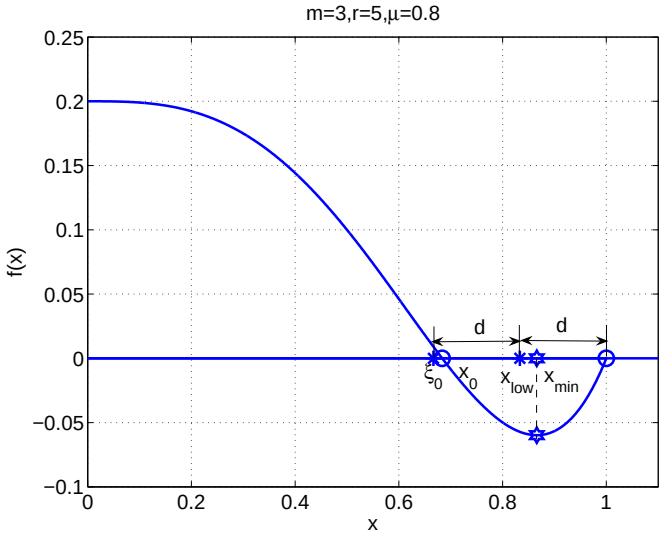

Figure 4.3. Approximation of the dominant root x_0 for $m = 3, r = 5, \mu = 0.8$: x_{min} is the local minimum between 0 and 1 and is approximated by x_{low}. ξ_0 is the approximation of x_0. In this case, the approximation error is within 2.5% although the traffic intensity ρ is only 3/4.

λ_0 can be derived from x_0, whose approximation is presented in Proposition 5.3.3.

Proposition 4.7.1 *Consider a polynomial* $f(x) = \mu x^r - x^m + 1 - \mu$. *The dominant root* x_0 *inside the unit circle can be well approximated by*

$$x_0 \approx 1 - \frac{2(1-\rho)}{\Delta\rho} \triangleq \xi_0, \tag{4.57}$$

where $\rho = m/(r\mu)$ *and* $\Delta = r - m$.

Proof Since i) $f(x)$ is continuous, ii) $f(0) = 1 - \mu > 0$, and iii) $f(x_0) = f(1) = 0$, a local minimum x_{min} exists between x_0 and 1. By equating the derivative of $f(x)$

to zero, we obtain x_{min},

$$x_{min} = \rho^{\frac{1}{\Delta}} < 1. \tag{4.58}$$

The first approximation is that the distances from x_{min} to the two real roots are equal, *i.e.*, $1 - x_{min} \approx x_{min} - x_0$ such that $x_0 \approx 2x_{min} - 1$. The second approximation is in x_{min}. Using two inequalities [2]

$$\ln x < x - 1, \quad x < 1, \tag{4.59}$$

$$\ln \rho > -\frac{1-\rho}{\rho}, \quad \rho < 1, \tag{4.60}$$

x_{min} is lower bounded by

$$x_{min} \gtrapprox 1 - \frac{1-\rho}{\Delta\rho} \triangleq x_{low}. \tag{4.61}$$

Then, $x_0 \approx 2x_{low} - 1$ is expressed by (5.5).

Remarks:

- The local minimum x_{min} of $f(x)$ is larger than $(1 + x_0)/2$. So, the approximation $x_0 \approx 2x_{min} - 1$ would yield an estimate larger than x_0. However, lower bounding x_{min} by x_{low} compensates for this so that (5.5) is quite tight, especially when r is large and ρ is close to 1.

- To guarantee that x_0 is a root inside the unit circle, (5.5) requires that $2(1 - \rho)/(\Delta\rho) < 1$, which is satisfied if $\Delta \geq 2$ and $\rho \geq 0.5$.

To simplify the delay distribution, plugging (5.5) into (4.39) and (4.40), the

delay mean and variance are approximated as

$$\overline{D} \approx \frac{\Delta\rho}{2(1-\rho)} \tag{4.62}$$

$$\sigma^2 \approx \Big(\frac{\Delta\rho}{2(1-\rho)}\Big)^2 - \frac{\Delta\rho}{1-\rho} \tag{4.63}$$

Plugging $\Delta = 1$ into (5.6) and variance (5.7), and comparing them with the accurate results (5.9) and (5.10), we conclude that the approximate analysis gets tight as $\rho \to 1$.

4.8 Comparison with Conventional D/Geom/1 Queueing Analysis

With conventional discrete-time queueing theory, the queue length and delay of the D/Geom/1 system with non-integer interarrival times are analyzed by converting the non-integer number to an integer. For example, $\Delta < m$, the interarrival time is rounded up to 2 and λ is solved as a root to a quadratic function $\lambda = (1 - \mu + \mu\lambda)^2$. Table 4.1 compares the positive real (effective) eigenvalue λ_0.

Apparently, there exists a huge gap in λ_0 if rounding the non-integer interarrival time up to an integer when m and r are closer, *e.g.*, $m = 3, r = 4$. Since both delay and queue length are geometric with λ_0 and x_0, the performance gap would be enlarged as the queue length and delay increase. Therefore, the study of non-integer interarrival times is necessary, especially for extremely heavy traffic $m/r \to 1$.

To confirm the tightness of the approximations (4.56) and (5.5), Fig. 4.4 compares the queue length distributions of (i) the exact one given by simulation; (ii) approximation I with π_n given by (4.56) and λ_0 calculated numerically; (iii) approximation II with π_n given by (4.56) and λ_0 approximated by (5.5); and (iv)

TABLE 4.1

COMPARISON OF EIGENVALUES FOR INTEGER AND NON-INTEGER INTERARRIVAL CASE WITH $m = 3, \mu = 0.8$

	$r = 4$	$r = 5$	$r = 6$
Our analysis x_0	0.8689	0.6836	0.6300
Our analysis λ_0	0.5699	0.1492	0.0625
Conventional analysis λ_0	0.0625	0.0625	0.0625

approximation obtained by using the conventional D/Geom/1 analytical results with r/m rounding to 2. Apparently, our analysis provides more accurate statistical performance analysis even with two approximations (4.56) and (5.5). Note that for $\Delta = 1$, we obtain the accurate delay distributions.

4.9 Conclusions

In order to statistically analyze the delay performance of TDMA, we establish a discrete-time G/Geom/1 system with non-integer interarrival times. An eigenvalue approach is used to solve steady-state system probabilities and the corresponding queue length and delay distributions. Due to the sparse structure of the characteristic matrix polynomial, the eigenvalue problem is reduced to a problem of polynomial roots, which substantially simplifies the computation. For special systems with heavy traffic intensity, numerical results show that it is sufficient to consider only the dominant real positive root and ignoring all other complex or negative roots. Moreover, by showing the performance gap with conventional D/Geom/1 queueing analysis, the necessity and usefulness of our analysis are

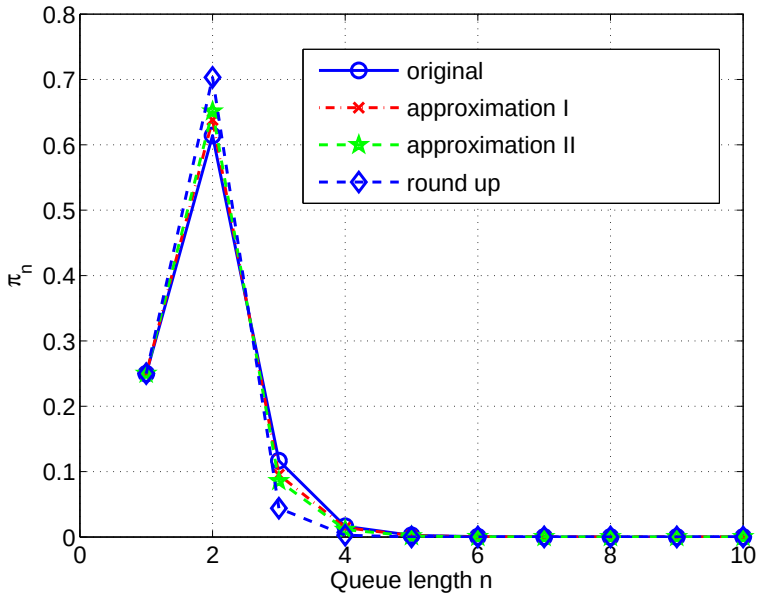

Figure 4.4. Comparison of the queue length distribution for $m = 3, r = 5, \mu = 0.8$. The original one is the accurate distribution. Approximation I comes from (4.56) with λ_0 calculated numerically. Approximation II comes from (4.56) with λ_0 approximated by (5.5). "Round up" is obtained by the conventional approach.

demonstrated.

CHAPTER 5

DELAY ANALYSIS OF TDMA AND ALOHA IN WIRELESS MULTIHOP NETWORKS (WMNs)

The delay analysis of TDMA at a single node in Chapter 4 can be extended to the multihop scenario although in WMNs, the analysis is significantly more challenging than in single-hop networks due to the delay accumulation at each hop. Many factors interact with each other, including the MAC scheme, the routing algorithm, the scheduling algorithm, the wireless channel and the resulting interference. In WMNs, there are two types of interference as shown in Fig. 5.1(a), *inter-flow interference* caused by cross-traffic flows and *intra-flow interference* caused by multiple nodes of a single flow [152]). The analysis is unlikely to be tractable if all these factors are considered together.

Since the focus of this dissertation is on MAC and scheduling, we assume a single flow so that the routing algorithm and the inter-flow interference can be neglected. This is a common scenario, *e.g.*, in sensor networks with a single phenomenon to be detected (Fig. 5.1(a)). A set of nodes around the phenomenon periodically detect, collect, and then forward the sensed data to a cluster head (node 0). A path is established from the cluster head to the base station (BS). Then, the two-dimensional (2-D) topology is reduced to one-dimensional (1-D), which can be further simplified to a chain network (Fig. 5.1(b)). Due to the zero

inter-flow interference assumption, the analysis of the chain network provides an upper performance bound for general 2-D networks.

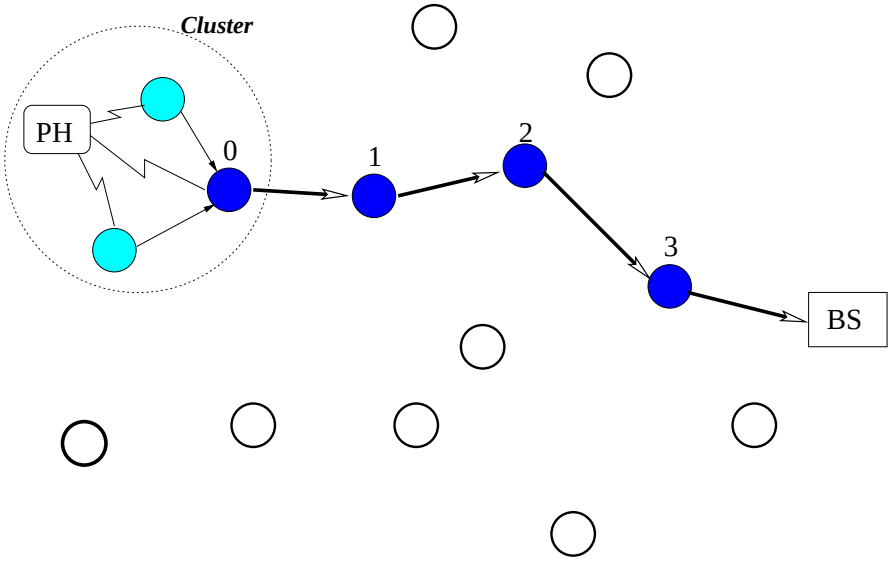

(a) General network (PH: phenomenon)

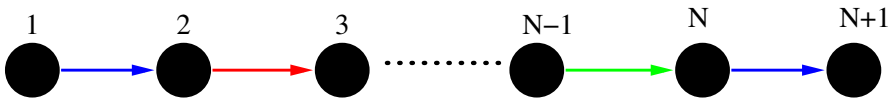

(b) Line network

Figure 5.1. Wireless multihop networks

For the single flow case, FIFO is sufficient for local scheduling, but the MAC scheme needs to be carefully designed since it needs to achieve two conflicting goals, eliminating interference and increasing spatial reuse. Moreover, efficient

MAC schemes may incur extra access delays, which trades off against throughput. Designing optimal MAC schemes in WMNs should be based on the performance metrics, *e.g.*, delay and throughput. As pointed out in Chapter 4, even for simple TDMA, the delay analysis could be very complicated because of the involvement of both the queueing delay and the access delay. For a tractable analysis, we consider two simple but typical wireless multihop MAC schemes, m-phase spatial TDMA [94] and slotted ALOHA. In TDMA, a node is scheduled to transmit once in m time slots, and nodes m hops apart can transmit simultaneously. In slotted ALOHA, every node independently transmits with probability p_m whenever it has packets. TDMA (with nodes fully cooperative) and ALOHA (with nodes completely independent) represent two extremes in terms of the level of the node coordination and thus provide an upper and lower performance bound for other meaningful MAC schemes.

5.1 Previous Work and Our Contributions

Previously, the analysis of MAC schemes was focused on the single-hop scenario [12, 94] and little work has been done on their multihop delay. From the perspective of delay analysis, the queueing delay is ignored for simplification. For example, in an "infinite population model", a new node is generated to represent the newly generated packet; or new packets are generated only when the buffer is empty [12, 16, 101, 149, 157] so that there is no queueing delay. However, in practice, the number of nodes is finite, and new packets may be generated when the buffer is non-empty, which results in queueing delays.

The impact of the wireless channel is another important MAC-related issue [12, 16, 101, 157]. With the "capture" property of the radio receiver, the throughput

of slotted ALOHA is improved [12, 101, 125]. In some MAC schemes, using the channel characteristics to control the backoff timer or the transmit power, the delay and throughput can be changed [149, 157]. Therefore, the channel model is critical for the analysis. The "disk model" [47], assuming a fixed transmission range, has been very popular because of its simplicity. In m-phase TDMA with m chosen appropriately (*e.g.*, $m = 3$ in [124]), the disk model results in error-free channels since the simultaneous transmissions of nodes m hops apart cause no interference or collisions [118, 124]. In reality, the transmission success depends on the received SNIR. So TDMA does not completely eliminate the interference unless spatial reuse is completely foregone. The "capture model" [112] is more appropriate, in which packet transmissions fail if the received SNIR is too low. The failed packets have to wait for the next transmission opportunity. The packets behind them need a local scheduler to solve the competition for the transmission opportunities.

With practical traffic and channel models, combining scheduling protocols with MAC schemes is meaningful. However, from the perspective of queueing theory, the joint queueing analysis might be difficult. For instance, the queueing analysis of multihop networks usually neglects the MAC-dependent access delay [54, 91, 93, 124]. Closed-form solutions for the delay of the chain network with a single source (like Fig. 5.1(b)) are provided when the traffic is geometric [54] or the channel is error-free [93]. For other traffic models and error-prone wireless channels, some approximations are needed, *e.g.*, the "independence" assumption: In [45], the delay variance of a two-node tandem network is derived by assuming that the two nodes are independent. Similarly, in [56], an IEEE 802.11 wireless ad hoc network is modeled as a series of *independent* M/G/1 systems to obtain a product-form

delay distribution. However, in most cases the "independence" assumption does not hold and would lead to a very loose performance expression.

In this chapter, we derive the e2e delay distribution of a chain line network (Fig. 5.1(b)), considering a two-level scheduling problem [146]. Local packet scheduling causes a queueing delay, while the global MAC scheme results in an access delay. Our analysis accounts for both the queueing delay and the access delay. The "capture" model for wireless channels and CBR traffic are practical (*e.g.*, voice data [33] and periodic traffic in sensor networks).

For CBR traffic, correlations exist between the delays experienced at different nodes, indicating that the "independence" assumption does not hold. Based on the simulation results, an empirical model for the correlation coefficient is established. Then, the line network is treated like a series of independent GI/Geom/1 systems, but the delay variances are scaled by this correlation coefficient. With the complete e2e delay distribution, we calculate the delay outage probability (the probability that the e2e delay exceeds a predetermined threshold) for delay-sensitive applications. As a complement to previous work focusing on the throughput, this paper compares TDMA and ALOHA in terms of the e2e delay and the outage probability.

5.2 System Model

The chain network under consideration (Fig. 5.1(b)) is composed of $N+1$ transmitting nodes. Denote node i by n_i and the delay experienced at n_i by D_i. More precisely, D_i is the interval between the instant that the packet is successfully received by n_i and the instant that the packet is successfully transmitted and thus received by n_{i+1}. Thus the e2e delay is the sum of the D_i's. A FIFO discipline is

used at the nodes. A CBR flow of fixed-length packets is generated at the source n_0, and all remaining nodes except the BS are pure relays. The time is slotted to one packet transmission duration, and the network is modeled as a discrete-time tandem queueing network. The traffic interarrival time is r slots ($r \in \mathbb{N}$). The channels are assumed to be subject to independent errors with capture probability $\mu = 1 - \varepsilon$ (*e.g.*, AWGN or block fading channels), where ε can be obtained from (1.11). The network is 100% reliable, *i.e.*, the failed packets will be retransmitted at each link until received successfully.

In queueing theory, the delay D_i is composed of two parts, the waiting time (from the arriving instant to the instant that the packet is about to be served) and the service time, as shown in Fig. 5.2. In TDMA, the node is given a transmission opportunity once in m time slots. When dividing the time into frames of m slots and setting the beginning of a frame as the slot allocated to the node, the service time is geometric with μ, denoted by $\mathcal{G}_\mu$. The access delay is hidden in the frame so that each node can be modeled as a GI/Geom/1 system at the frame level. In ALOHA, busy nodes make a transmission decision at every time slot. A packet is correctly received if and only if the node attempts to transmit and the transmission is successful, with probability $s \triangleq \mu p_m$ (given that the arrival and the channel state are independent[1]). Overall, the service time is $\mathcal{G}_s$. This way, it is not necessary to distinguish the access delay from the failed transmission attempts. Then each node can be modeled as a GI/Geom/1 at the slot level.

Based on the characterization of the output process of the upstream node, the individual nodes can be analyzed as a GI/Geom/1 system, deriving the complete distribution of W_i, with the mean denoted by $\overline{W}_i$ and the variance by σ_i^2. Note

[1]To account for the half-duplex restriction, here μ is the conditional capture probability given that the receiver is listening.

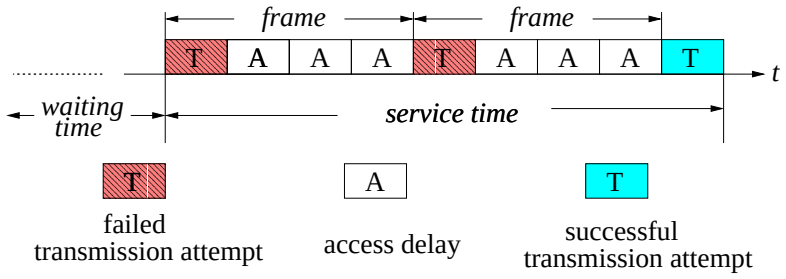

(a) TDMA

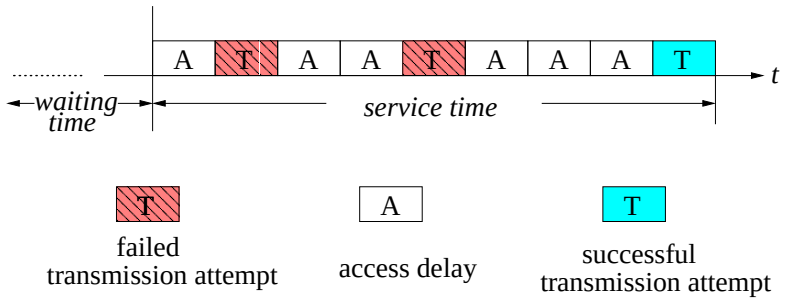

(b) ALOHA

Figure 5.2. Packet transmission procedure in TDMA and ALOHA

that W_i is difference from D_i since W_i is obtained as if each node is independent of each other, which is not true in practice. It is known that except for memoryless Poisson and geometric traffic, the output of node n_i, or the input to the following node n_{i+1}, depends on the input and service process of n_i [54]. Therefore, the delay D_{i+1} is correlated with the delay D_i.

It is hardly feasible to explicitly derive the e2e delay distribution if all correlations are considered. Instead, we propose an approximative approach that includes the long-distance correlations in the correlation between neighboring nodes. Then the line network can be modeled as a series of queueing systems which are correlated only with their neighbors. Since all nodes have an identical channel and all nodes except for the source node are pure relays, we further assume that the correlation coefficient $\eta \triangleq \mathrm{cor}(D_i, D_{i+1})$ is independent of i. Since correlations do not affect the delay means, from the analysis of W_i, the e2e delay mean and variance are:

$$\overline{D} = \sum_{i=0}^{N} \overline{W}_i, \quad \sigma^2 = \sum_{i=0}^{N} \sigma_i^2 + \sum_{i=0}^{N-1} \eta \sigma_i \sigma_{i+1}. \tag{5.1}$$

For the variance, if the D_i's were independent like W_i's ($\eta = 0$), then σ^2 would be the sum of σ_i^2, as assumed in previous work [45, 56]. However, the D_i's are not independent ($\eta \neq 0$), and a gap appears between the real e2e delay variance (the "simulation" line in Fig. 5.3(b)) and the sum of σ_i^2 (the "independence" line). The variance σ^2 is either greater or smaller than the sum of σ_i^2, depending on whether the correlation is positive or negative.

Intuitively, for bursty traffic, if a packet experiences a long delay at n_i because of a bad channel or the long accumulated queue, node n_{i+1} probably has cleared its buffer during this period so that when the packet arrives at n_{i+1}, it is likely to experience a short delay, and vice versa. In other words, the correlation is expected

to be negative ($\eta < 0$), hence the e2e delay variance σ^2 is smaller than the sum of σ_i^2. This effect becomes more prominent as the traffic intensity increases. So, it is reasonable to conclude that the correlation is a function of the intensity. The detailed derivation of the correlation coefficient η will be given in the following sections for TDMA and ALOHA separately.

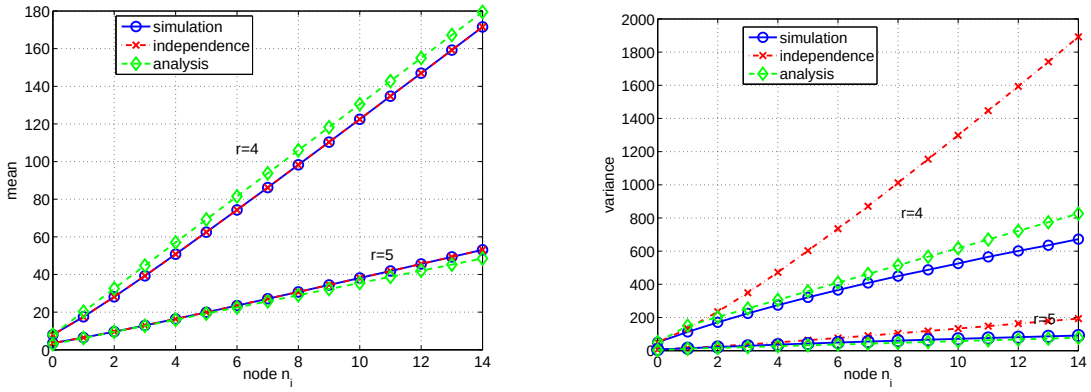

(a) Delay mean

(b) Delay variance

Figure 5.3: Comparison of the e2e delay performance in the TDMA network with $m = 3, \mu = 0.8, N = 14, r = 4, 5$

5.3 Analysis of the m-Phase TDMA Network

In m-phase TDMA networks, each node can be modeled as a D/Geom/1 system with service rate μ at the frame level. The average arrival rate is m/r, where m/r is a reduced fraction. We further assume $r < 2m$ for heavy traffic. Define the traffic intensity as $\rho \triangleq m/(r\mu)$ and constrain it to $\rho < 1$ for stability. Note

that previous MAC-related work implicitly assumed $\rho = 1$. As the source node, $D_0 = W_0$.

5.3.1 Delay Analysis of the Source Node n_0

The source n_0 is fed with a CBR flow of interarrival time r. At the frame level, n_0 is modeled as a D/Geom/1 but the interarrivel time r/m is an integer for $m < r < 2m$. Such D/Geom/1 system has been studied in Chapter 4. We summarize the results in the following theorems.

Theorem 5.3.1 *Consider a D/Geom/1 system with interarrival time r/m ($r, m \in \mathbb{N}$ and r/m is a reduce fraction) and service rate μ. The equilibrium probability $Q_l(u)$ for $l \geq 1$ is*

$$Q_l(u) \approx \rho \lambda_0^l a^{u-1}(a-1), \quad \textit{where} \quad a = \lambda_0^{-1/r}, \tag{5.2}$$

and λ_0 is a real positive eigenvalue of the matrix $\mathbf{M}(\lambda)$

$$\mathbf{M}(\lambda) = \mathbf{M_0} + \mathbf{M_1}\lambda + \mathbf{M_2}\lambda^2, \tag{5.3}$$

with $\mathbf{M_i}$ ($i = 0, 1, 2$) given in (4.13).

Theorem 5.3.2 *Consider a general D/Geom/1 queueing system with interarrival time r/m and service rate μ. Then, the probability generating function (pgf) of the delay distribution is*

$$G_{D_0}(z) \approx \frac{(a-1)(a^m - z^m)\beta z^m}{(a-z)(1-\beta z^m)}, \tag{5.4}$$

where $a^r = \lambda_0$ and $\beta = a^{-m}$.

An closed-form approximation for x_0 is presented in Proposition 5.3.3.

Proposition 5.3.3 *Consider the polynomial $\mu x^r - x^m + 1 - \mu = 0$. The real positive root x_0 inside the unit circle can be well approximated by*

$$x_0 \approx 1 - \frac{2(1-\rho)}{\Delta\rho}, \quad \rho = m/(r\mu), \quad \Delta = r - m < m. \tag{5.5}$$

The approximation (5.5) is tight when Δ is large and/or ρ is close to 1, both of which also guarantee $x_0 \lessapprox 1$. The delay mean and variance can be directly calculated from $G_{D_0}(z)$ (4.36),

$$\overline{D}_0 \approx \frac{a}{a-1} \approx \frac{\Delta\rho}{2(1-\rho)}, \tag{5.6}$$

$$\begin{aligned}\sigma_0^2 &\approx \frac{a(2-a)}{(a-1)^2} \approx \Big(\frac{\Delta\rho}{2(1-\rho)}\Big)^2 - \frac{\Delta\rho}{1-\rho} \\ &= \overline{D}_0(\overline{D}_0 - 2).\end{aligned} \tag{5.7}$$

For a special case $r = m + 1$,

Theorem 5.3.4 *Consider a D/Geom/1 queueing system with interarrival time $(m+1)/m$ and service rate μ. Then, the pgf and the mean and variance of the delay D_0 are*

$$G_{D_0}(z) = \frac{(z^m - 1)z}{z(1-z^m) - \mu(1-z^{m+1})} \cdot \frac{1-\rho}{\rho} \tag{5.8}$$

$$\overline{D}_0 = \frac{1}{2(1-\rho)}, \qquad \rho = \frac{m}{r\mu} \tag{5.9}$$

$$\sigma_0^2 = \frac{1}{4(1-\rho)^2} - \frac{m+2}{6(1-\rho)}. \tag{5.10}$$

Comparing the approximate delay analysis (5.6), (5.7) (setting $\Delta = 1$) and the accurate analysis (5.9), (5.10), we find that even for small Δ, the approximation

is tight if $\rho \to 1$.

5.3.2 Delay Analysis of the Relay Nodes

The relay nodes are fed with the output of the source node n_0. In Chapter 4, it has been proved that the output process of D/Geom/1 systems with $r < 2m$ is a correlated on-off process, as repeated in Theorem 5.3.5.

Theorem 5.3.5 *Consider a D/Geom/1 queueing system with service rate μ and interarrival time r/m ($m < r < 2m$). Then the output process is a correlated on-off with transition probabilities $a_{01} = \mu$ and $a_{10} = \Delta\mu/m$, where $\Delta = r - m$.*

Therefore, the first relay node n_1 is GI/Geom/1 system with on-off input. The queue length distribution is derived in [31], and the packet delay is shown to be geometric in [104] without calculating the parameter of the geometric distribution, which is derived in Lemma 5.3.6.

Lemma 5.3.6 *Consider a discrete-time GI/Geom/1 queueing system with service rate μ and on-off arrival, whose transition probabilities are a_{01} and a_{10}. Then, the delay is geometrically distributed with parameter*

$$\xi = \frac{1-\mu}{\mu a_{10} + (1-\mu)(1-a_{01})}. \tag{5.11}$$

Proof Using the delay model [69], denote the system state by the delay of the HOL packet. Negative states indicates an idle server. All probabilities of going

beyond a delay -1 are included in the state -1. The transition probability Z_{jk} is

$$Z_{jk} = \begin{cases} \mu b_l(j),\ j \geq 0,\ k \leq j \\ 1-\mu,\ j \geq 0,\ k = j+1 \text{ or } j = -1,\ k = j \\ a_{01}, \quad j = -1,\ k = 0, \end{cases} \tag{5.12}$$

where $l = j - k + 1$, $b_l = t_l$ and $b_l(j) = b_l$ for $j > -1$, and $b_l(j) = \sum_{h=l}^{\infty} b_h = a_{10}(1-a_{01})^{l-2}$ for $j = -1$. Manipulating the balance equations, the steady-state probability is $z_j = z_0 \xi^j$ $(j \geq 0)$. Since the delay probabilities involve only non-negative states (as in (4.42)), the delay distribution is geometric with ξ.

For the relay node n_1, with $a_{10} = \Delta\mu/m$ and $a_{01} = \mu$, the delay probabilities are $\pi_{jm+1} = (1-\xi)\xi^j$ at the time slot level. Therefore, the mean and variance are

$$\overline{W}_1 = 1 + \frac{m\xi}{1-\xi} = 1 + m\tau, \quad \tau \triangleq \frac{\rho}{1-\rho}\frac{1-\mu}{\mu} \tag{5.13}$$

$$\sigma_1^2 = \frac{m^2\xi}{(1-\xi)^2} = m^2\tau(1+\tau). \tag{5.14}$$

The output of n_1 is also bursty and correlated, but too complicated to be characterized by a simple traffic model. It is stated in [104] that the output process of tandem GI/Geom/1 queues converges to a Bernoulli (geometric) process as the number of nodes goes to infinity. However, in practical wireless networks, the route is often too short for the output to converge to a geometric process. Considering that on-off is a simple yet accurate model for bursty and correlated traffic, we use the derived on-off process with $\{a_{01}, a_{10}\}$ to characterize the inputs to all relay nodes. As a matter of fact, simulation results confirm that the delays W_i $(i \geq 1)$ of the relay nodes are close to the geometric process described in Lemma 5.3.6.

5.3.3 Estimation of the Correlation Factor

The inputs to relay nodes are correlated and bursty and result in correlations between the delays D_i's. As mentioned in Section 7.1, the correlation is generally a function of the traffic intensity $\rho = m/(r\mu)$. However, in a TDMA tandem network, the operations of the servers are successive, *i.e.*, the neighboring nodes cannot be served simultaneously. This behavior affects the correlation. It also implies that the correlation might not be solely determined by ρ. If $\rho = 0$, there is no traffic, and $D_i \equiv 0$. So, there is no correlation and $\eta = 0$. On the other hand, if $\mu = 1$, the channel is perfect, and every packet can be successfully transmitted with only one attempt regardless of ρ, *i.e.*, $D_i \equiv 1$ $(i \geq 1)$. Then, the correlation is expected to be $\eta = 0$ as well even if $\rho \neq 0$. In this sense, the correlation depends at least on two parameters ρ and μ although ρ itself is a function of μ since $\mu = 1$ does not necessarily lead to $\rho = 0$. From (5.13) and (5.14), it is verified that the delay D_i $(i \geq 1)$ is a function of τ. Accordingly, we assume that the correlation coefficient η is a function of τ.

It is unclear how τ impacts the correlation coefficient η. A set of simulation results (obtained by MATLAB) are provided to establish an empirical model of η. As shown in Fig. 5.4, i) the correlation is indeed negative; ii) the magnitude of the correlation can be regarded as exponentially increasing with τ. Based on the least-square principle, the curve is fitted as follows

$$\eta(\tau) = x_1 + x_2 e^{-x_3 \tau^{x_4}}, \quad \tau = \frac{\rho}{1-\rho} \cdot \frac{1-\mu}{\mu}, \tag{5.15}$$

where $x_1 = -0.0023$, $x_2 = -0.7350$, $x_3 = 0.2315$, $x_4 = -0.5598$. With the empirical η and assuming that all relay nodes behave identically, the e2e delay

mean and variance are further simplified from (5.1) to the following

$$\overline{D} = \overline{D}_0 + N\overline{W}_1 \tag{5.16}$$

$$\begin{aligned}\sigma^2 &= \sigma_0^2 + \sigma_1^2 + \eta\sigma_0\sigma_1 + (N-1)\eta\sigma_1^2 \\ &\approx \sigma_0^2 + N(1+\eta)\sigma_1^2. \end{aligned} \tag{5.17}$$

Then, the tandem network can be treated as a series of *independent* discrete-time

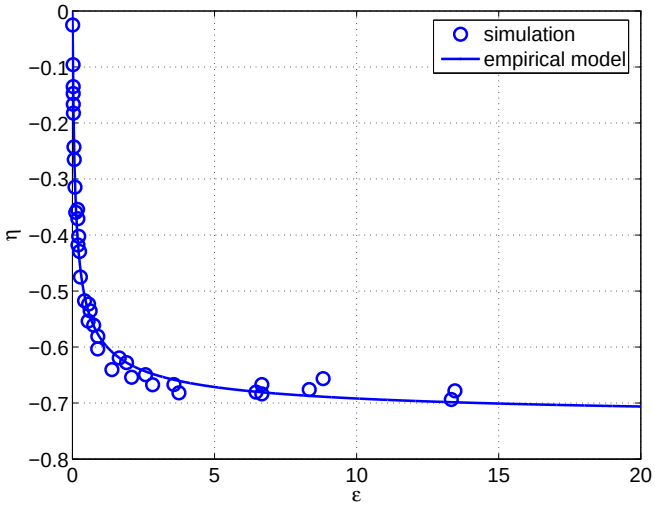

Figure 5.4. The estimation of the correlation coefficient η in TDMA: η vs. τ (see (5.15))

servers. The first one is the source with mean $\overline{D}_0$ and variance σ_0^2. The others are identical relays with mean $\overline{W}_1$ and scaled variance $(1+\eta)\sigma_1^2$. According to the Law of Large Numbers, the e2e delay will converge to a Gaussian distribution, and

the mean and variance are linear with the number of nodes N. Simulation results in Fig. 5.5 and Fig. 5.3 confirm the quick convergence to a "sampled" Gaussian and the linearity even for relatively short networks.

In Fig. 5.3 ($m = 3, \mu = 0.8, N = 14$ for $r = 4$ and $r = 5$, respectively), we compare the mean and variances in three cases: 1) the simulated e2e delay; 2) the sum of the simulated delays of the individual nodes, *i.e.*, the e2e delay when all servers are independent; and 3) the analytical delay with mean (5.16) and scaled variance (5.17). It is obvious that, with respect to the variance, the correlation causes a huge gap between the real case 1) and the "independence" case 2). In other words, the "independence" assumption is not accurate for the calculation of the variance. Our analytical results (case 3)) use the empirical correlation coefficient η and are much closer to the simulated variance.

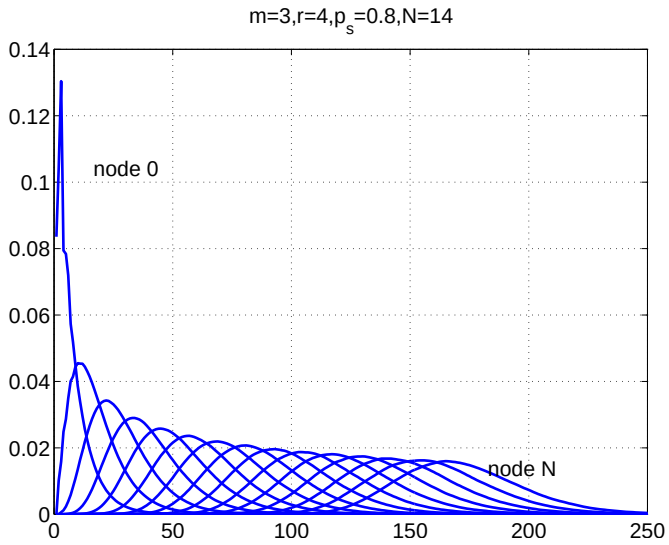

Figure 5.5. Pmf of the packet cumulated delay in TDMA with $m = 3, r = 4, \mu = 0.8, N = 14$

The other observation revealed in Fig. 5.3 is the impact of the traffic rate $1/r$. As r increases, the delay mean and variance unsurprisingly decrease. However, the delay decreases at a much faster speed than the increase of r. Comparing $r = 4$ and $r = 5$, with r increasing by 20%, the mean decreases by 70% and the variance by 87%. The reason is that the traffic intensity is determined by three parameters m, r, μ ($\rho = m/(r\mu)$). With m and μ fixed, a small change in r probably causes a huge change in ρ, and in μ (5.13) and σ^2 (5.14). Previous work usually assumed $\rho = 1$ thereby preventing a study of the impact of the traffic rate.

5.4 Analysis of the Slotted ALOHA Network

m-phase TDMA achieves the optimal performance but also incurs a substantial amount of overhead to establish the frame structure and requires a complete cooperation between all nodes involved. In wireless networks, slotted ALOHA may be more practical since every node operates in a completely independent way. However, unless the traffic is light, its random and independent transmission pattern generally results in poor performance. This section analyzes the delay of ALOHA networks using a similar technique as in TDMA since the individual node is also modeled as a GI/Geom/1 system. The difference is that the ALOHA network is analyzed at the time slot level. Note that the source node n_0 is modeled as a D/Geom/1 queueing system with an integer interarrival time r. The delay distribution is derived in the following Corollary 5.4.1 to Theorems 5.3.1 and 5.3.2.

Corollary 5.4.1 *Consider a D/Geom/1 queueing system with interarrival time $r \in \mathbb{N}$ and service rate s. Then the delay is $\mathcal{G}_{1-\alpha}$, where α is a positive real root*

of the polynomial

$$sy^r - y + 1 - s = 0. \tag{5.18}$$

The delay mean and variance are approximately expressed in an explicit form

$$\overline{D}_0 = \frac{1}{1-\alpha} \approx \frac{(r-1)\rho}{2(1-\rho)}, \quad \rho = \frac{1}{sr} \tag{5.19}$$

$$\sigma_0^2 = \frac{\alpha}{(1-\alpha)^2} \approx \Big(\frac{(r-1)\rho}{2(1-\rho)}\Big)^2 \Big(1 - \frac{2(1-\rho)}{(r-1)\rho}\Big). \tag{5.20}$$

Proof As a special case $m = 1$ of Theorem 5.3.1, the polynomial (4.18) is modified to (5.18) by replacing μ with s and setting $m = 1$. There is only one root inside unit circle, denoted by α. Plugging $a = 1/\alpha$ and $\beta_0 = \alpha$ into (4.36) (Theorem 5.3.2), the pgf of the delay distribution is

$$G_{D_0}(z) = \frac{(1-\alpha)z}{1-\alpha z}, \tag{5.21}$$

which is corresponding to a geometric distribution with parameter $1 - \alpha$. Using the same technique as in Proposition 5.3.3 but replacing Δ by $r - 1$, if $r \gtrapprox 4$ and $\rho \gtrapprox 0.5$, α is well approximated by

$$\alpha \approx 1 - \frac{2(1-\rho)}{(r-1)\rho}. \tag{5.22}$$

Then, the delay mean $\overline{D}_0$ and variance σ_0^2 are approximated as in (5.19) and (5.20).

The output process of n_0 is more complex in ALOHA than in TDMA since the system idle time ranges from 0 to $r - 1$ time slots. But it can be approximated

as an on-off process, as stated in Lemma 5.4.2 by using a similar technique in Theorem 5.3.5.

Lemma 5.4.2 *Consider a D/Geom/1 queueing system with interarrival time $r \in \mathbb{N}$ and service rate s. Then, the output process is approximately an on-off with transition probabilities $a_{01} = (1-s)/((r-1)\alpha)$ and $a_{10} = (1-s)/\alpha$.*

Then the relay nodes are modeled as GI/Geom/1 with on-off input $\{a_{01}, a_{10}\}$. According to Lemma 5.3.6, the delay W_i $(i \geq 1)$ is geometric with ξ

$$\begin{aligned} \xi &= \frac{1-s}{sa_{10} + (1-s)a_{00}} \\ &= \frac{(r-1)\alpha\rho}{1-(1-(r-1)\alpha)\rho} \approx 1 - \frac{1-\rho}{r\rho - 1}. \end{aligned} \tag{5.23}$$

The mean and variance are

$$\begin{aligned} \overline{W}_1 &= \frac{1}{1-\xi} = 1 + \frac{(r-1)\rho\alpha}{1-\rho} \approx \frac{r\rho - 1}{1-\rho}. \\ \sigma_1^2 &= \frac{\xi}{(1-\xi)^2} = \frac{(r-1)\rho\alpha}{1-\rho}\big(1 + \frac{(r-1)\rho\alpha}{1-\rho}\big) \\ &\approx \Big(\frac{r\rho - 1}{1-\rho}\Big)^2 - \frac{r\rho - 1}{1-\rho}. \end{aligned} \tag{5.24}$$

The correlations in ALOHA are different from those in TDMA because i) the nodes are not served successively; ii) the service rate is $s = \mu p_m$, which cannot reach to 1 for $p_m < 1$ even if the channel is perfect. In other words, it might not be necessary to include μ explicitly in the calculation of the correlation. Therefore, as stated in Section 7.1, we assume that the correlation in ALOHA is a function of the traffic intensity ρ. Through simulation results (Fig. 5.6), η is found to be

composed of two parts and characterized as follows

$$\eta = x_1 + x_2\rho + \frac{x_3}{x_4 - \rho}, \tag{5.25}$$

where $x_1 = -0.2483$, $x_2 = -0.5415$, $x_3 = 0.0096$, $x_4 = 1.0088$. The intuition behind this shape of $\eta(\rho)$ is: as the traffic intensity increases, the queueing delay will increase and so does the resulting correlation magnitude $|\eta|$. However, if ρ increases to 1, all delays increase to infinity. Then, $|\eta|$ might decrease rather than continue to increase. So, interestingly, a transition point $\rho \approx 0.93$ exists. Therefore, it is not suggested in ALOHA to set the traffic intensity ρ higher than this transition point because of both the increasing delay and the almost-zero correlation.

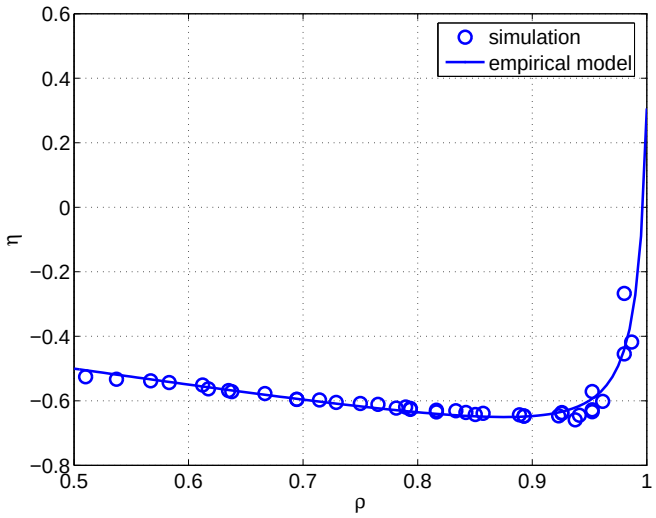

Figure 5.6. The estimation of the correlation coefficient η in ALOHA: η vs. ρ (see (5.25))

The remaining part of the ALOHA analysis is similar to TDMA. The simulated pmf (Fig. 5.7) of the delay verifies the convergence to Gaussian. The delay mean and variance are presented in Fig. 5.8. The 20% increase of r causes 73% decrease of the mean and 92% of the variance.

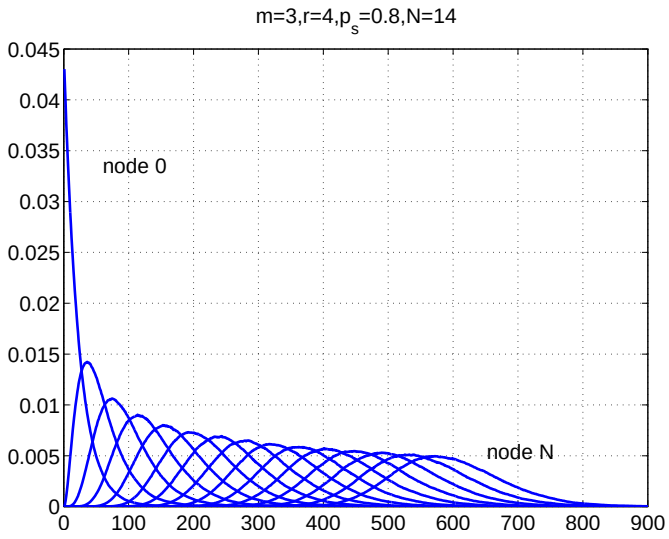

Figure 5.7. Pmf of the packet cumulated delay in ALOHA with $m = 3, r = 4, \mu = 0.8, N = 14$

5.5 Comparison

Table 5.1 lists the delay statistics of the individual node for TDMA and ALOHA. As the number of nodes N increases, the e2e delay statistics are mainly determined by those of the relay nodes. Therefore, the delay of TDMA and

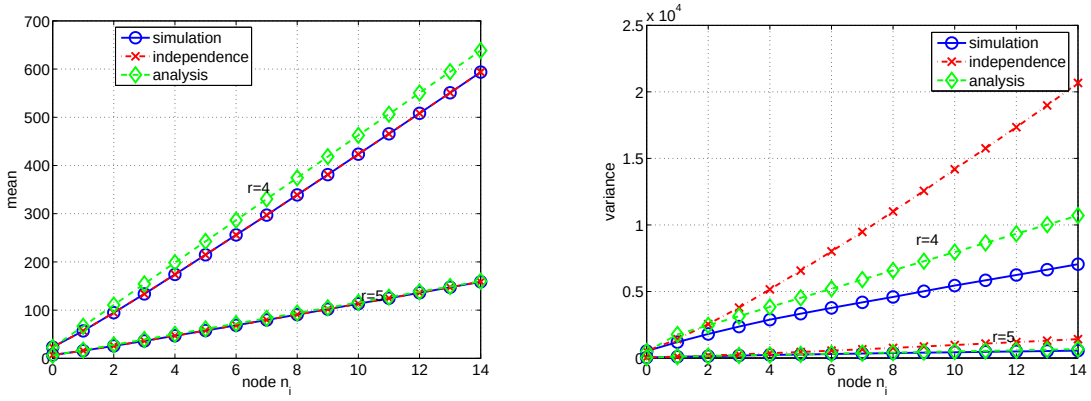

(a) Delay mean

(b) Delay variance

Figure 5.8: Comparison of the delay performance in the ALOHA network

ALOHA can be compared as follows:

$$\frac{\mu_{\text{TDMA}}}{\mu_{\text{ALOHA}}} \approx \frac{m}{r-1} \cdot \frac{1-\mu}{\mu\alpha} \approx \frac{m}{r-1} \cdot \frac{1-\mu}{\mu} < 1, \tag{5.26}$$

$$\frac{\sigma^2_{\text{TDMA}}}{\sigma^2_{\text{ALOHA}}} \approx \left(\frac{1+\eta_{\text{TDMA}}}{1+\eta_{\text{ALOHA}}}\right)\left(\frac{m}{r-1}\right)^2 \cdot \frac{1-\mu}{\mu} \cdot \left(\frac{1-\mu}{\mu} + \frac{1-\rho}{\rho}\right) < 1, \tag{5.27}$$

where η_{TDMA} and η_{ALOHA} are given in (5.15) and (5.25), respectively. The mean for ALOHA is $(r-1)\mu/m(1-\mu)$ times than TDMA. The ratio of the variance depends on the correlation coefficients η. The ratio of $1+\eta_{\text{TDMA}}$ to $1+\eta_{\text{ALOHA}}$ lies between 0.5 and 2.5. So, $\sigma^2_{\text{TDMA}}/\sigma^2_{\text{ALOHA}} \ll 1$ for $m \geq 3, m < r < 2m, \mu > 0.5$. As an example, for $r = 4, \mu = 0.8$ and $m = 3$ (corresponding to $p_m = 1/3$ for ALOHA), (5.26) and (5.27) shows that the mean and variance of ALOHA are 4 and 11.9 times than those of TDMA, respectively. The simulation results in Fig. 5.3 and Fig. 5.8 confirm that the delay mean of ALOHA is about four times greater than that of TDMA, while the variance is about 11 times larger. Theoretically, we proved that TDMA achieves better performance than ALOHA not only in the throughput but also in the e2e delay. This comparison is based on the assumption of equal μ for TDMA and ALOHA. If the network were interference-limited, TDMA would have a larger μ than ALOHA (if the other parameters are the same), which would further increase the performance gap.

In addition, with the Gaussian approximation of the e2e delay, we are able

TABLE 5.1

COMPARISON OF LOCAL DELAYS FOR TDMA AND ALOHA

	Source node		Relay node	
	mean $\overline{D}_0$	variance σ_0^2	mean $\overline{W}_1$	variance σ_1^2
TDMA	$(r-m)\cdot\frac{\rho}{2(1-\rho)}$	$\overline{D}_0(\overline{D}_0-2)$	$1+m\cdot\frac{\rho}{1-\rho}\cdot\frac{1-\mu}{\mu}$	$(\overline{W}_1-1)(\overline{W}_1-1+m)$
ALOHA	$(r-1)\cdot\frac{\rho}{2(1-\rho)}$	$\overline{D}_0(\overline{D}_0-1)$	$1+(r-1)\cdot\frac{\rho}{1-\rho}\cdot\alpha$	$\overline{W}_1(\overline{W}_1-1)$

to calculate the delay outage probability $p_L(d) = \Pr\{D > d\}$ for delay-sensitive applications, where d is the regarded as a hard delay bound. Given the mean $\overline{D}$ and variance σ^2, $p_L(d)$ is

$$p_L(d) = \Pr\{D > d\} = \frac{1}{2}\Big(1 - \mathrm{erf}\big(\frac{d-\overline{D}}{\sqrt{2}\sigma}\big)\Big). \tag{5.28}$$

Fig. 5.9 shows $p_L(d)$ for $m = 3, r = 4, \mu = 0.8, N = 10$. Compared to previous work that assumed independent D_i's, our analysis provides more accurate insight on $p_L(d)$. For example, given $d = 185$ for TDMA, we calculate $p_L(d) = 0.0093$ while the independence assumption would lead to $p_L(d) = 0.09$, which is almost 10 times higher. Similarly, for ALOHA, given $d = 600$, our analysis yields $p_L(d) = 0.0087$ while the independence assumption leads to $p_L(d) = 0.0891$. Since $p_L(d)$ is an important measure for the design of real-time networks, our more accurate analysis is clearly preferred. Besides, Fig. 5.9 also shows how much worse ALOHA behaves in terms of the delay outage probability. In order to achieve $p_L(d) \leq 10\%$, ALOHA requires a delay bound of $d = 570$, about 3.5 times than the delay bound $d = 160$ of TDMA.

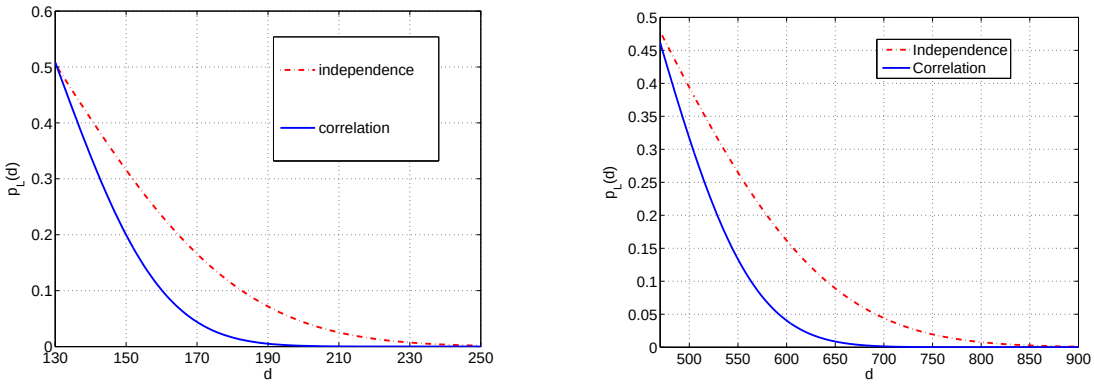

(a) TDMA (b) ALOHA

Figure 5.9: The delay outage probability $p_L(d)$ for $m = 3, r = 4, \mu = 0.8, N = 10$

5.6 Conclusions

Discrete-time queueing theory is useful to statistically compare TDMA and ALOHA, in which the access delays are incorporated into the prolonged service time in TDMA and the decreased service rate in ALOHA. Given the same traffic load and original service rate, we proved that prolonging the service time by a factor of m as in TDMA causes less delay than decreasing the service rate by $p_m = 1/m$ on average as in ALOHA in terms of both the mean and variance.

The e2e delay, especially the variance, is significantly affected by the negative correlations between the delays experienced at single nodes. Previous work ignored the correlations and assumed an "independence" instead. Using simulation results we estimate an empirical correlation coefficient, which leads to a more accurate expression for the e2e delay variance which has been paid little attention in the literature. The complete delay distribution can be used to calculate a delay outage probability $p_L(d)$, a critical measurement for delay-sensitive applications.

CHAPTER 6

CROSS-LAYER ANALYSIS OF PHYSICAL LAYER, MAC AND TRAFFIC STATISTICS

In Chapter 5, the performance of MAC schemes is analyzed assuming that the channel outage probability ε is a constant. However, in practice, the channel states that determine the SNIR at the receiver and, in turn, the success of the transmissions, are time- and location-dependent. Due to this interaction, MAC schemes should be analyzed jointly with the physical layer. In interference-limited networks, ε is a function of the interference or SIR. The interference is related to the multiple access protocol and referred to as multiple access interference (MAI) [123]. In the saturation state (when the nodes are always backlogged), the MAI depends on the MAC scheme. However, the saturation state could result in infinite buffers and an unstable network. Realistically, all stable networks are non-saturated. In non-saturated networks, the nodes may have empty buffers upon being scheduled and thus will not transmit and interfere. Then, the MAI is not only MAC-dependent, but also coupled with the node buffer occupancy, which, based on queueing theory, depends on the arrival process (traffic) and the service process (channel). Hence, the physical channel, the MAC scheme and traffic are correlated through the MAI-dependent ε, or the link rate $p_s = 1 - \varepsilon$.

The most often studied traffic statistics include the rate and burstiness. In multihop networks, an additional feature should be taken into account – the traffic

correlation. Unlike in single-hop networks, a traffic flow is usually relayed over several hops. So the arrival process to a node is the aggregation of the local flow and relayed flows. Even if the source flows are generated independently, the overall arrival processes to the nodes of the same path are correlated. The node buffer occupancies under correlated and independent flows could be quite different even in a simple two-node network [63]. The correlation is affected by the channel quality and the MAC scheme and, in turn, may affect the real-time buffer occupancy and change the channel quality. A comprehensive study of the traffic correlation should therefore explore the interaction between the physical layer, the MAC layer and traffic statistics.

Previous cross-layer studies between the MAC and the physical layer were focused on power control [134] and considered only the saturated mode [50, 88, 155]. The traffic correlation is ignored by assuming that all flows in the network are independent. [117] discussed the correlation in the channels inherited from the multihop topology but the correlated relationship is simply expressed by a predetermined constant without specifying how it is calculated.

This chapter investigates how the MAC scheme, the physical channel, and the traffic statistics interact with each other, how the correlations affect the network throughput and delay, and establishes the *network capacity*, *i.e.*, the maximum stable throughput [143]. The investigation of the correlations includes the auto-correlation in the channels, the cross-correlation between traffic and channels, and the traffic correlation, and their impact on the delay and throughput. Since the node busy probability is MAC- and traffic-dependent, we consider two typical MAC schemes, m-phase TDMA and slotted ALOHA, and three often used traffic models, constant bit rate (CBR) for voice applications, on-off for data applica-

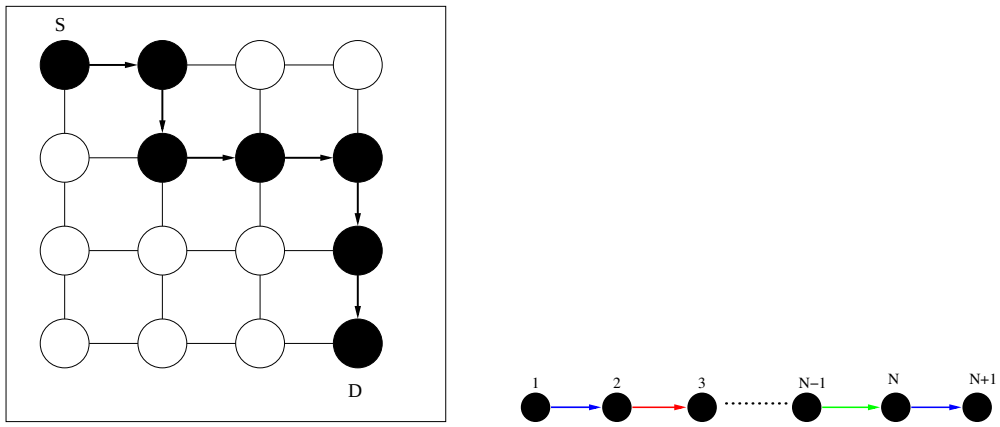

(a) Manhattan street network (b) Line network

Figure 6.1. Regular wireless multihop networks

tions, and memoryless Bernoulli processes. For a tractable analysis, two extreme traffic correlation cases are explored, independent and completely correlated traffic. Simulation results are provided to compare the influence of these models.

6.1 Interaction Between the Channel, MAC Schemes, and Traffic

In certain wireless networks such as vehicular networks, the topology is quite likely to be regular, like a square grid (Fig. 6.1(a)) or a regular line (Fig. 6.1(b)). Small changes in the distances between nodes are overshadowed by fading. Hence, it is reasonable to assume fixed distances when the channel is modeled as slow fading. The channel quality is measured by its probability $1 - p_s$ of successful reception or capture rate [26]. To guarantee 100% reliability, failed packets will be retransmitted until being received correctly.

The multihop network (Fig. 6.1) is composed of N nodes. Denote node i by

n_i. Each node independently generates a flow of fixed-length packets with rate R_i. The aggregated traffic rate is $\lambda_i = \sum_{k \in \mathcal{R}_i} R_k$, where $\mathcal{R}_i$ is the set of nodes whose flows traverse n_i, accounting for both the local traffic r_i and the relayed traffic R_k ($k \in \mathcal{R}_i \backslash \{n_i\}$).

Assume equal distance between neighboring nodes. The transmit power P_i is assumed to be identical for all nodes, $P_i \equiv P$. Specially, given the path loss exponent α, in Rayleigh fading channels, the received power is exponentially distributed with mean $P d_i^{-\alpha}$, where d_i is the distance from n_i to the receiver under consideration. The variations in the received power stems from both fading and varying distances due to motion. In certain networks, such as vehicular networks, since the transmit energy consumption is not critical, so the noise power can be ignored. The transmission is successful if the received SIR is greater than a threshold Θ [50, 77, 88], *i.e.*,

$$\begin{aligned} p_{s,i} &= \mathbb{P}\{\mathrm{SIR}_i > \Theta\} \\ &= \prod_{k \in \mathbb{I}_i} \Big(1 - \frac{p_t(k,i)}{1 + (\frac{d_k}{d_i})^{\alpha}/\Theta}\Big). \end{aligned} \tag{6.1}$$

where $\mathbb{I}_i$ is the interference set of n_i, consisting of all potential interferers of n_i. Θ is determined by the communication hardware and the modulation and coding scheme. $p_t(k,i)$ is the effective transmit probability of the potential interferer n_k when n_i is transmitting. Note that (6.1) holds if the transmissions of the nodes are independent of each other. Therefore it is not applicable to the MAC schemes with cooperation like hand-shaking and carrier sensing (CSMA, IEEE 802.11). Moreover, even if the scheduling process is independent like ALOHA, the "independence" condition is not satisfied for non-saturated networks since the

transmissions take place only at non-idle nodes. Note that $p_t(k,i)$ can be used to model some level of dependence if it can be solved explicitly.

The relationship between the node buffer occupancy and the transmission occurrence can be reflected quantitatively through (6.1), where the effective transmit probability is $p_t(k,i) \triangleq p_{m,k}p_b(k,i) \leq 1$. $p_{m,k}$ is the MAC-dependent access probability of n_k and $p_b(k,i) \leq 1$ is the conditional busy probability of n_k given that n_i is transmitting. For simplicity, we assume $p_{m,k} = p_m$, *i.e.*, spatial stationarity. The main difference from previous work lies in $p_b(k,i)$, which was neglected because $p_b(k,i) \equiv 1$ for saturated networks. The neglect leads to $p_t(k,i) = p_m$ and decouples n_k and n_i. It also results in an overestimation of the cumulated interference and a very conservative $p_{s,i}$ when $p_b(k,i) \ll 1$.

To explain how n_i and n_k are correlated, consider the simple two-node tandem network in Fig. 6.2 (set $i = 1, k = 2$). The channel can be regarded as a demultiplexer which forwards a fraction $p_{s,i}(t)$ of the flow to the following node while returning a fraction $1-p_{s,i}(t)$ to the buffer of n_i for retransmission. In general, the buffer occupancy B_i is determined by the arrival process and the service process $p_{s,i}(t)$. Since the latter is connected to $p_{s,k}(t)$ through feedback, B_i and B_k are correlated, so are the transmissions of n_i and n_k.

The calculation of $p_b(k,i)$ is analytically complicated due to the involvement of the correlated queueing systems of n_k and n_i. The correlation is mainly caused by the arrival processes $A_i(t)$. As shown in Fig. 6.2, $A_2(t)$ is composed of three parts,

$$A_i(t) = p_{s,i-1}(t-1)A_{i-1}(t-1) + (1 - p_{s,i}(t-1))A_i(t-1) + S_i(t), \qquad (6.2)$$

which is obviously correlated with $A_1(t)$ even if the local flows $S_1(t)$ and $S_2(t)$ are

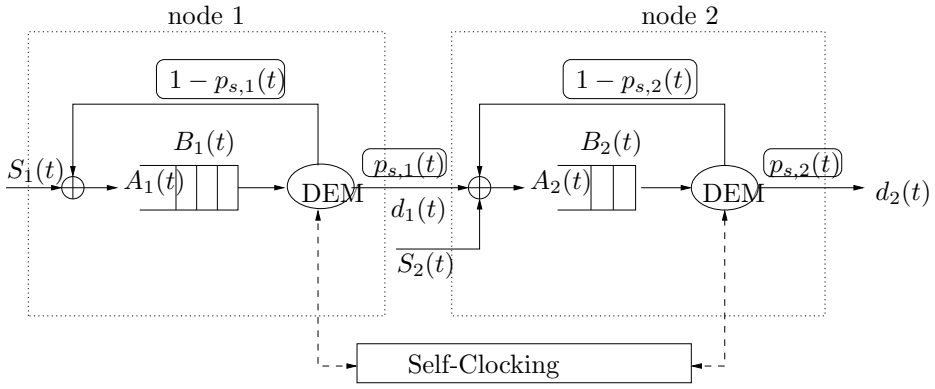

Figure 6.2. The correlations in a two-node tandem network

generated independently.

However, if approximating $p_b(k,i) \approx \Pr\{B_k > 0 | B_i > 0\}$, it is clear that $p_b(k,i)$ is monotonically increasing with its arrival rate λ_k and decreasing with its service rate $p_{s,k}$[1]. Plugging $p_t(k,i) = p_m p_b(k,i)$ into (6.1), we can see the following correlations,

- *Auto-correlation in channels*: the increase of $p_{s,k}$ leads to a decrease of $p_b(k,i)$ and $p_t(k,i)$ such that $p_{s,i}$ is enhanced, and vice versa. This positive feedback (correlation) [117] is consistent with the observation in Fig. 6.2. For instance, if $p_{s,2}$ increases, B_2 will be emptied quickly. Then, when n_1 is transmitting, it is highly likely that $B_2 = 0$, implying that n_2 will not interfere with the transmission of n_1 so that the transmission succeeds with high probability and $p_{s,1}$ increases.

- *Cross-correlation between channels and traffic rates*: The increase of λ_k leads to an increase of $p_b(k,i)$ and $p_t(k,i)$ such that $p_{s,i}$ is reduced, and vice

[1]In [114], it is stated that the correlation is positive in terms of the queue lengths if n_k and n_i are immediate neighbors. Moreover, the correlation increases with the traffic rate and the burst size.

versa. In Fig. 6.2, if λ increases, the buffer size B_1 increases and n_1 has to transmit more frequently to deliver these extra packets. Then, when n_2 is transmitting, $B_1 > 0$ with a high probability and n_1 interferes with n_2's transmission, which makes $p_{s,2}$ decrease.

Note that due to the above correlations, the correlation in the arrival processes $A_i(t)$ becomes more complicated, which, in turn, further complicates the correlations in channels and traffic. For tractable analysis, we consider two extreme cases,

$$\begin{cases} A_i(t) = S_i(t) + (1 - p_{s,i}(t-1))A_i(t-1) \\ A_i(t) = p_{s,i-1}(t-1)A_{i-1}(t-1) + (1 - p_{s,i}(t-1))A_i(t-1), \quad \text{with} \\ \qquad A_1(t) = S_1(t) + (1 - p_{s,1}(t-1))A_1(t-1). \end{cases} \tag{6.3}$$

In the first case, there are only local traffic flows, *i.e.*, the flows are terminated after one-hop transmission. Then $A_i(t)$ is merely correlated with each other due to the correlated channel qualities $p_{s,i}$. In the second case, $S_i(t) \equiv 0$ for all $i > 1$, corresponding to a single-flow in the network. Then, $A_i(t)$ is explicitly correlated with each other. If $p_{s,i} \equiv 1$ (perfect channel), in the first case, $A_i(t) = S_i(t)$ is independent of each other and referred to as "independent" flows; in the second case, $A_i(t) = S_1(t)$ is completely correlated with each other and referred to as "completely correlated" flows. Therefore, the two cases provide upper and lower bounds for other correlation levels. For fair comparison, we set the rate $R_i = \lambda$. If $p_{s,i} < 1$, the failed packets will be retransmitted and then make $A_i(t)$ different from $A_{i-1}(t)$. The difference between $A_i(t)$ and $A_{i-1}(t)$ is the measurement of how closely $A_1(t)$ and $A_2(t)$ is correlated.

The correlations are evaluated via the conditional probability $p_b(k, i)$, which

can be interpreted as the probability that the busy periods of n_k and n_i overlap. The unconditional busy probability is ρ_k, the traffic intensity, defined as the ratio of the arrival rate to the service rate. We are interested in how $p_b(k,i)$ is close to ρ_k in the presence of the correlations.

- The line network behaves like a Markov chain. The correlation between two nodes diminishes as their distance increases. Therefore, if n_k and n_i are far away from each other, there is no correlation and $p_b(k,i) \to \rho_k$. The impact of the correlations is overshadowed by the long distance between n_i and n_k. The distance between n_i and its interferers is determined by the MAC scheme. Here we study two typical MAC schemes, m-phase TDMA and slotted ALOHA.

- If $\rho_k \to 1$, the busy periods of n_k will cover the whole time slot and certainly overlap with that of n_i regardless of the buffer occupancy of n_i, *i.e.*, $p_b(k,i) \to \rho_k \approx 1$. In other words, the impact of the correlations is overshadowed by the heavy traffic load.

- Traffic burstiness has an impact on $p_b(k,i)$ even for memoryless Bernoulli traffic [114]. In Fig. 6.2, if packets arrive in batches at n_1, then n_1 has packets buffered after it delivers one packet to n_2. At the following instant, both n_1 and n_2 are busy, *i.e.*, $p_b(k,i) \to 1$. On the other hand, for smooth traffic, the two arrivals are usually separated by a non-zero interval. n_1 is probably idle after delivering a packet to n_2 and their busy periods are not overlapped. Naturally, bursty traffic results in higher $p_b(k,i)$ than smooth traffic.

To distinguish the impact of traffic burstiness, we consider three typical models,

CBR, on-off and Bernoulli. In CBR, the packet interarrival time is a constant $r = 1/\lambda$. In on-off, the arrival process is modulated by a two-state Markov chain that alternates between ON (1) and OFF (0) states. A packet is generated only when the Markov chain is in state ON. The transition probabilities between ON and OFF are a_{01} and a_{10}, respectively. This model generates a stream of correlated bursts and silent periods both of which are geometrically distributed in length. The mean burst length is $B = 1/a_{10}$. The average rate $\lambda = a_{01}/(a_{10} + a_{01})$. Bernoulli is a special on-off model with $a_{01} + a_{10} = 1$. The generated burst and silent periods are independent so that Bernoulli traffic is memoryless.

6.2 m-phase TDMA

In m-phase TDMA [94], every node is allocated to transmit once in m time slots, and nodes m hops apart can transmit simultaneously. Then, the interferers of n_i are lm ($l = 1, 2, \ldots$) hops away from n_i with $p_m = 1$. Using the shortest path first routing protocols, the receiver is n_{i+1}. Then, the distance from the interferer n_k to the receiver is $d_k/d_i = lm + 1$ if n_k is on the left side of n_{i+1}, referred to as left interferer, and $d_k/d_i = lm - 1$ if n_k is on the right side of n_{i+1}, referred to as right interferer. Based on the statement in Section 6.1, the impact of the correlations is overshadowed by the long distance between n_i and n_k. With m chosen appropriately, $p_b(k, i) \approx \rho_k$. In TDMA, $\rho_k = m\lambda/p_{s,k}$ at the frame (m slots) level [142], in which the traffic rate λ is multiplied by a factor m to account for the packet accumulation in the frame. Plugging $p_t(k, i) \approx \rho_k$ into (6.1), we have

$$p_{s,i} = \prod_{k \in \mathbb{I}_i} \Big(1 - \frac{m\lambda}{p_{s,k}(1 + (lm \pm 1)^\alpha/\Theta)}\Big), \tag{6.4}$$

where $\mathbb{I}_i = \{k|(k \bmod m) = (i \bmod m)\}$ and $d_k/d_i = lm \pm 1$. Positive feedback in $p_{s,i}$ and $p_{s,k}$ and negative feedback in $p_{s,i}$ and λ are explicitly revealed in (6.4). Given the parameter m, define the network throughput $\lambda_{\max}$ as the maximum rate accommodated by the network. The network capacity λ_C is obtained by maximizing $\lambda_{\max}$ over m.

6.2.1 Network Throughput and Capacity

The network throughput is determined at the bottleneck area where the nodes experience the worst channel quality $p_{sL} \leq p_{s,i}$. The network traffic distribution can be classified into *heterogeneous* and *homogeneous*, distinguished by whether the arrival rates at each node are identical or not. For the homogeneous traffic distribution, $\lambda_i = \lambda_k = \lambda$ and the network throughput and capacity are calculated when $\lambda = \max_i\{\lambda_i\}$. Thus, p_{sL} occurs at the center nodes that have approximately the same number of right and left interferers, which is denoted by K

$$K = \lceil \frac{\lfloor \frac{N}{m} \rfloor}{2} \rceil - 1. \tag{6.5}$$

Replacing $p_{s,k} \geq p_{sL}$ into (6.4), we approximate p_{sL} as follows

$$p_{sL} \leq \prod_{l=1}^{K} \Big(\Big(1 - \frac{m\lambda}{p_{sL}\big(1+(lm+1)^{\alpha}/\Theta\big)}\Big)\Big(1 - \frac{m\lambda}{p_{sL}\Big(1+(lm-1)^{\alpha}/\Theta\Big)}\Big)\Big) \quad (6.6)$$

$$\approx 1 - \frac{m\lambda}{p_{sL}} \sum_{l=1}^{K} \Big(\frac{1}{1+(lm+1)^{\alpha}/\Theta} + \frac{1}{1+(lm-1)^{\alpha}/\Theta} \Big) \quad (6.7)$$

$$\lessapprox 1 - \frac{2m\lambda}{p_{sL}} \sum_{l=1}^{K} \frac{1}{1+(lm)^{\alpha}/\Theta} \quad (6.8)$$

$$\approx 1 - \frac{2m\lambda}{p_{sL}} \int_{0.5}^{K+0.5} \frac{\Theta}{\Theta+(mx)^{\alpha}} dx, \quad (6.9)$$

$$\triangleq 1 - \frac{2m\lambda}{p_{sL}} g(m,\Theta,\alpha), \quad (6.10)$$

The approximation in (6.7) comes from the fact that for $0 \leq m\lambda/p_{sL} \leq 1$ and $1/(1+(lm \pm 1)^{\alpha}/\Theta) \ll 1$, the product can be approximated by the sum [21]. The approximation in (6.8) uses the convexity of the function $1/(1+x^{\alpha}/\Theta)$. Since $m^{-\alpha}$ is very small, the sum in (6.8) is approximated by an integral in (6.9), where the integral is denoted by $g(m,\Theta,\alpha) \geq 0$. Note that $g(m,\Theta,\alpha)$ monotonically decreases with m and α, and increases with Θ.

For heterogeneous traffic distribution, $\lambda_i \neq \lambda_j$. A simple example is that every node generates a traffic flow of identical rate $r_i \equiv r$. In the line network, $\lambda_i = ir$ and $\lambda = Nr$. Let L denote the index of the node where p_{sL} occurs. Then,

$$L = Km + \mathrm{Rem}\big(\frac{N}{m}\big), \quad N = L + (K-1)m.$$

A similar calculation as in (6.9) yields the upper bound (replacing λ by $(L-lm)r$

and $(L+lm)r$ for the distance $lm+1$ and $lm-1$, respectively)

$$\begin{aligned} p_{sL} &\lessapprox 1 - \frac{m\lambda}{p_{sL}} \sum_{l=1}^{K} \frac{1}{1+(lm)^{\alpha}/\Theta} \\ &\approx 1 - \frac{m\lambda}{p_{sL}} g(m,\Theta,\alpha). \end{aligned} \tag{6.11}$$

Apparently, the obtained p_{sL} is greater than that obtained for the homogeneous traffic distribution. Since the network throughput and capacity are determined by the worst-case scenario, they are studied based on the homogeneous traffic distribution (6.9), from which p_{sL} can be solved as a root to a quadratic equation,

$$p_{sL} \approx \frac{1}{2}\left(1 + \sqrt{1 - 8m\lambda g(m,\Theta,\alpha)}\ \right). \tag{6.12}$$

The integral can be calculated numerically. Specially, for $\alpha = 2$, (6.12) is simplified to

$$\begin{aligned} p_{sL} &\approx \frac{1}{2}\left(1 + \sqrt{1 - 8\lambda\sqrt{\Theta}\Big(\arctan\big(\frac{(K+0.5)m}{\sqrt{\Theta}}\big) - \arctan\big(\frac{m}{2\sqrt{\Theta}}\big)\Big)}\ \right) \\ (\text{for } K \to \infty) &\approx \frac{1}{2}\left(1 + \sqrt{1 - 8\sqrt{\Theta}\lambda\Big(\frac{\pi}{2} - \arctan\big(\frac{m}{2\sqrt{\Theta}}\big)\Big)}\ \right) \end{aligned} \tag{6.13}$$

For fixed Θ and α, p_{sL} is a function of the traffic rate λ and MAC parameter m. If $\lambda_i \neq \lambda_k$, the calculation will be more complex. But (6.6) shows that the obtained p_{sL} will be better than in the case $\lambda_i = \lambda_k = \lambda = \max_i\{\lambda_i\}$. The inclusion of λ distinguishes (6.12) from previous work for saturated networks [50, 88, 155]. Plugging $p_b(k,i) \equiv 1$ into (6.4), we obtain a p_{sL}^F at the saturated state,

$$p_{sL}^F \approx 1 - 2g(m,\Theta,\alpha), \tag{6.14}$$

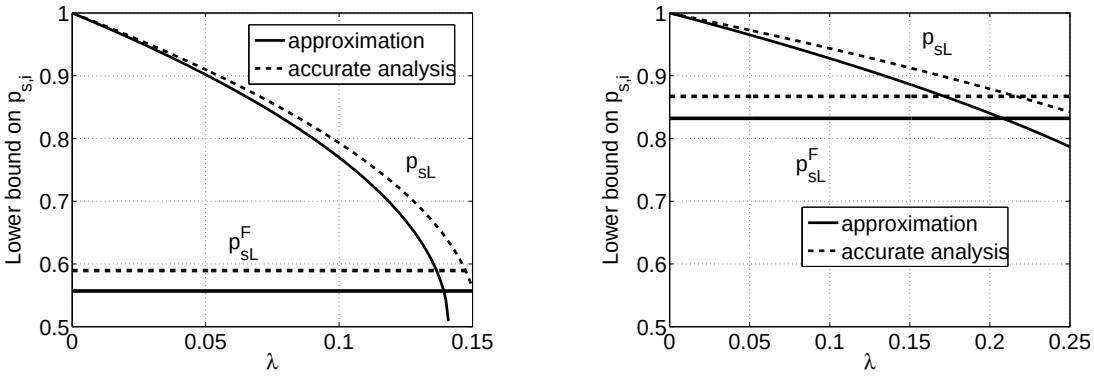

(a) $\alpha = 3$ (b) $\alpha = 4$

Figure 6.3. Comparison of the lower bound on $p_{s,i}$ for non-saturated and saturated TDMA line networks with $\Theta = 10, m = 4$

which is independent of λ. Fig. 6.3 compares p_{sL} and p_{sL}^F for $\Theta = 10, m = 4$ where p_{sL}^F is a constant. For light traffic (non-saturated state), a huge gap exists between p_{sL} and p_{sL}^F. The real channel p_{sL} performs much better than p_{sL}^F. The resulting buffer occupancy and packet delay are thus shorter than at the saturated state.

To guarantee network stability, the nodes experiencing p_{sL} should be stable with $\rho = m\lambda/p_{sL} < 1$. Plugging p_{sL} (6.12) into the stability condition,

$$2m\lambda < 1 + \sqrt{1 - 8m\lambda g(m, \Theta, \alpha)}, \tag{6.15}$$

we are able to calculate the network throughput $\lambda_{\max}$ as

$$\lambda_{\max} = \frac{1 - 2g(m, \Theta, \alpha)}{m}. \tag{6.16}$$

Fig. 6.4 shows $\lambda_{\max}$ as a function of m for $\Theta = 10$ with $\alpha = 3$ and $\alpha = 4$,

in which $\lambda_{\max}(m)$ is not monotonic. Increasing m will decrease the potential interference and improve the channel capacity p_{sL}. However, it also implies smaller spatial reuse, which potentially decreases the network throughput. Note that as the maximum achievable traffic rate, the throughput $\lambda_{\max}$ is obtained by $\rho = 1$. Therefore, applying p_{sL}^F (6.14) for the saturated network to the stability condition leads to the same result of $\lambda_{\max}$. The network capacity $\lambda_C = \max_m\{\lambda_{\max}\}$ is obtained by maximizing over m. More specifically, differentiating $\lambda_{\max}$ (6.16) by m and equating to zero,

$$1 - 2g(m, \Theta, \alpha) + 2mg'_m(m, \Theta, \alpha) = 0, \tag{6.17}$$

the solution m^* is the optimum value of m achieving λ_C. Plugging m^* into (6.16), we obtain λ_C

$$\lambda_C = \frac{1 - 2g(m^*, \Theta, \alpha)}{m^*} = -2g'_m(m^*, \Theta, \alpha) \leq \frac{1}{m^*}. \tag{6.18}$$

Since $g(m, \Theta, \alpha)$ is non-negative, the network capacity cannot exceed $1/m^*$. Fig. 6.5 displays the capacity λ_C, which is monotonically decreasing with Θ. Generally, the higher SIR threshold Θ restricts spatial reuse and therefore results in lower capacity.

6.2.2 Simulation Results

In TDMA, the impact of the correlations can be neglected as m is large. The lower bound p_{sL} on the success probability $p_{s,i}$, the network throughput and capacity are all derived based on the assumption of $p_b(k, i) = \rho_k$ as if the nodes were independent. To validate the accuracy of the assumption, simulation results

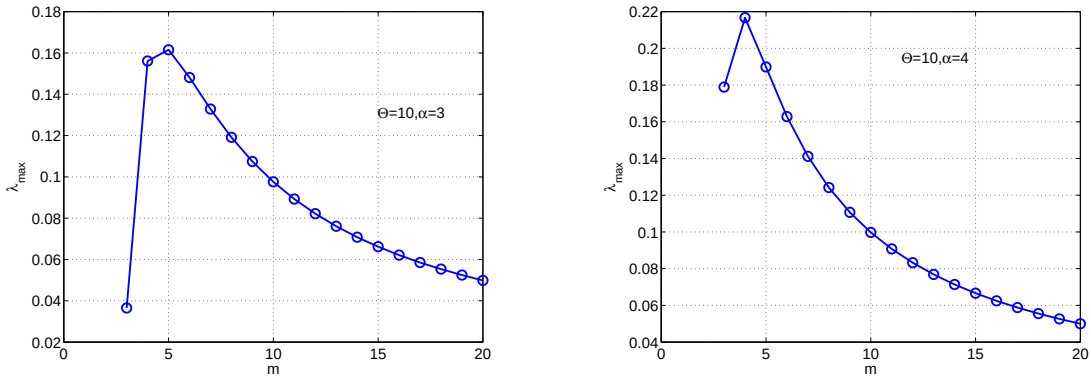

(a) $\alpha = 3$ (b) $\alpha = 4$

Figure 6.4. Network throughput $\lambda_{\max}$ as a function of TDMA parameter m in a line network with $\Theta = 10$

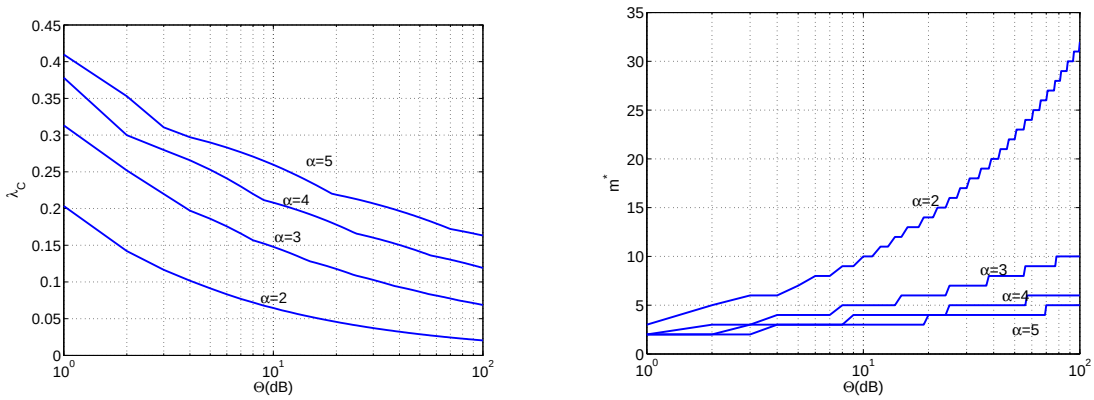

(a) λ_C (b) m^*

Figure 6.5. The network capacity λ_C of TDMA line networks

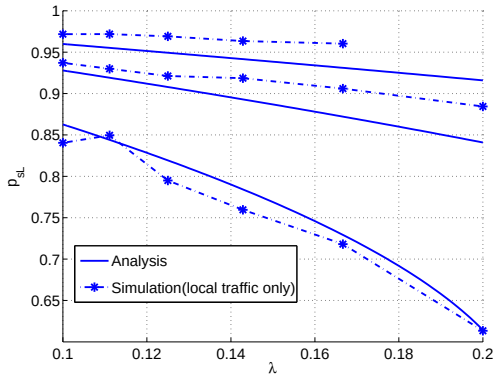

(a) Comparison of the analysis and simulations

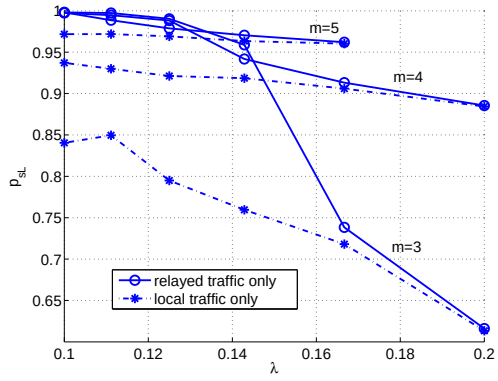

(b) Channel quality of networks with independent and correlated traffic flows

Figure 6.6. The channel quality p_{sL} in TDMA networks with CBR traffic and $\alpha = 4, \Theta = 10$

are provided. First, in Fig. 6.6(a) with independent flows, the simulated channel quality p_{sL} is very close to the analytical result (6.12), particularly with λ increasing. Second, in Fig. 6.6(b), we compare the channel performance under the two extreme cases, independent flows and completely correlated flow. As long as the traffic rate λ is equivalent, the channels behave similarly regardless of the traffic flows are correlated themselves. Therefore, the analytical results on the lower bound p_{sL}, the network throughput $\lambda_{\max}$ and capacity λ_C are quite accurate in TDMA networks with m large enough.

On the other hand, if m is small, the correlation at the arrivals become more important. In our simulations, the more closely correlated the arrivals, the better the channel quality p_{sL} (Fig. 6.6(a), light traffic with $\lambda < 0.15$). However, the channel performance improvement is less apparent as the traffic rate λ and thus the normalized traffic intensity ρ_k increases. In other words, in terms of p_{sL}, the

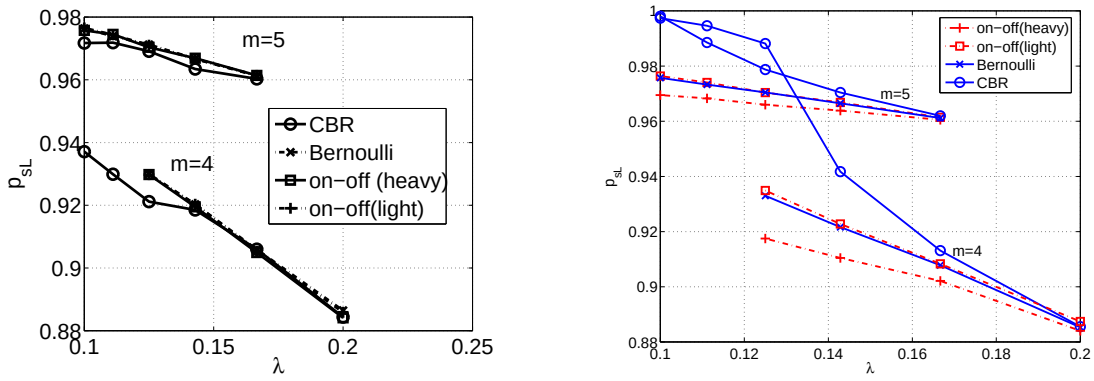

(a) Independent traffic flows

(b) Dependent traffic flows

Figure 6.7. The impact of traffic burstiness in TDMA networks with $\alpha = 4, \Theta = 10$

impact of traffic intensity overshadows that of the traffic correlation.

In Fig. 6.7, we can see that traffic burstiness plays a role mainly in networks with correlated traffic flows. Here the light and heavy bursty on-off processes are defined based on the burst size. Set $1/(1-\lambda)$ (the burst size of Bernoulli traffic) as the standard burst size. Light on-off has a burst size of $(1/(1-\lambda)-(1-\lambda))/2$ while heavy on-off has a burst size of $\lambda/2$. As expected in Section 6.1, bursty traffic results in a higher $p_b(k,i)$ and thus a lower channel quality p_{sL} than smooth traffic (Fig. 6.7(b)). The heavier the burstiness, the worse the channel. But the impact of burstiness is overshadowed by the traffic intensity since with λ increasing, the channel quality p_{sL} converges regardless of traffic burstiness.

In summary, $p_b(k,i)$ is affected by the following factors in an order of 1) distance m between n_k and n_i; 2) traffic intensity ρ_k or traffic rate λ; 3) traffic correlation; and finally 4) burstiness.

6.3 Slotted ALOHA

6.3.1 Network Throughput and Capacity

In ALOHA [4], every node independently transmits with access probability p_m when *it has packets*. ALOHA can be regarded as a special case of TDMA with $m = 1$ and $p_m \neq 1$. So the interference set is $\mathbb{I}_i = \{k | k \neq i\}$, which means that the distance between the transmitter and interferers may be too small to neglect the correlation between them as in TDMA. Due to the complexity of deriving the correlations, ALOHA is mainly studied through simulation results. But as shown in Section 6.2.1 for TDMA, the throughput and capacity are calculated when the network is at the saturated state and can be directly derived by p_{sL}^F, which does not involve in the conditional probability $p_b(k,i)$. Plugging $p_t(k,i) = p_m p_b(k,i) = p_m$ and $d_k/d_i = 0, 1, 2, \ldots$ (p_{sL} occurs at the center) into (6.1), we obtain

$$\begin{aligned} p_{sL}^F &\leq (1-p_m)(1-\frac{p_m}{1+1/\Theta})\Big(\prod_{k=2}^{\infty}\big(1-\frac{p_m}{1+k^\alpha/\Theta}\big)\Big)^2 \\ &\triangleq (1-p_m)(1-\frac{p_m}{1+1/\Theta})\big(g(p_m,\Theta,\alpha)\big)^2. \end{aligned} \tag{6.19}$$

Like in [51], for small p_m, $\log(1-p_m/(1+k^\alpha/\Theta)) \lessapprox -p_m/(1+k^\alpha/\Theta)$, which leads to $g(m,\Theta,\alpha) \approx e^{-p_m/\sigma}$, where

$$\sigma^{-1} = \sum_{k=2}^{\infty}\frac{1}{1+k^\alpha/\Theta}. \tag{6.20}$$

Specially, for $\alpha = 2$ and $\alpha = 4$, $g(m,\Theta,\alpha)$ is further simplified to

$$\begin{cases} g(m,\Theta,\alpha)(1-\dfrac{p_m}{1+1/\Theta}) \approx \dfrac{e^{\sqrt{2}y_1}}{\sqrt{1-p_m}e^{\sqrt{2}y_2}} & \alpha = 2 \\ g(m,\Theta,\alpha)(1-\dfrac{p_m}{1+1/\Theta}) = \dfrac{\cosh^2(y_1)-\cos^2(y_1)}{\sqrt{1-p_m}(\cosh^2(y_2)-\cos^2(y_2))} & \alpha = 4, \end{cases} \tag{6.21}$$

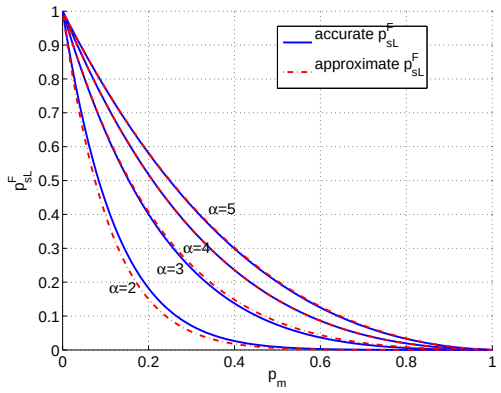

(a) Lower bound p_{sL}^F on $p_{s,i}$ for $\Theta = 10$

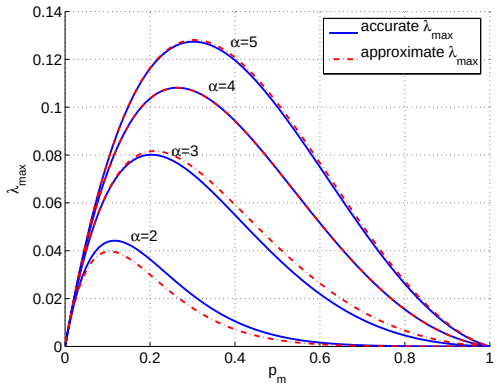

(b) Network throughput $\lambda_{\max}$

Figure 6.8. The network throughput and capacity in ALOHA networks

where $y_1 := \pi \sqrt[\alpha]{\Theta(1-p_m)}/\sqrt{2}$ and $y_2 := \pi \sqrt[\alpha]{\Theta}/\sqrt{2}$. Fig. 6.8(a) verifies that the approximation of $g(p_m, \Theta, \alpha)$ is accurate for p_{sL}^F when $\alpha > 2$. Plugging p_{sL}^F into the stability condition $\rho_k = \lambda/(p_m p_{sL}^F) < 1$, we obtain the network throughput $\lambda_{\max}$,

$$\lambda_{\max} \lessapprox p_m(1-p_m)(1-\frac{p_m}{1+1/\Theta})e^{-p_m/\sigma}. \tag{6.22}$$

Like in TDMA, Fig. 6.8(b) shows that $\lambda_{\max}$ is not monotonic with the MAC parameter p_m. To calculate the capacity λ_C, maximizing $\log(\lambda_{\max})$ over p_m, which is equivalent to maximizing $\lambda_{\max}$ over p_m, yields the optimal p_m to achieve the capacity, denoted by $p_m^* = \arg\max_{p_m} \lambda_{\max}$

$$c_0(p_m^*)^3 + c_1(p_m^*)^2 + c_2 p_m^* + c_3 = 0, \tag{6.23}$$

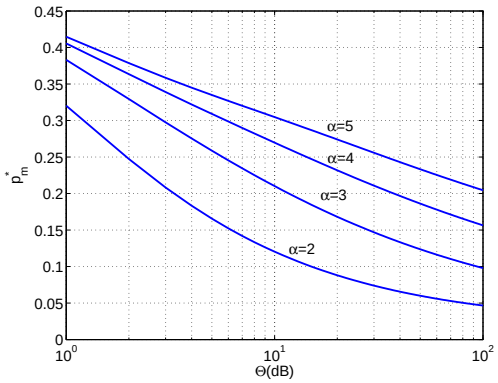

(a) The optimal p_m^* to achieve the capacity

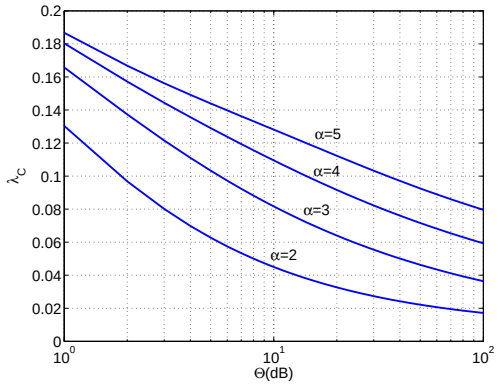

(b) The network capacity λ_C

Figure 6.9. The capacity of ALOHA line networks

with

$$\begin{cases} c_0 = 2\Theta\sigma^{-1}, \quad c_1 = -(2\sigma^{-1} + 3\Theta + 4\Theta\sigma^{-1}) \\ c_3 = -(1+\Theta), \; c_2 = 2(1 + 2\Theta + \sigma^{-1} + \Theta\sigma^{-1}). \end{cases} \tag{6.24}$$

p_m^* is the solution to the above third order polynomial. Fig. 6.9(a) displays p_m^* as a function of the SIR threshold Θ. The network capacity λ_C is

$$\lambda_C = p_m^*(1-p_m^*)(1 - \frac{p_m^*}{1+1/\Theta})e^{-p_m^*/\sigma}, \tag{6.25}$$

which is exhibited in Fig. 6.9(b). In a saturated network, if all nodes transmits independently, a higher access probability p_m allows more nodes to transmit simultaneously but results in more severe interference. The network capacity λ_C is achieved at a small p_m, typically $p_m \leq 0.4$ (Fig. 6.9(a)).

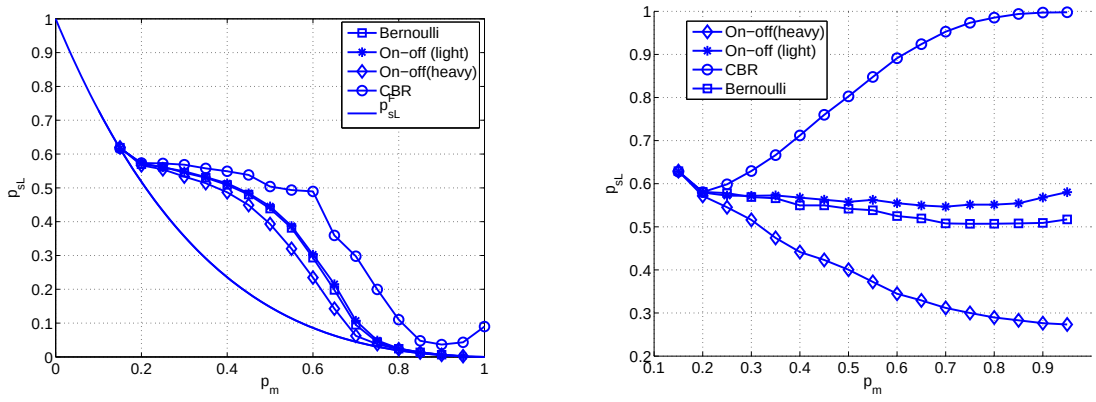

(a) Independent flows

(b) Correlated flows

Figure 6.10. Realistic channel performance in ALOHA networks with $\lambda = 0.1, \Theta = 10, \alpha = 4$.

6.3.2 Correlated Traffic Flows in ALOHA Networks

Practical networks are not saturated, so $p_b(k,i) \equiv 1$ does not hold. Fig. 6.10(a) displays the difference between the analytical lower bound p^F_{sL} (6.19) and the simulated minimum success probability p_{sL} for four traffic types with rate $\lambda = 0.1$. The traffic intensity $\rho = \lambda/(p_m p_{sL})$ is close to 1 when i) p_m is too small, in which the node keeps holding the packets too long and increases the buffer occupancy; ii) p_m is too large, in which more nodes transmit simultaneously and decrease the transmission success probability. Therefore, the analysis p^F_{sL} is tight when $p_m < 0.3$ or $p_m > 0.6$. Other than that, the real channel quality p_{sL} is much better than at the saturated state. Simply assuming $p_b(k,i) \equiv 1$ will underestimate the channel quality and lead to inefficient admission control.

Moreover, traffic burstiness has a more obvious impact on p_{sL} than in TDMA. Even if the traffic flows are independent themselves, for CBR traffic, p_{sL} remains

approximately unchanged with $p_m \in (0.2, 0.6)$, while for heavy bursty on-off, p_{sL} sharply decreases from 0.6 to 0.2. If the traffic flows are correlated, the impact of burstiness becomes more visible Fig. 6.10(b). For CBR traffic, the channel quality p_{sL} surprisingly does not decrease with increasing p_m as expected. Instead, p_{sL} converges to 1, like a perfect channel (Fig. 6.10(b)). On the other hand, for heavy bursty on-off traffic, p_{sL} varies with p_m in a similar way as in independent flows. However, for Bernoulli and light bursty on-off traffic, p_{sL} turns out to be less affected by p_m since it is like a constant between 0.5 and 0.6 when p_m increases from 0.2 to 1. In short, unlike TDMA, traffic correlation plays a important role in ALOHA with random transmission orders.

Recall that the traffic correlation mainly affects the conditional busy probability $p_b(k, i)$ of n_k given that n_i is transmitting. As an example, consider $p_b(k, 1)$ given that n_1 is the only source node in the network. In Fig. 6.11(a), $p_b(k, 1)$ is compared to the unconditional busy probability ρ_k. A small p_m, *e.g.*, $p_m = 0.15$, implies heavy traffic intensity and a large ρ_k, in which $p_b(k, 1) \approx \rho_k \to 1$. As p_m increases but does not cause serious interference, the traffic intensity ρ_k will decrease, so will the node busy periods. Then, $p_b(k, 1) \leq \rho_k < 1$, as shown in Fig. 6.11(a) for $p_m = 0.4$, in which the immediate neighbor n_2 of n_1 is idle more often with $p_b(2, 1) = 0.1$ when n_1 is transmitting than in equilibrium with $\rho_2 = 0.3$. That is why in ALOHA it is not appropriate to approximate $p_b(k, i) \approx \rho_k$.

Particularly, as p_m is close to 1, *e.g.*, $p_m = 0.85$, most nodes are quite silent with $p_b(k, 1) \to 0$ except n_{10} and its neighbors. It is no coincidence that the CBR flow is of rate $\lambda = 0.1$ with a constant interarrival time of 10 slots. Therefore, in Fig. 6.11(b), we emphasize two nodes with respect to the source node n_1, the closest neighbor n_2 and the node n_{11} of 10 hops away. With p_m increasing, the

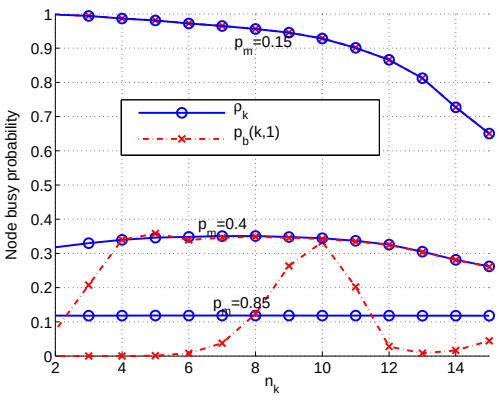

(a) Conditional busy probability $p_b(k,1)$

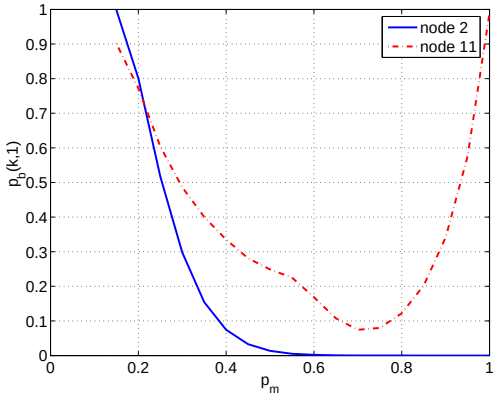

(b) Special cases of $p_b(k,1)$ with $k=2$ and $k=11$

Figure 6.11. The impact of traffic correlations on $p_b(k,i)$ in ALOHA with CBR traffic and $\Theta = 10, \alpha = 4$

smoothness of CBR traffic is better preserved, which leads the most influential interferer n_2 to be more silent and n_{11} to be more synchronous with n_1. At $p_m = 1$, ALOHA behaves like m-phase TDMA with $m = 1/\lambda$ if $1/\lambda$ is an integer.

Then, it is interesting to determine under which circumstance ALOHA can emulates TDMA. First, the traffic smoothness needs to be preserved, which takes place at $p_m \to 1$ for CBR traffic. That is why on-off and Bernoulli traffic cannot benefit from the increasing p_m (Fig. 6.11(b)) and possess better channel performance (Fig. 6.12(b)). But smoothness preservation is not sufficient. In Fig. 6.12(a), we present the conditional busy probabilities $p_b(k,1)$ of CBR traffic with different rate $\lambda = 1/m$. Denote a virtual interference set of n_1 by $\tilde{\mathbb{I}}_1 = \{k | k = 1 + lm\}$ $(l = 1, 2, \ldots)$. Note that in ALOHA, the interference set of n_1 is $\mathbb{I}_1 = \{k | k = 2, 3, \ldots\}$, larger than $\tilde{\mathbb{I}}_1$. With n_1 transmitting, only the nodes in $\tilde{\mathbb{I}}_1$ transmit with high probability $p_b(k,1) \to 1$ while all other nodes are most likely

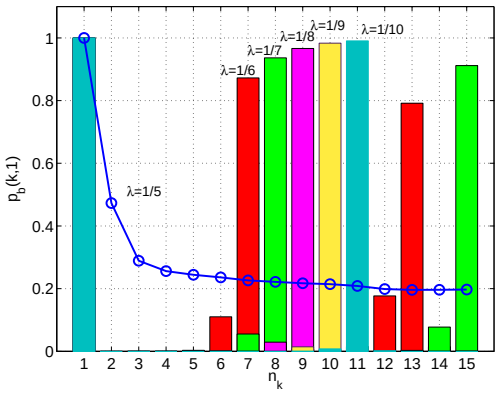

(a) The impact of traffic rate λ on the conditional busy probability $p_b(k,1)$

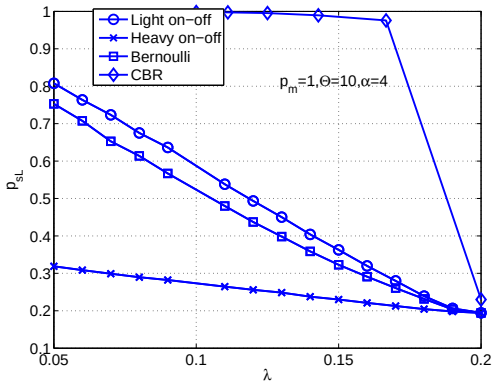

(b) The impact of traffic models on lower bound p_{sL} on the success probability

Figure 6.12. The conditions on which ALOHA emulates TDMA to generate a natural spacing between simultaneous transmitting nodes: i) CBR traffic; ii) $p_m = 1$; iii) traffic rate λ. ($\Theta = 10, \alpha = 4$)

to keep silent with $p_b(k,1) \to 0$. This phenomenon can be interpreted as that a natural spacing is formed between n_1 and its potential interferers, which narrows down the interference set to be $\tilde{\mathbb{I}}_1$. However, this spacing does not always exist. As λ increases to $\lambda = 0.2$, there is no obvious difference in $p_b(k,1)$ between $k \in \tilde{\mathbb{I}}_1$ and $k \notin \tilde{\mathbb{I}}_1$. In other words, the spacing disappears and the channel performance will be sharply degenerated as confirmed in Fig. 6.12(b). Therefore, ALOHA emulates TDMA only if the traffic rate is below the network capacity $\lambda_C = 0.2$. It is worth pointing out that the capacity for correlated flows is greater than for independent flows (Fig. 6.9(b), $\lambda_C = 0.1$ for $\Theta = 10, \alpha = 4$).

More importantly, even if the traffic rate is close to λ_C, say $\lambda = 1/6$, the channel quality p_{sL} is still very good and even slightly better than in TDMA. This benefit not only the network throughput and capacity, but also the end-to-

end delay. Based on queueing theory, with p_{sL} unchanged, a large p_m implies a smaller access delay and thus a smaller overall waiting delay. Since the traffic correlation exists in most multihop networks, it is important to investigate its advantages.

6.4 ALOHA with Packet Dropping Policy

The traffic correlation plays a distinct role in ALOHA. Counter-intuitively, for CBR and light bursty on-off traffic, increasing the access probability and having more nodes transmit simultaneously does not necessarily degenerate the channel performance. Instead, as long as the traffic rate is below the network capacity, for smooth traffic, the traffic correlation induces an almost equal spacing between transmitting nodes that makes ALOHA emulate TDMA and thus leads to enhanced channel qualities. But, there is one disadvantage that the spacing between simultaneously transmitting nodes is mainly determined by the traffic rate as $m = 1/\lambda$. If λ is small, the spacing factor m would be much larger than the optimum m^*, reducing spatial reuse. To solve this problem, we use packet dropping to control the spacing factor m. We begin with a simple strategy where the failed packet is discarded immediately. Then, queueing is excluded and every node has at most one packet in the buffer. The arrival process at n_{i+1} completely depends on n_i, including its arrival and channel $p_{s,i}$. More specifically, n_{i+1} has a non-empty buffer at time t only if n_i successfully delivers a packet to it at time $t-1$. Therefore, all correlations are excluded except for the traffic correlation.

Prior to study the transmission of n_i at time t, we first observe the transmission of n_{i-1} at time $t-1$. n_i is able to transmit at t only if n_{i-1} succeeded in transmission at $t-1$. Then, at $t-1$, the following events occur (Fig. 6.13),

1. the desired receiver n_i did not transmit at $t-1$ and thus n_{i+1} has no packets to transmit at t;

2. n_{i-1} cannot receive at $t-1$ as a half-duplex transceiver and it has no packet to transmit at t as well;

3. n_{i+1} did not transmit to n_{i+2} at $t-1$ since its transmission would interfere with that of n_{i-1} at n_i. As the most influential interferer, the impact of n_{i+1} would lead to a failed transmission even if the channel is capable of capture. Thus n_{i+2} has no packet at t;

4. n_{i-3} did not transmit because of the same reason as 3). Thus, n_{i-2} has no packet at t.

In summary, when n_i transmits at t, at least its four closest neighbors n_{i-2}, n_{i-1}, n_{i+1}, n_{i+2} do not transmit and interfere. In practice, simulation results show that the transmissions to n_{i-3} and n_{i+3} are hardly successful at $t-1$. Therefore, these two nodes can be excluded from the interference set so that the nearest interferers are n_{i-4} and n_{i+4}. Similarly, if n_{i-4} or n_{i+4} does transmit, the other interferers are at least four hops away from them. In other words, this simple dropping policy leads ALOHA to emulate m-phase TDMA with $m = 4$. The difference lies in: i) the spacing is naturally generated without the overhead of establishing the frame structure; ii) there is no access delay because $p_m = 1$.

Due to the similarity with TDMA, the performance of this network can be derived in a similar way as in TDMA. For the case of correlated flows, n_1 is the only source generating a CBR flow of rate λ. The failed packets are discarded at

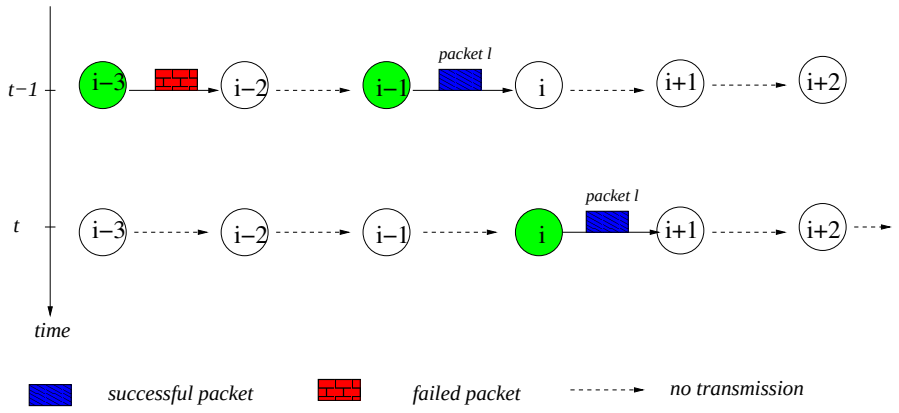

Figure 6.13. Transmission order in ALOHA with $p_m = 1$ and dropping policy

probability $1 - p_{s,i}$. Then, the arrival rate at n_i is

$$\lambda_i = \lambda \prod_{k=1}^{i-1} p_{s,k} \geq \lambda p_{sL}^{i-1}. \tag{6.26}$$

Since there is no access delay and no packets accumulation, unlike in TDMA, the traffic intensity is $\rho_k = \lambda_k / p_{s,k}$, m times less than in TDMA. That is why the obtained p_{sL} is better than in TDMA, as shown in the following. Due to the non-homogeneous traffic loads, the lower bound p_{sL} occurs at n_{m+1}. Plugging ρ_k into (6.6), we have

$$\begin{aligned}
p_{sL} &\approx \Big(1 - \frac{\lambda}{p_{sL}(1+(m+1)^\alpha/\Theta)}\Big) \prod_{k=1}^{\infty} \Big(1 - \frac{\lambda p_{sL}^{(k+1)m}}{p_{sL}(1+(km-1)^\alpha/\Theta)}\Big) \\
&\approx 1 - \frac{\lambda}{p_{sL}} \Big(\frac{1}{1+m^\alpha/\Theta} + p_{sL}^m \sum_{k=1}^{\infty} \frac{p_{sL}^{km}}{1+(km)^\alpha/\Theta} \Big) \\
&\approx 1 - \frac{\lambda}{p_{sL}} \big(\frac{1}{1+m^\alpha/\Theta} + \frac{p_{sL}^{2m}}{1+m^\alpha/\Theta} \big), \quad \beta \triangleq \frac{1}{1+m^\alpha/\Theta} \\
&= 1 - \frac{\lambda\beta}{p_{sL}} \big(1 + p_{sL}^{2m}\big),
\end{aligned} \tag{6.27}$$

where the term with the infinite sum is replaced by βp_{sL}^{2m} with a small error. Then, p_{sL} is solved as a root to the following polynomial

$$f(x) = bx^{2m} + x^2 - x + b. \quad b \triangleq \lambda\beta \tag{6.28}$$

In order to obtain an explicit expression, we use the second-order Taylor expansion at $x = 1$ to yield a quadratic equation. For $m = 4$, considering $f(1) = 2b$, $f^{'}(1) = 8b + 1$, and $f^{''}(1) = 56b + 2$,

$$p_{sL} = \frac{1 + 48b + \sqrt{1 + 8b - 160b^2}}{2(1 + 28b)}. \tag{6.29}$$

For small λ, Fig. 6.14(a) shows that $p_{sL}(\lambda)$ is linearly decreasing. The e2e dropping probability is upper bounded by $p_d \leq 1 - p_{sL}^N$, which is almost linear with λ for $\alpha \geq 4$ (Fig. 6.14(b)). Note that due to the packet dropping policy, the network throughput and capacity are not determined by the stability condition $\rho_k = \lambda_k / p_{sL} < 1$. Instead, based on the definition, the throughput is the number of packets that are successfully transmitted to the destination,

$$\lambda_{\max} = \lambda(1 - p_d) \geq \lambda p_{sL}^N, \tag{6.30}$$

which is shown in Fig. 6.14(c). Since $m = 4$ is predetermined by the dropping policy[2], the network capacity $\lambda_C = \lambda_{\max}$. The optimum m^* in TDMA to achieve the capacity ($m^* = 4$ for $\Theta = 10, \alpha = 4$) is obtained by using the dropping policy, which substantially improves spatial reuse.

The cost of dropping packets en route is low reliability that can be resolved by introducing redundancy. For instance, using erasure correcting codes [82], more

[2]In practice, $m > 4$ depending on α and Θ.

packets will be injected into the source node such that the destination node can recover the data even a portion of the data are lost. In Fig. 6.14(c), if a traffic flow of higher rate $\lambda = 0.3$ with 50% redundancy is injected, a throughput of $\lambda_{\max} = 0.2$ is guaranteed for $\alpha = 4, \Theta = 10$. Note that $\lambda_{\max} = 0.2$ ($\alpha = 4$) is the highest rate achievable in TDMA, while in this ALOHA with packet dropping the throughput is enhanced to $\lambda_{\max} > 0.3$ as $\lambda \to 1$. In other words, relaxing reliability requirement can improve throughput.

Meanwhile, in Fig. 6.14(a), at rate $\lambda = 0.3$, the channel is almost perfect with $p_{sL} > 0.95$, while in TDMA, at $\lambda_{\max} = 0.2$, the channel quality $p_{sL} < 0.9$ (Fig. 6.5(a)). As mentioned before, good channel qualities p_{sL} also imply short delays. Many applications can tolerate a small part of packet loss but are delay-sensitive. Moreover, from the perspective of energy efficiency, reducing reliability within a tolerable threshold is more efficient than keep retransmitting the failed packets. The latter consumes more energy on the packets which may be out-of-date at the destination due to long delays. In overall, it is beneficial to drop a small fraction of packets to save energy, reduce e2e delay and enhance throughput.

6.5 Conclusions

In this chapter we investigated the impact of the correlations in WMNs. First, the auto-correlation in the channel quality p_{sL} and the cross-correlation between p_{sL} and the traffic rate λ over Rayleigh fading channels are exposed through an explicit expression of p_{sL}. Second, the impact of the traffic correlation is reflected through the conditional node busy probability. In TDMA networks, due to the spacing between the transmitter and interferers, the statistical traffic parameters like burstiness and correlation are not as significant as the deterministic param-

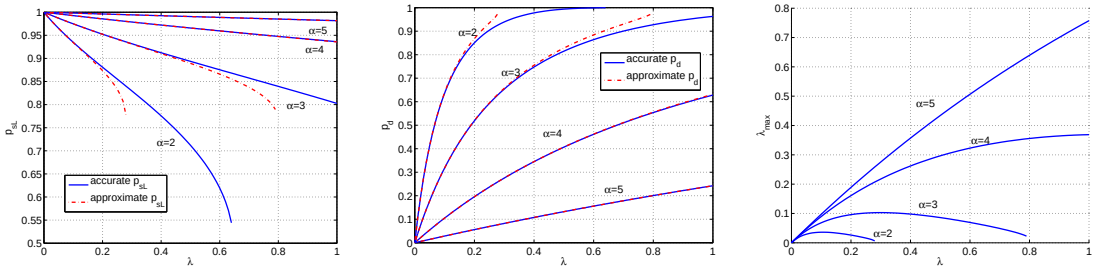

(a) Channel quality p_{sL}

(b) Packet dropping probability p_d

(c) Network throughput $\lambda_{\max}$

Figure 6.14. The network performance of ALOHA with dropping strategy and $\Theta = 10$

eter, traffic rate, in affecting the channel performance. We derive the network throughput and capacity by approximating the conditional busy probability by the unconditional probability.

In ALOHA networks, the statistical traffic parameters become dominant, particularly the traffic correlation. The throughput and capacity derived under independent traffic flows cannot capture the channel properties under correlated flows, especially for CBR traffic. In [146], it is found that the smoothness of CBR traffic is destroyed by the error-prone wireless channel with fixed success probability $1 - p_s$. In interference-limited Rayleigh fading channels, the success probability is time-varying. But, with the traffic correlation, the smoothness of CBR traffic is preserved by the traffic correlation even without MAC. This CBR-fed ALOHA network emulates TDMA to have a spacing naturally formed between the transmitting nodes. Since there is no overhead to establish the frame structure like in TDMA, the obtained performance is better than TDMA's in terms of throughput, capacity and channel quality p_{sL}. Then, it is helpful to combine the MAC scheme

with traffic regulation that can smooth bursty traffic flows.

To further explore the traffic correlation, we apply a packet dropping strategy to control the formation of the natural spacing for more efficient spatial reuse. Analysis shows that a simple dropping policy can lead to optimum m^* derived in TDMA. Although reliability is reduced because of packet dropping, the network throughput and channel performance are improved. If an intelligent dropping strategy is used instead of simply dropping the outdated packets, a better tradeoff between reliability, throughput and delay can be achieved.

CHAPTER 7

TRADEOFF BETWEEN DELAY AND RELIABILITY IN WIRELESS NETWORKED CONTROL SYSTEMS

The analysis in Chapter 5 shows that the e2e delay is very sensitive to the channel quality which dynamically changes in the wireless environment. The long delay incurred by bad channels cannot be tolerated by delay sensitive applications, *e.g.*, in WSNs, where data communication is required to be real-time and reliable. It is difficult, if not impossible, to guarantee hard delay bounds with full reliability. However, Section 6.4 reveals that dropping packets is an energy efficient approach to guarantee packet delays. Many delay-sensitive applications can tolerate a small amount of data loss, *e.g.*, network sensing and control systems (NSCS) [18, 71, 73, 77]. Then, it is sufficient to provide a balanced guarantee between the delay and reliability.

In previous work, the delay was guaranteed by allowing only one transmission attempt [73, 77]. Then the network is rather unreliable since reliability completely depends on the channel condition μ. If $\mu \ll 1$, the packet loss rate $p_L = 1 - \mu$ will be too large to be tolerable. On the other hand, in the fully reliable network, the failed packets will be retransmitted until they are received successfully. Similarly, the resulting delay is tightly controlled by the channel condition μ. If $\mu \ll 1$, the delay will be very long and cannot be tolerated by real-time applications. Besides, more energy will be wasted to retransmit packets that are outdated and should

be discarded. From the perspective of network stability, the traffic rate cannot be greater than μ. In interference-limited networks, Chapter 6 shows that μ at the hotspot nodes are very small. Then, only light traffic can be accommodated.

A balance between latency and reliability can be achieved by intentionally dropping a small percentage of outdated packets. Three packet dropping strategies discussed in [156] are Finite Buffer (FB), Bounded Delay (BD), and Limited Attempts (LA). Among them, BD can ensure a hard delay bound and will be used in this chapter. The dropping strategy is usually associated with the node scheduling algorithm to determine which packets are eliminated. For instance, if applications prefer the new packets over the old packets, priority scheduling (high priority to new packets) or Last-Come-First-Serve (LCFS) scheduling are used to drop outdated packets and yield the buffer space for new packets.

The network using the BD strategy is referred to as Delay Bounded (DB)-network. Compared to the fully reliable network, the DB network has several advantages. First, network stability is not an issue. Even if the traffic load is too heavy to be accommodated, the network is still able to self-stabilize after discarding some packets. Hence, a higher traffic rate than μ is allowed in the DB network. Second, less energy is wasted to retransmit packets that will be dropped eventually (refer these packets to as "marked" packets). Given the multihop topology, the sooner the marked packets are dropped, the better. Third, in interference-limited networks, as the overall traffic load decreases, the channel reception probability μ will be enhanced and more traffic flows will be admitted.

Unreliability caused by the BD strategy is measured by the packet loss rate p_L. As long as p_L is smaller than a predetermined threshold, the BD strategy is a sensible solution for the tradeoff between latency and reliability. Denote

the e2e delay bound by D_B. In this chapter, we derive the relationship between D_B and p_L, in particular for Networked Control Systems (NCSs) [144]. The tradeoff between the e2e delay, reliability, and the sampling rate is *jointly* studied with the consideration of the MAC scheme, the dropping strategy and multihop communication.

7.1 System Model

The system model for a NCS is outlined in Fig. 7.1(a), where the source (*e.g.*, sensor) data are transmitted over multiple wireless hops to the controller. Nodes 1 to N are relays. The data generated at the source node is time-critical, *e.g.*, periodic data used for updating controller output. A loop exists between the source, the controller and plant. Focusing on the MAC schemes, we consider a regular line network as shown in Fig. 7.1(b), which disposes of the routing and inter-flow interference problem. The obtained performance provides an upper bound for general two-dimensional networks because 1) the inter-flow interference is zero; 2) networks with equal node distances achieve better performance than those with unequal or random node distances [77]. Then, the set of communication links is modeled as a chain network (Fig. 7.1(b)). If packets are of fixed length, the objective is to analyze the discrete-time tandem queueing network controlled by wireless MAC schemes.

Two MAC schemes are studied, m-phase TDMA with frame length m and slotted ALOHA with transmit probability p_m. The wireless channel is characterized by its reception probability μ. The sampled source data (generated by the source in Fig. 7.1(a)) is assumed to be CBR of rate $1/r$. To simplify the analysis, the local scheduling algorithm is FCFS. Other scheduling algorithms like LCFS and

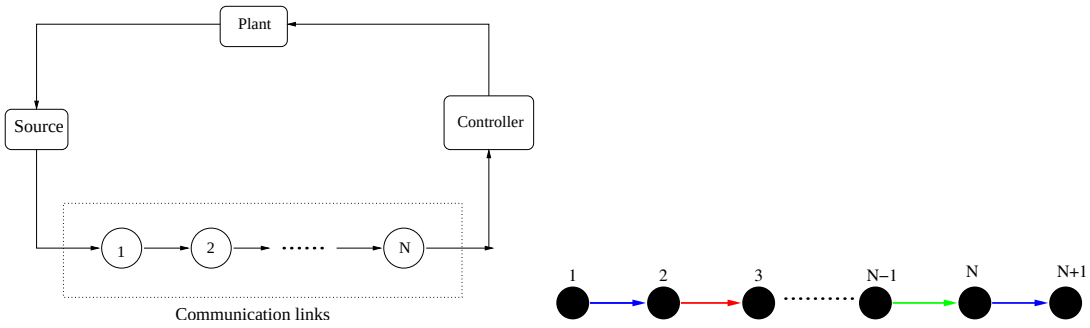

(a) Multihop NCS model (b) Regular line network

Figure 7.1. System models

priority scheduling can be chosen to better serve the NCS application demand.

The CBR arrival results in a non-Markovian queueing system, which substantially complicates the analysis. Despite of the enormous queueing theory literature, it is still difficult to track the transient behavior of non-Markovian systems [135], while the BD strategy is implemented based on the system transient behavior. Even if the source is deterministic and smooth, calculating the delay distribution in a time-dependent BD strategy is still a challenge. In addition, non-Poisson arrival causes correlations between the delays and queue lengths at individual nodes. Closed-form solutions exist only for some special networks, like Jackson networks, which do not include the networks considered here. In other words, accurate analyses are almost impossible in a multihop network with a long path. Therefore, we start the analysis with the first node, then investigate the network performance through simulation results.

From the perspective of energy efficiency, it is not recommended to drop the packet only when its e2e delay exceeds D_B, which often happens when the packet

reaches the last few nodes to the destination. The longer the route the packet traverses, the more energy is wasted. So, a local BD strategy is preferred. In order to determine how the local BD strategy is implemented, we first review the cumulated delay distribution in non-dropping tandem networks.

In [142], a fully reliable tandem queueing network is studied. CBR Traffic is transformed to correlated and bursty through the error-prone wireless channels. Even with correlation, the e2e delay is approximately linear in the number of nodes with respect to both the delay mean and delay variance, as confirmed by simulation results in Fig. 7.2. Then, it is reasonable to uniformly allocate D_B among nodes based on their relative distances to the source node [102], *i.e.*, the local delay bound D_i is set to be $D_i = iD_B/N = iD$ ($i \in [1, N]$, $D_i \in \mathbb{N}$). Packets are dropped at node i if their cumulated delay exceeds D_i. Intuitively, if a node experiences a delay at node i longer than D_i, then it is highly possible that it has delay longer than D_B at the final node N. Parameters of interest include the cumulated delay d_i and the packet loss rate p_L^i at node i ($1 \leq i \leq N$).

As proved in [142], the e2e delay mean of ALOHA is about $\mu/(1-\mu)$ times than that of TDMA. The gap is even larger for the delay variance as shown in Fig. 7.2(b). However, in WMNs, TDMA is not feasible for implementation, and simple MAC schemes like ALOHA are more desirable, even though TDMA substantially outperforms ALOHA in terms of both throughput and delay. The BD strategy is a solution to reduce the performance gap between TDMA and ALOHA.

Note that in the DB network, the packets are dropped according to their delays. Conventional queueing theory keeps track of the buffer size and cannot capture the packet dropping event [156]. So, we use a delay model [69], in which

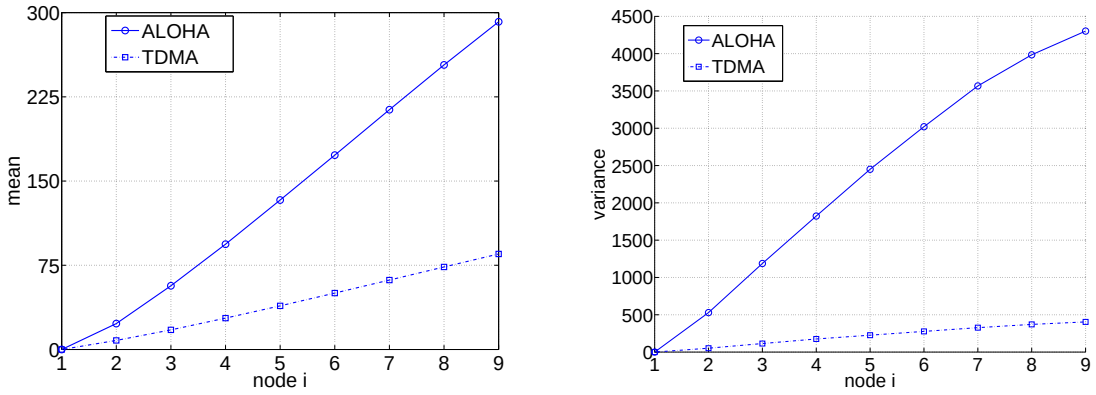

(a) delay means

(b) delay variances

Figure 7.2. Comparison of delay performance in the TDMA and ALOHA network with $m = 3, r = 4, \mu = 0.8, N = 8$

the system state is denoted by the packet delay such that the delay-dependent packet dropping event can be directly depicted through the system state.

7.2 Delay Bounded WMNs

7.2.1 m-phase TDMA

In TDMA networks, nodes $i, m+i, 2m+i, \ldots$ $(1 \leq i \leq m)$ can transmit simultaneously. The time is divided into frames of m slots. A transmission can be either a transmission of a new packet or a retransmission of a failed packet. For a node, the beginning of a frame is the beginning of the time slot allocated to this node. The transmission rate is $1/m$, and the transmission is successful with probability μ. To guarantee system stability, $r > m$. For heavy traffic, we assume $m < r < 2m$. At the frame level, the service time is geometric with μ. We start with the first node since it determines the traffic pattern of all subsequent nodes.

At the frame level, the interarrival time $1 < r/m < 2$ is not an integer even though it is a constant. Therefore, a standard Markov chain cannot be established as usual to keep track of the buffer size. Instead, we resort to the delay model that denotes the delay of the Head of Line (HOL) packet as the system state [69]. The system state is the waiting time of the HOL packet in terms of time slots, but the state transitions happen at the frame boundaries. Since the waiting time is the difference between the present time and the packet arrival time, the state value might be negative when the queue is empty and the next packet arrival does not happen. The absolute value of the negative state represents the remaining time till the next packet arrival. With a constant interarrival time r, the transition probability matrix $\mathbf{P} = \{P_{ij}\}$ is:

$$P_{ij} = \begin{cases} \mu & 0 \le i \le D-m, \quad j = i - \Delta, \\ 1-\mu & 0 \le i \le D-m, \quad j = i + m, \\ 1 & D-m < i \le D, \ \ j = i - \Delta \ \text{ or } \ i < 0, \ j = i + m, \end{cases} \tag{7.1}$$

where $\Delta := r - m > 0$. At frame t, let the HOL packet be packet k and its waiting time $w_k(t)$. If the transmission is successful, packet k departs at frame t, and the subsequent packet $k+1$ becomes the HOL packet at frame $t+1$. The waiting time of packet $k+1$ at frame t is $w_{k+1}(t) = w_k(t) - r$. It increases by m up to $w_{k+1}(t+1) = w_k(t) - r + m = w_k(t) - \Delta$ at frame $t+1$. Therefore, the system state transit from $w_k(t)$ to $w_k(t) - \Delta$ with probability μ. If $w_k(t) < \Delta$, packet k is the last packet in the buffer and the buffer becomes empty after its transmission. Then, the system transits to a negative state $i = -(\Delta - w_k(t)) < 0$. For $m < r < 2m$, the server idle time does not exceed one frame. Then, there must be a packet arrival during frame $t+1$. This new packet may arrive in the

middle of frame $t+1$ and cannot be transmitted immediately. The waiting time to access the channel is $m+i>0$. Then the negative state i transits to a positive state $m+i$ with probability 1.

If the transmission is failed and $w_k(t) \leq D-m$, the HOL packet remains in the buffer and will be retransmitted after one frame. Its delay increases by m up to $w_k(t+1) = w_k(t)+m \leq D$ with probability $\varepsilon = 1-\mu$. If $w_k(t) > D-m$, this HOL packet k will experience a delay greater than D after one frame and be discarded (maybe in the middle of the frame). Then, at the beginning of frame $t+1$, packet $k+1$ becomes the HOL packet with a delay $w_{k+1}(t+1) = w_k(t)-\Delta$. Recall that if the transmission is successful, the positive state $w_k(t)$ transits to state $w_k(t)-\Delta$, as well. In other words, if $w_k(t) > D-m$, the system state always transits to $w_k(t)-\Delta$ with probability 1, regardless of whether the transmission is successful or failed.

The steady-state probability distribution $\{\pi_i\}$ can be obtained either iteratively or by using mathematical tools to solve $\pi = \pi\mathbf{P}$. For the critical case $\Delta = 1$, $\{\pi_i\}$ is derived in terms of π_0 as follows:

$$\pi_i = \begin{cases} \frac{\pi_0}{\mu^i}\left(1+\varepsilon\sum_{k=1}^{K_i}(-\varepsilon\mu^m)^k g(k)\right) & i \leq D-m \\ \varepsilon\sum_{j=i-m}^{D-m}\pi_j & i > D-m \end{cases} \tag{7.2}$$

where

$$g(k) = \binom{i-km+1}{k} - \binom{i-km}{k}\mu,\ K_i = \left\lfloor \frac{i+1}{m+1} \right\rfloor$$

If the HOL packet is transmitted successfully, its delay at the first node is $w_k(t)$ plus one time slot for transmission. Therefore, the delay distribution $\{d_i\}$ is

completely determined by the probabilities of non-negative states,

$$d_i = \frac{\pi_{i-1}}{\sum_{j\geq 0}\pi_j}. \tag{7.3}$$

In the m-phase TDMA network, the node transmits at the frame boundaries. A packet may be dropped in the middle of a frame if it experiences a delay greater than $D-m$ at the beginning of this frame and fails to be transmitted. The packet dropping probability is

$$p_L^{(1)} = \frac{\varepsilon \sum_{i=D-m+1}^{D}\pi_i}{\lambda}, \quad \lambda = \frac{m}{r} \tag{7.4}$$

By inspecting the balance equations, we obtain

$$\pi_i = \begin{cases} \varepsilon \sum_{j=1}^{i}\pi_j + \pi_0 & 1 \leq i < m \\ \varepsilon \sum_{j=i-m}^{k}\pi_j & i \geq m, \end{cases} \tag{7.5}$$

where $k = \min\{i, D-m\}$. (7.5) holds for the delay distribution $\{d_i\}$ as well. Apparently, d_i is jointly determined by $l = \min\{i, m, B-i\}$ consecutive states below i, which results in a backward iteration. If $D - m > m$, the probability mass function (pmf) of the first node delay is composed of three sections, $[1, m]$, $[m+1, D-m+1]$, and $[D-m+2, D+1]$. If $D < 2m$, the pmf will be simpler. Since a smaller D causes a higher dropping probability, a general condition for the delay constraint is $D > 2m$ to ensure that every packet has at least one transmission opportunity. Because both m and D are positive integers, the smallest possible value of D is $2m + 1$.

Note that as $D \to \infty$, [142] has shown that the output of the first node is a correlated on-off process. This correlation exists even if $D < \infty$. Then, the

following relay nodes are fed with bursty and correlated traffic, which makes it difficult to analyze the resulting network. So, for $D < \infty$, the network performance is investigated through simulation results.

The e2e delay is the sum of all local delays. The delay mean $\overline{D}$ and the dropping probability p_L can be upper bounded as follows:

$$\overline{D}=\sum_{i=1}^{N} d_i \leq N\overline{D}_1 \tag{7.6}$$

$$p_L=1-\prod_{i=1}^{N}(1-p_L^{(i)}) \leq 1-(1-p_L^{(1)})^N. \tag{7.7}$$

The tightness of these upper bounds depends on $p_L^{(1)}$. The fewer packets are dropped, the closer $p_L^{(i)}$ to $p_L^{(1)}$, and the tighter is the bound.

7.2.2 Slotted ALOHA

In slotted ALOHA, each node independently transmits with probability p_m. Note that p_m represents the node transmission opportunity. The node actually transmits only if it is given a transmission opportunity *and* it has packets to transmit, which depends on its buffer occupancy. Traffic and the channel model are the same as in TDMA. Again, we start with the first node, which is observed at the time slot level. Given the success probability μ, a packet departs the node if and only if the node is scheduled to transmit and the transmission is successful, with a probability $a = \mu p_m$. Otherwise, the packet is retained in the buffer or discarded. The service time is geometric with a. The system state is the waiting

time of the HOL packet. The state transition probabilities are

$$P_{ij} = \begin{cases} 1-a & i \in [0, D),\ j = i+1 \\ a & i \in [0, D),\ j = i-r+1 \\ 1 & i < 0, \quad j = i+1 \quad \text{or } i = D,\ j = D-r+1. \end{cases} \tag{7.8}$$

At slot t, assume that the HOL packet is packet k with delay $w_k(t)$. If $w_k(t) < D$ and the packet successfully departs the node with probability a, the next packet becomes the HOL packet at slot $t+1$ with delay $w_{k+1}(t+1) = w_{k+1}(t) + 1 = w_k(t) - r + 1$. Otherwise, if the packet fails to depart the node with probability $(1-a)$, it remains as the HOL packet with its delay increased by one. If $w_k(t) = D$, either the packet is transmitted successfully or not, it has to be deleted from the buffer since its delay exceeds the bound D at slot $t+1$. In this case, the system state transits from D to $D-r+1$ with probability 1. The negative states indicate an empty buffer and the system is waiting for the next new packet arrival.

The delay distribution $\{d_i\}$ is calculated based on $\{\pi_i\}$ and (7.3) like in TDMA. Since the packet dropping possibly occurs at the time slot boundaries, the packet dropping probability is

$$p_L^{(1)} = \frac{(1-a)\pi_D}{\lambda} = r(1-\mu p_m)\pi_D. \tag{7.9}$$

Rewriting the balance equations, we obtain

$$\pi_i = \begin{cases} a\sum_{j=k}^{i+r-1} \pi_j & i < D-r+1 \\ (1-a)\pi_{i-1} & D-r+1 \le i \le D, \end{cases} \tag{7.10}$$

where $k = \max\{0, i\}$. (7.10) holds for $\{d_i\}$, as well. Different from the TDMA

network, (7.10) exhibits that d_i is jointly determined by $r-1$ consecutive states above i, which results in a forward iteration. The pmf essentially consists of three sections, $[1, D-2r+2]$, $[D-2r+3, D-r+1]$, and $[D-r+2, D+1]$. A general setting is $D > 2(r-1)$, so that the pmf contains all three sections.

Note that the node transmits with probability p_m when its buffer is non-empty. In other words, the effective transmit probability is $p_t = P_B p_m$, where P_B is the node busy probability. In previous work, the traffic load is so heavy that $P_B = 1$. Then the effective transmit probability p_t is identical to the transmit probability p_m so that the performance of ALOHA networks can be optimized by manipulating p_m. However, if the traffic load is light and $P_B \ll 1$[1], which is highly possible in ALOHA networks, simply optimizing p_m does not necessarily lead to optimization of the network performance.

As a matter of fact, based on queueing theory, the busy probability of node i is $P_B^i = \lambda_i/(\mu p_m)$, where λ_i is the arrival rate to node i. As the delay bound D goes to infinity, it is easy to show that $\lambda_i = 1/r$ for all i and thus $P_B = 1/(r\mu p_m)$. Naturally, the effective transmit probability $p_t = 1/(r\mu)$ depends only on the traffic rate $1/r$ and the channel reception probability μ, and is completely independent of p_m. Since the network performance is essentially determined by the effective transmit probability p_t, this observation implies that the ALOHA parameter p_m does not contribute to the change of the network performance. In the DB-ALOHA network, due to packet dropping, the arrival rate λ_i to node i is a function of the loss rate $p_L^{(i)}$, $\lambda_i = \lambda_{i-1}(1 - p_L^{(i)})$. The packet loss rate $p_L^{(i)}$ depends on the delay bound D, the service rate $a = 1/(\mu p_m)$ and the arrival rate λ_{i-1}. Intuitively, p_t is not completely independent of p_m. However, in most cases the loss rate is required to be relatively small. Then $P_B^i \approx 1/(r\mu p_m)$, and it is

[1] P_B is essentially a function of p_m.

reasonable to say that p_t is independent of p_m.

From the analysis in [142] we can see that the longer delay of ALOHA is mostly caused by the longer access delay, which is proportional to $1/p_m$. When the traffic load is light, a large p_m will lead to a small access delay and significantly improve the e2e delay. In this sense, to optimize the delay performance of ALOHA, p_m should be chosen based on the traffic load, which has been ignored in previous work because of the heavy traffic assumption. For example, in [76], the throughput is maximized by $p_m = 1/N$ without consideration that the node does not need contend for transmission opportunities when its buffer is empty.

7.3 Simulation Results

A set of extensive simulation results are provided to expose the performance of the DB-TDMA and DB-ALOHA network. First of all, the fully reliable (non-dropping) TDMA network is compared with the DB-TDMA network in Fig. 7.3. We set $m = 3$ and $\mu = 0.8$ for both networks. For the DB network, we additionally set the interarrival time $r = 4$ and $D = 4$, which results in an e2e dropping probability $p_L \approx 0.20$. It implies that 20% packets will be discarded and the throughput is $(1 - 0.2)/r = 1/5$. In the non-dropping network, all generated packets will be successfully delivered to the sink and the throughput is exactly the traffic rate $1/r$. Accordingly, for the non-dropping network, we set the interarrival time $r = 5$ such that both networks are compared under the identical throughput.

With the BD strategy, the e2e delay decreases. A substantial improvement is particularly reflected on the delay variance that is reduced by 60%. On the one hand, simply reducing the traffic load at the first node does not improve the network performance significantly. On the other hand, although introducing re-

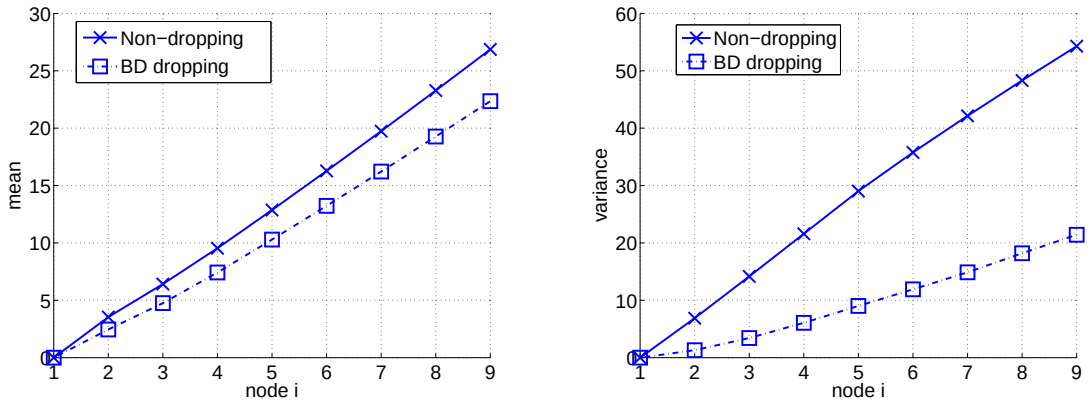

(a) Delay means

(b) Delay variances

Figure 7.3. Comparison of the non-dropping and DB-TDMA network with $m = 3, N = 9, \mu = 0.8$

dundant packets does increase the traffic load, it enhances the delay performance. In addition, the lost packets can be compensated for by the redundant packets, which ensures reliability. In this sense, the BD strategy is very helpful to achieve a good balance between latency and reliability.

7.3.1 m-phase TDMA

Throughout this section, the m-phase TDMA network is assumed to have $m = 3, r = 4, N = 8$. Compared to the pmf of the non-dropping TDMA network, the pmf of the cumulated delays from node 0 to node i $(1 \leq i \leq N)$ is truncated based on D_B/D (Fig. 7.4) . For $D > 2m$, the pmf of the cumulated delay is scaled. In Fig. 7.5, the e2e delay mean and variance are shown for $\mu = 0.8, D = 10$. The delay mean approximately linearly increases with the number of nodes. In comparison with the non-dropping TDMA network ($D = \infty$), the delay mean is

reduced by 40% and the delay variance by 75%. The resulting e2e packet loss rate $p_L = 0.0414$ (as listed in Table 7.1) is acceptable.

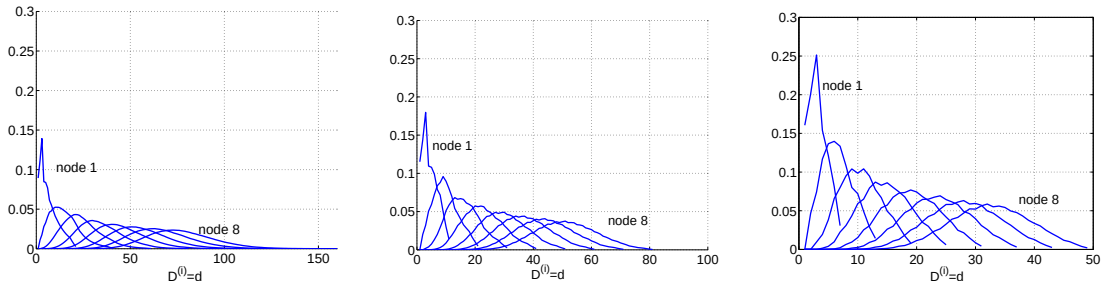

(a) $D = 20$ (b) $D = 10$ (c) $D = 6$

Figure 7.4: pmf of the cumulated delay in the TDMA network with $m = 3, r = 4, p_r = 0.8, N = 8$

The dropping probability is to be traded off against the delay. A smaller D results in a smaller delay and a higher local dropping probability $p_L^{(i)}$ at node i, which is shown in Fig. 7.6(a). As D increases, $p_L^{(i)}$ decreases more slowly. It implies that the major packet loss occurs at the first few nodes of the chain. This property is desirable since the downstream nodes do not need to spend energy to transmit packets that will finally be discarded. For large D, the per-node dropping probability asymptotically converges to zero.

Fig. 7.7 demonstrates the effects of D. Both the delay mean and the delay variance are nearly linear in D, particularly when D is small. As expected, the e2e dropping probability p_L asymptotically decreases with D. For large D, say

TABLE 7.1

E2E DROPPING PROBABILITIES FOR THE TDMA NETWORK WITH $m = 3, r = 4, N = 8$

μ	D				
	1	5	10	15	20
0.7	0.9615	0.3742	0.2183	0.1678	0.1431
0.75	0.9331	0.2621	0.1229	0.0803	0.0589
0.8	0.8880	0.1550	0.0414	0.0142	0.0058

$D > 10$, the decrease of p_L becomes very slow. Thus, simply increasing D does not help to improve reliability, but does harm the delay performance. There may exist an optimal D to achieve the best balance between the delay and the packet loss. Unlike in fully reliable networks [142], the delay performance is not severely deteriorated by the drop of μ (Fig. 7.8). Moreover, as long as D is sufficiently large, even if the traditional stability condition does not hold, the resulting e2e dropping probability is so moderate that both the data latency and reliability are guaranteed. For instance, considering the critical case $\mu = m/r = 0.75$, for $D \geq 20$, the packet loss $p_L \leq 0.05$ is negligible. For small D like $D = 10$ and $p_L \leq 0.13$, it is not difficult to introduce redundant packets for reliability.

7.3.2 Slotted ALOHA

This section discusses the performance of the DB-ALOHA scheme. To compare with TDMA, we set $p_m = 1/m$ and $m = 3, r = 4, N = 8$. Different from the TDMA system, the pmf tail is both truncated and twisted by applying the BD

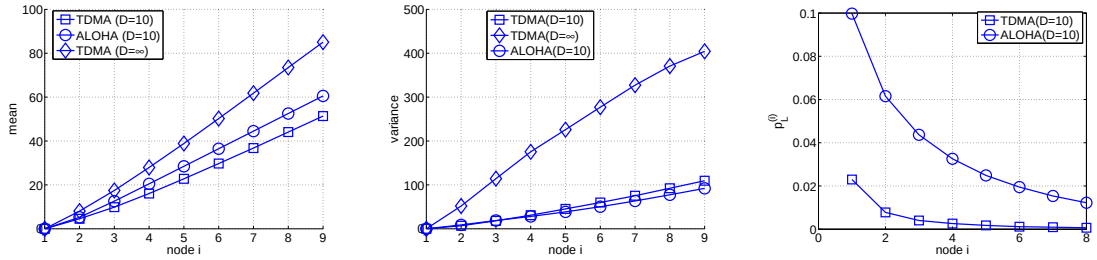

(a) Delay means (b) Delay variances (c) Dropping probability

Figure 7.5. Performance comparison of the system with $m = 3, r = 4, N = 8, \mu = 0.8, D = 10$

scheme (Fig. 7.9). But the delay central moments and the dropping probability behave similarly as in TDMA. Specifically, the delay mean and variance linearly increase with the number of nodes (Fig. 7.5(a) andFig. 7.5(b)), and the per-node dropping probability $p_L^{(i)}$ decreases with the node index i, and the first node experiences the maximum packet loss (Fig. 7.5(c) and Fig. 7.6(b)). The e2e dropping probability p_L is listed in Table 7.2.

Like the TDMA network, both the delay mean and variance are approximately linear with D (Fig. 7.10(a) and Fig. 7.10(b)). The dropping probability p_L (Fig. 7.10(c)) sharply decreases with small D. However, for D sufficiently large, say $D \geq 30$, the decreasing speed is decelerated and p_L eventually converges to zero. Apparently, a larger D is needed for p_L to reach zero. The impact of μ is displayed in Fig. 7.11. Again, the drop of μ causes a very small difference in the delay mean and variance, but results in an increase of the per-node packet dropping rate. Moreover, the per-node dropping probability asymptotically converges to zero.

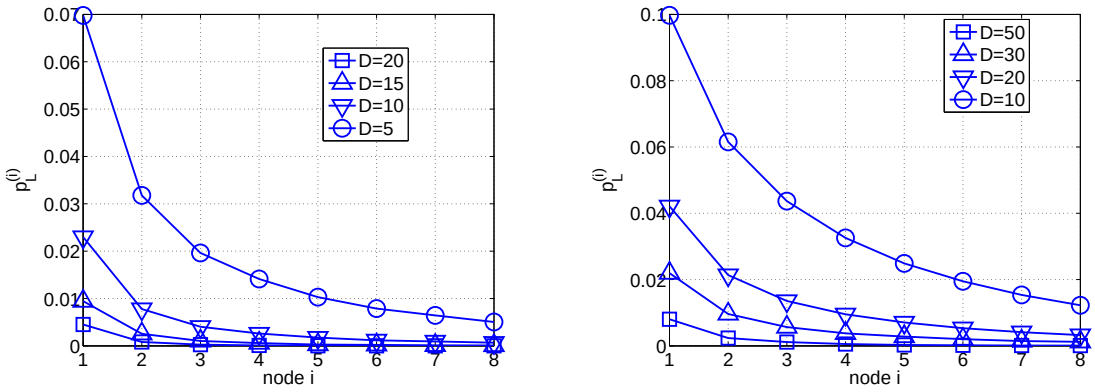

(a) TDMA

(b) ALOHA

Figure 7.6. Packet dropping performance for the system with $m = 3, r = 4, N = 9, \mu = 0.8$

7.3.3 Comparison

In the fully reliable network, the TDMA network substantially outperforms the ALOHA network in terms of the delay (Fig. 7.2). In the DB network, the performance gap between TDMA and ALOHA becomes fairly small. As shown in Fig. 7.5, the difference of the delay mean between the TDMA and ALOHA network decreases from 300% (reliable) to 20% (DB); while the delay variance difference changes from 750% (reliable) to 10% (DB). The main performance degradation caused by the random access is the dropping probability. For ALOHA, the local dropping probability $p_L^{(i)}$ at node i is almost five times than that of TDMA. Moreover, $p_L^{(i)}$ of ALOHA converges to zero more slowly than TDMA. However, if the packet loss rate does not exceed the predetermined threshold, ALOHA is is a practical MAC scheme that achieves a good delay performance. As a tradeoff, when the gap in p_L is reduced, the gap in the delay moments will be increased.

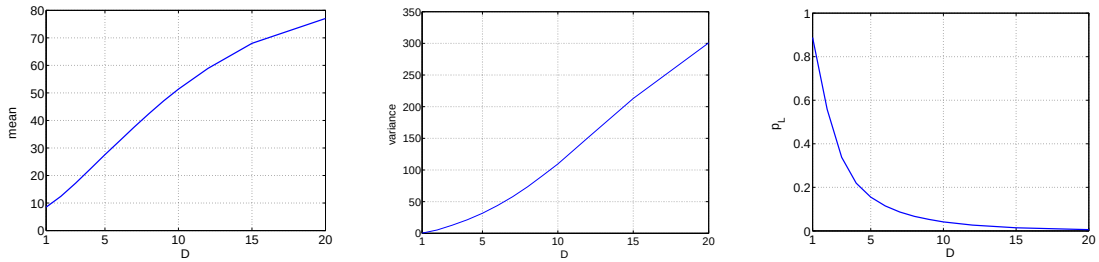

(a) Delay means (b) Delay variances (c) p_L

Figure 7.7: The impact of D in the m-phase TDMA network with $m = 3, r = 4, N = 8, p_r = 0.8$

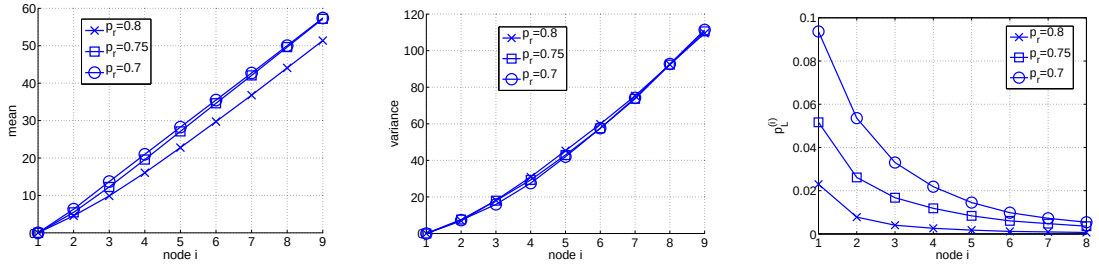

(a) Delay means (b) Delay variances (c) $p_L^{(i)}$

Figure 7.8: The impact of μ in the m-phase TDMA network with $m = 3, r = 4, N = 9, D = 10$

The pair (D_B, p_L) can be used in the controller design to optimize the NCS performance as shown in [76, 97]. With nonzero packet loss p_L and the maximum packet delay B, the controller system can be formulated as a Markovian Jump Linear System (MJLS). Optimizing the MJLS system can optimize the NCS network with MAC schemes.

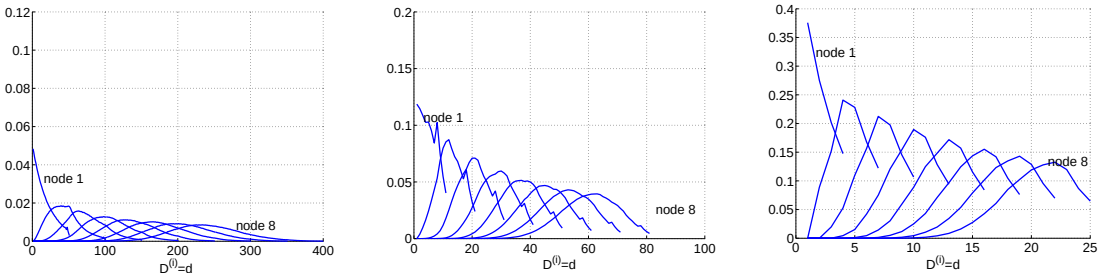

(a) $D = 50$ (b) $D = 10$ (c) $D = 3$

Figure 7.9: pmf of the cumulated delay in the ALOHA network with $m = 3, r = 4, p_r = 0.8, N = 8$

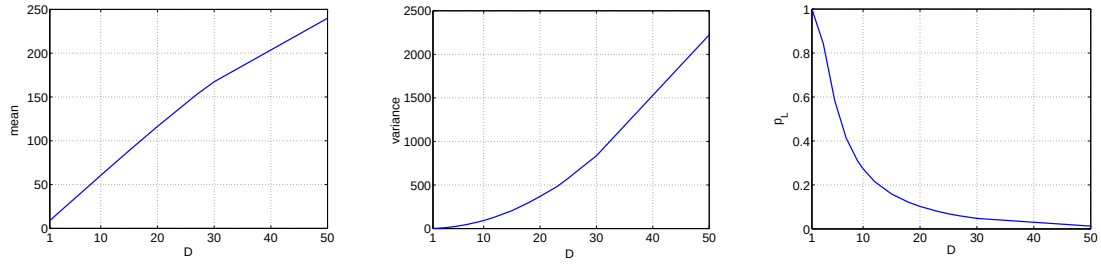

(a) Delay means (b) Delay variances (c) p_L

Figure 7.10: The impact of D in the ALOHA network with $m = 3, r = 4, N = 8, p_r = 0.8$

7.4 Conclusions

In DB WMNs, the QoS paramaters delay and packet loss rate are derived. The e2e delay mean and variance are approximately linear with the number of nodes. The local dropping probabilities $p_L^{(i)}$ asymptotically converge to zero. A moderate delay bound D_B is sufficient to guarantee a small packet loss and thus achieve a good balance between reliability and latency.

Compared to fully reliable networks, the e2e delay of DB networks becomes

TABLE 7.2

E2E DROPPING PROBABILITIES FOR THE ALOHA NETWORK WITH $m = 3, r = 4, N = 8$

μ	D						
	1	10	20	30	40	50	100
0.70	0.9999	0.4243	0.2505	0.1911	0.1599	0.1423	0.1048
0.75	0.9999	0.3481	0.1784	0.1164	0.0863	0.0692	0.0341
0.80	0.9998	0.2731	0.1020	0.0477	0.0238	0.0127	0.0000

less sensitive to the channel reception probability μ. This improvement is desirable since the network performance is not expected to rapid fluctuate with μ, which basically cannot be controlled. Besides, with the BD strategy, the delay performance gap between TDMA and ALOHA is reduced. Due to the implementation complexity and overhead, TDMA is less favored than ALOHA. But ALOHA has poor delay performance. With the reduced performance gap, ALOHA becomes more practical.

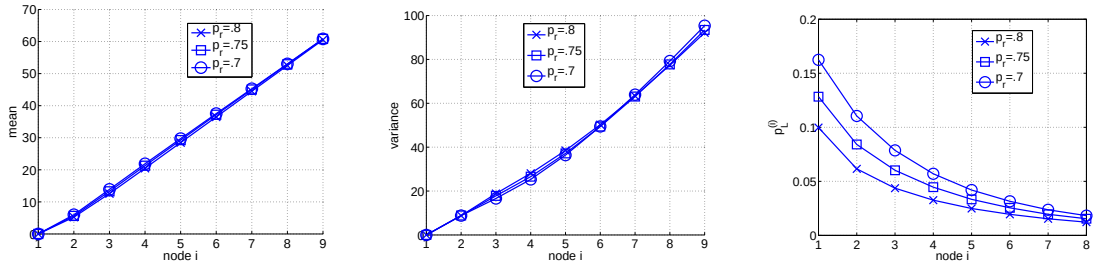

(a) Delay means (b) Delay variances (c) $p_L^{(i)}$

Figure 7.11: The impact of μ in the ALOHA network with $m = 3, r = 4, N = 8, D = 10$

CHAPTER 8

CONCLUDING REMARKS

8.1 Conclusions from our Work

In this dissertation, we use discrete-time queueing theory to analyze packet scheduling algorithms and MAC schemes in WMNs. It is revealed that

- a priority algorithm with Bounded Delay (BD) dropping can provide balanced delay guarantees. When the wireless channel is not bad on average (small error rate), which is reasonable in practice, the queueing performance of flows with low priorities is mainly determined by that of the high priorities, rather than the channel itself. Moreover, if the delay bounds are chosen appropriately and the low priority traffic load is light, the loss rate in the LP packets is small.

- TDMA and ALOHA can be statistically analyzed using queueing theory by incorporating the access delays into the prolonged service time (TDMA) or the decreased service rate (ALOHA). Given the same traffic load and original service rate, prolonging the service time by m times causes less delay than decreasing the service rate by $p_m = 1/m$ times in terms of both the mean and variance.

- in one-dimensional WMNs, the e2e delay, especially the variance, is significantly affected by the negative correlations between the delays experienced

at single nodes. Previous work based on the "independence" assumption led to very conservative call admission control because the accurate e2e delay variance is much smaller than the sum of delay variances at individual nodes. The complete delay distribution can be used to calculate a delay outage probability $p_L(d)$, a critical measurement for delay-sensitive applications.

- there exist correlations in traffic flows, multiple access interference, and delays in WMNs. These correlations can be taken advantage of to design distributed and cooperative MAC and packet scheduling protocols in multihop networks. In TDMA networks, due to the spacing between the transmitter and interferers, the statistical traffic parameters like burstiness and correlation are not as strongly as the deterministic parameter traffic rate. On the other hand, in ALOHA networks, these statistical traffic parameters become dominant, particularly the traffic correlation. With the traffic correlation, the smoothness of CBR traffic is preserved even without MAC. Moreover, the traffic correlation helps the CBR-fed ALOHA network to emulate TDMA and form a natural spacing between the transmitting nodes. Since there is no overhead to establish the frame structure like in TDMA, the performance is better than TDMA in terms of throughput, capacity and channel quality μ_L. It is helpful to combine the MAC scheme with traffic regulation that can smooth bursty traffic flows.

- in delay-bounded WMNs, the e2e delay mean and variance are approximately linear with the number of nodes. The local dropping probabilities $p_L^{(i)}$ asymptotically converge to zero. A moderate delay bound D_B is sufficient to guarantee a small packet loss and thus achieve a good balance

between reliability and latency.

Compared to fully reliable networks, the e2e delay of DB networks becomes less sensitive to the channel reception probability μ. This improvement is desirable since the network performance is not expected to rapid fluctuate with μ, which basically cannot be controlled. Besides, with the BD strategy, the delay performance gap between TDMA and ALOHA is reduced. Due to the implementation complexity and overhead, TDMA is less favored than ALOHA. But ALOHA has poor delay performance. With the reduced performance gap, ALOHA becomes more practical.

8.2 Future Work

8.2.1 Energy-Efficient Rate-Adaptive Scheduling

Throughout this dissertation, when MAC is studied, packet scheduling is set to be FIFO for tractable analysis. In practice other scheduling algorithms such as LCFS and priority scheduling that favor the newly arriving packets, may be more desirable for delay-sensitive WMN applications. It will be interesting to explore the performance of WSNs when associating with these scheduling algorithms.

For example, as stated in Chapter 2, *Longest Queue First (LQF)* or *Largest Delay First (LDF)* scheduling is throughput-optimal even in the wireless environment from the perspective of energy efficiency [9, 10, 14, 67, 120, 130]. One future direction is to use the Telatar model to design and analyze LQF-based scheduling algorithms under log-normal shadowing and Rayleigh fading channels.

Assume that a set of discrete transmission rates $\mathcal{R} = \{0, 1, \ldots, M\}$ correspond to the time-varying channel conditions. At any time slot t, the rate $R_i(t) \in \mathcal{R}$ $(i = 1, 2, \ldots, N)$ indicates the number of packets that can be transmitted reliably

in this slot. The arrival process is denoted by $A_i(t)$, the number of packets arriving in time t. Then, if the node i is selected for transmission, its queue length evolves according to

$$Q_i(t+1) = (Q_i(t) + A_i(t) - C_i(t))^+, \tag{8.1}$$

where $C_i(t) = \min\{R_i(t), Q_i(t)\}$.

Unlike previous LQF-based scheduling, the queue length of each session is weighed by a reserved rate r_i, not the real transmission rate $R_i(t)$. Recall that in a Generalized Processing Sharing system, given a set of weights $\{\phi_i, i = 1, \ldots, N\}$, each backlogged session is guaranteed a minimum service rate

$$r_i = \frac{\phi_i}{\sum_{j=1}^{N} \phi_j} C. \tag{8.2}$$

If $C = 1$, session i should receive a fraction r_i of the total bandwidth. This parameter can be used to control the fairness. The misbehavior of nodes with small r_i will not affect other nodes significantly. Note that this parameter is unable to guarantee a "real" fairness. Define a non-decreasing function of r_i, $f(r_i)$. The queue length is weighed by $f(r_i)$.

The scheduler chooses user $i^*(t)$ to transmit according to

$$i^*(t) = \arg\max_i(\alpha R_i(t) + (1-\alpha) f(r_i) Q_i(t)), \tag{8.3}$$

where the parameter α is used to trade-off between energy efficiency and throughput. Given the constant transmit power per time slot, the scheduler transmits $R_i(t)$ packets under the specific channel condition. Note that if the SNR is too low, the scheduler decides not to serve this node. Next, we specify how the rate $R_i(t)$ is determined on the basis of the channel condition.

If the fading channel is characterized by a composite log-normal shadowing-Rayleigh fading distribution, with a pdf given by (1.12), then the distribution of L is derived to have an approximate pdf:

$$f(x) = \frac{a}{\sqrt{2\pi}\sigma x^2}\big(1 + \frac{1}{e^{\frac{a}{x}} - 1}\big) \times \exp\Big(- \frac{\Big[\ln(1+\rho) - \mu + \ln(e^{\frac{a}{x}} - 1)\Big]^2}{2\sigma^2}\Big), \quad (8.4)$$

where

$$a = \frac{\rho \ln K - \ln \eta_i}{\rho}.$$

The cumulative density function (cdf) of this random variable, fortunately, shows a similarity to the Poisson distribution. From Fig. 8.1, we can see that for a composite log-normal-Rayleigh fading channel with $\mu = 0$ and $\sigma = 0.3454$, the cdf of L can be approximated by a Poisson distribution with $\lambda = 10$. As a matter of fact, the smaller the variance σ of the channel, the more accurate this approximation.

Approximating L by a Poisson distribution significantly simplifies the analysis of this scheme. For the case $\lambda \gg 1$, the pdf of L can be approximated even by a Gaussian distribution. This permits a qualitative analysis of the LQF-based scheduling system to verify that this system indeed succeeds to balance between energy efficiency, throughput, and fairness. The Telatar model can be used for the queueing analysis of the packet delay and packet loss probability. In addition, the QoS requirements on delay and loss rate will be taken into account when deciding the transmission schedule.

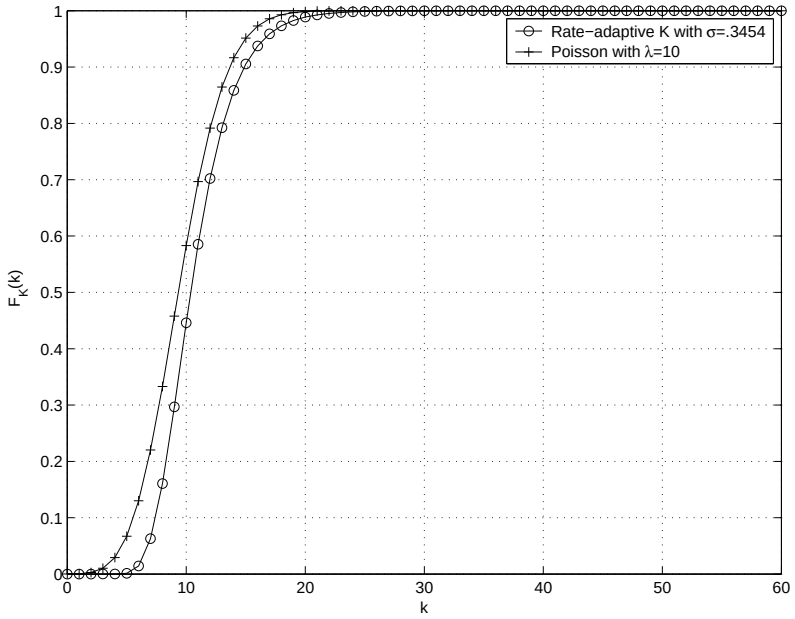

Figure 8.1. Approximating the CDF of L by a Poisson distribution

8.2.2 MAC Schemes with Network Coding for Bidirectional Flows on Line Networks

Network coding is a recent field in information theory that allows nodes to recombine several input packets into one or several output packets [5]. With linear network coding, outgoing packets are linear combinations of the original packets [36]. Network coding is compelling because of the benefits in the increased capacity and improved robustness and adaptability. As an application, network coding can improve throughput of a line network when the traffic between two end nodes are bidirectional and both nodes have a similar number of packets to exchange.

In Fig. 8.2, nodes A and C exchange packets via an intermediate node B. A (resp. C) sends a packet a (resp. c) to B (resp. A), which then broadcasts $a \oplus c$

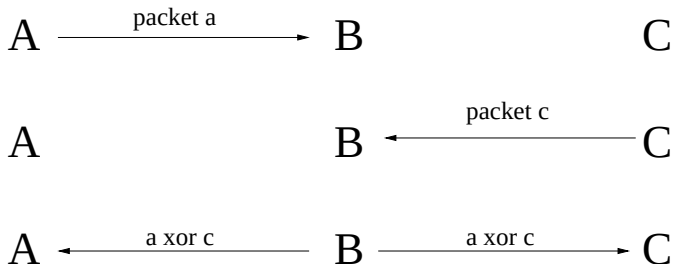

Figure 8.2. A simple network coding example. Nodes A and C exchange packets via an intermediate node B. A (resp. C) sends a packet a (resp. c) to B (resp. A), which then broadcasts $a \oplus c$ instead a and c in sequence. Both A and C can recover the packet of interest, while the number of tranwsmissions is reduced.

instead a and c in sequence. Both A and C can decode the packet of interest, while the number of transmissions is reduced. Besides, overhearing a packet of neighbor that is coded over information previously forwarded to the neighbor serves as a passive acknolwedgement. If associating network coding with multihop MAC schemes, transmission opportunities could be better used at nodes that combine new packets with an old packet for the opposite direction. Both throughput and delay can be improved.

BIBLIOGRAPHY

1. http://www.scalable-networks.com/publications/documentation.php.

2. http://functions.wolfram.com/ElementaryFunctions/Log/29/.

3. Network Simulator ns2 – a discrete event simulator targeted at networking research. The VINT Project. UC Berkeley, LBL, USC/ISI, and Xerox PARC. Available at http://www.isi.edu/nsnam/ns/.

4. N. Abramson. The Aloha System - Another Alternative for Computer Communications. In *Proceedings of Fall Joint Computer Conference, AFIPS Conference*, page 37, 1970.

5. R. Ahlswede, N. Cai, S-Y. Robert Li, and R. W. Yeung. Network Information Flow. *IEEE Transactions on Information Theory*, 46(4):1204–1216, July 2000.

6. I. F. Akyildiz, W. Su, Y. Sankarasubramaniam, and E. Cayirci. Wireless Sensor Networks: a Survey. *Computer Networks*, 38(4):393–422, 2002.

7. Ian F. Akyildiz, Weilian Su, Yogen Sankarasubramaniam, and Erdal Cayirci. A Survey on Sensor Networks. *IEEE Communications Magazine*, 40(8):102–114, August 2002.

8. Ian F. Akyildiz, Xudong Wang, and Weilin Wang. Wireless mesh networks: A survey. *Computer Networks*, 47(4):445–487, March 2005.

9. Matthew Andrews, Krishnan Kumaran, Kavita Ramanan, Alexander Stolyar, Rajiv Vijayakumar, and Phil Whiting. Scheduling in a Queueing System with Asynchronously Varying Service Rates. *Probability in the Engineering and Informational Sciences*, 14:191–217, 2004.

10. Matthew Andrews, Krishnan Kumaran, Kavita Ramanan, Alexander Stolyar, Phil Whiting, and Rajiv Vijayakumar. Providing Quality of Service over a Shared Wireless Link. *IEEE Communication Magazine*, pages 150–154, February 2001.

11. V. Annamalai, S. K. S. Gupta, and L. Schwiebert. On Tree-Based Convergecasting in Wireless Sensor Networks. In *Wireless Communications and Networking (WCNC)*, volume 3, pages 1942 –1947, 2003.

12. Jens C. Arnbak and Wim Van Blitterswijk. Capacity of Slotted ALOHA in Rayleigh-Fading Channels. *IEEE Journal on Selected Areas in Communications*, 5(2):261–269, February 1987.

13. Randall A. Berry and Robert G. Gallager. Communication Over Fading Channels with Delay Constraints. *IEEE Transactions on Information Theory*, 48(5):1135–1149, May 2002.

14. Pravin Bhagwat, Partha Bhattacharya, Arvind Krishna, and Satish K. Tripathi. Enhancing Throughput over Wireless LAN using Channel State Dependent Packet Scheduling. *Wireless Networks Journal*, 3(1), 1997.

15. IEEE Standards Board. Part 11: Wireless LAN Medium Access Control (MAC) and Physical Layer (PHY) Specifications, 1997.

16. Flaminio Borgonovo and Michele Zorzi. Slotted ALOHA and CDPA: A Comparison of Channel Access Performance in Cellular Systems. *ACM Wireless Networks*, 3(1):43–51, March 1997.

17. S. Borst and P. Whiting. Dynamic Rate Control Algorithms for HDR Throughput Optimization. In *IEEE INFOCOM*, volume 2, pages 976–985, 2001.

18. Michael S. Branicky, Stephen M. Phillips, and Wei Zhang. Stability of Networked Control Systems: Explicit Analysis of Delay. In *IEEE American Control Conference*, 2000.

19. Raffaele Bruno, Marco Conti, and Enrico Gregori. Mesh Networks: Commodity Multihop Ad Hoc Networks. *IEEE Communication Magazine*, pages 123–131, March 2005.

20. Y. Cao and V. O. K. Li. Scheduling Algorithms in Broadband Wireless Networks. *Proceedings of the IEEE*, 89(1):76–87, 2001.

21. Marcelo M. Carvalho and J. J. Garcia-Luna-Aceves. A Scalable Model for Channel Access Protocols in Multihop Ad Hoc Networks. In *ACM MobiCom'04*, September 2004.

22. Dave Cavalcanti, Dharma Agrawal, Carlos Cordeiro, Bin Xie, and Anup Kumar. Issues in Integrating Cellular Networks, WLANs, and MANETs: A Futuristic Heterogeneous Wireless Network. *IEEE Wireless Communications*, pages 30–41, June 2005.

23. Arnab Chakrabarti, Ashutosh Sabharwal, and Behnaam Aazhang. Multi-Hop Communication is Order-Optimal for Homogeneous Sensor Networks. In *IPSN'04*, April 2004.

24. M. L. Chaudhry, U. C. Gupta, and J. G. C. Templeton. On the Relations Among the Distributions at Different Epochs for Discrete-Time GI/Geom/1 Queues. *Operations Research Letters*, 18:247–255, 1996.

25. Imrich Chlamtac, Marco Conti, and Jennifer J.-N. Liu. Mobile Ad Hoc Networking: Imperatives and Challenges. *Ad Hoc Networks*, 1(1):13–64, July 2003.

26. A. Chockalingam, Michele Zorzi, Laurence B. Milstein, and Pallapa Venkataram. Performance of a Wireless Access Protocol on Correlated Rayleigh-Fading Channels with Capture. *IEEE Transactions on Communications*, 46(5):644–655, May 1998.

27. Byung-Gon Chun and Mary Baker. Evaluation of Packet Scheduling Algorithms in Mobile Ad Hoc Networks. *ACM Mobile Computing and Communications Review (MC2R)*, 6:36–49, July 2002.

28. John N. Daigle and Matthew Roughan. Queue-Length Distributions for Multi-Priority Queueing Systems. In *IEEE INFOCOM*, volume 2, pages 21–25, March 1999.

29. Ilker Demirkol, Cem Ersoy, and Fatih Alagoz. MAC Protocols for Wireless Sensor Networks: A Survey. *IEEE Communication Magazine*, pages 115–121, April 2006.

30. David A. Eckhardt and Peter Steenkiste. Effort-limited Fair (ELF) Scheduling for Wireless Networks. In *IEEE INFOCOM*, volume 3, pages 1097–1106, 2000.

31. Itamar Elhanany, Michael Kahane, and Dan Sadot. On Uniformly Distributed On/Off Arrivals in Virtual Output Queued Switches with Geometric Service Times. In *IEEE International Conference on Communications (ICC'03)*, volume 1, pages 173–177, May 2003.

32. A. Elwalid and D. Mitra. Analysis, Approximations and Admission Control of a Multi-Service Multiplexing System with Priorities. In *IEEE INFOCOM95*, pages 463–472, 1995.

33. Farshad Eshghi, Ahmed K. Elhakeem, and Yousef R. Shayan. Performance Evaluation of Multihop Ad Hoc WLANs. *IEEE Communications Magazine*, pages 107–115, March 2005.

34. D. Estrin, John Heidemann, Ramesh Govindan, and Satish Kumar. Next Century Challenges: Scalable Coordination in Sensor Networks. In *ACM MobiCom*, Seattle, WA, August 1999.

35. Hossam Fattah and Cyril Leung. An Overview of Scheduling Algorithms in Wireless Multimedia Networks. *IEEE Wireless Communications*, pages 76–83, October 2002.

36. Christina Fragouli, Jean-Yves Le Boudec, and Jorg Widmer. Network Coding: An Instant Primer. *ACM SIGCOMM Computer Communication Review*, 36(1):63–68, January 2006.

37. Donald A. Gall and H. R. Mueller. Waiting-Time Distributions and Buffer Overflow in Priority Queueing Systems. *IEEE Transactions on Communications*, 20(5):865–877, October 1972.

38. R. G. Gallager. Energy Limited Channels: Coding, Multiaccess, and Spread Spectrum, November 1987. M. I. T. LIDS Rep. LIDS–P–1714.

39. Abbas El Gamal, Chandra Nair, Balaji Prabhakar, Elif Uysal-Biyikoglu, and Sina Zahedi. Energy-Efficient Scheduling of Packet Transmissions over Wireless Networks. In *IEEE INFOCOM*, pages 1773–1782, 2002.

40. E. N. Gilbert. Capacity of a Burst-Noise Channel. *Bell Sys. Tech. J.*, 39:1253–1266, 1960.

41. A. J. Goldsmith and S. G. Chua. Variable-Rate Variable-Power MQAM for Fading Channels. *IEEE Transactions on Communications*, 45(10):1218–1230, October 1997.

42. Andrea J. Goldsmith and Stephen B. Wicker. Design Challenges for Energy-Constrained Ad Hoc Wireless Networks. *IEEE Wireless Communications*, pages 8–27, August 2002.

43. Munish Goyal, Anurag Kumar, and Vinod Sharma. Power Constrained and Delay Optimal Policies for Scheduling Transmission over a Fading Channel. In *IEEE INFOCOM*, 2003.

44. Winfried K. Grassmann. Finding Equilibrium Probabilities of QBD Process by Spectral Methods When Eigenvalues Vanish. *Linear Algebra and Its Applications*, 386:207–223, 2004.

45. Nalan Gulpinar, Peter Harrison, and Berc Rustem. Mean-Variance Optimization of Response Time in a Tandem M/GI/1 Router Network with Batch Arrivals. In *The 3rd International Working Conference on Performance Modeling and Evaluation of Heterogeneous Networks*, July 2005.

46. Gaurav Gupta and Mohamed Younis. Load-Balanced Clustering in Wireless Sensor Networks. In *IEEE ICC*, Anchorage, AK, 2003.

47. Piyush Gupta and P. R. Kumar. The Capacity of Wireless Networks. *IEEE Transactions on Information Theory*, 46(2):388–404, March 2000.

48. M. Haenggi. Energy-Balancing Strategies for Wireless Sensor Networks. In *IEEE International Symposium on Circuits and Systems (ISCAS'03)*, Bangkok, Thailand, May 2003.

49. M. Haenggi and D. Puccinelli. Routing in Ad Hoc Networks: A Case for Long Hops. *IEEE Communications Magazine, Series on Ad Hoc and Sensor Networks*, 43:93–101, October 2005.

50. Martin Haenggi. On the Local Throughput of Large Interference-Limited Wireless Networks. In *39th Annual Conference on Information Sciences and Systems (CISS'05)*, Baltimore, MD, March 2005.

51. Martin Haenggi. Outage and Throughput Bounds for Stochastic Wireless Networks. In *IEEE International Symposium on Information Theory (ISIT'05)*, Adelaide, Australia, September 2005.

52. W. Heinzelman, A. Chandrakasan, and H. Balakrishnan. Energy-Efficient Communication Protocol for Wireless Microsensor Networks. *IEEE Transactions on Wireless Communications*, 1(4):660–670, October 2002.

53. Gavin Holland, Nitin Vaidya, and Paramvir Bahl. A Rate-Adaptive MAC Protocol for Multi-Hop Wireless Networks. In *ACM/IEEE MOBICOM'01*, Rome, Italy, July 2001.

54. J. Hsu and P. J. Burke. Behavior of Tandem Buffers with Geometric Input and Markovian Output. *IEEE Transactions on Communications*, 24(3):358 – 361, March 1976.

55. Jeffrey J. Hunter. *Mathematical Techniques of Applied Probability*. Academic Press, October 1983. ISBN:0123618029.

56. Philippe Jacquet, Amina Meraihi Naimi, and Georgios Rodolakis. Routing on Asymptotic Delays in IEEE 802.11 Wireless Ad Hoc Networks. In *RAWNET 2005*, 2005.

57. A. Jalali, R. Padovani, and R. Pankaj. Data Throughput of CDMA-HDR a Efficiency-High Data Rate Personal Communication Wireless System. In *IEEE VTC*, 2000.

58. Christine E. Jones, Krishna M. Sivalingam, Prathima Agrawal, and Jyh Cheng Chen. A Survey of Energy Efficient Protocols for Wireless Networks. *Wireless Networks*, 7(4):343–358, 2001.

59. V. Kanodia, C. Li, A. Sabharwal, B. Sadeghi, and E. Knightly. Distributed Multi-Hop Scheduling and Medium Access with Delay and Throughput Constraints. In *ACM MobiCom*, Rome, Italy, July 2001.

60. V. Kanodia, C. Li, A. Sabharwal, B. Sadeghi, and E. Knightly. Ordered Packet Scheduling in Wireless Ad Hoc Networks: Mechanisms and Performance Analysis. In *ACM MOBIHOC*, Lausanne, Switzerland, July 2002.

61. Vikram Kanodia, Chengzhi Li, A. Sabharwal, B. Sadeghi, and E. Knightly. Distributed Priority Scheduling and Medium Access in Ad Hoc Networks. *Wireless Networks*, 8:455–466, 2002.

62. Vikas Kawadia and P. R. Kumar. A Cautionary Perspective on Cross-layer Design. *IEEE Wireless Communications*, pages 3–11, February 2005.

63. Charles Knessl. An Explicit Solution to A Tandem Queueing Model. *Queueing Systems*, 30:261–272, 1998.

64. Ramana Rao Kompella and Alex C. Snoeren. Practical Lazy Scheduling in Sensor Networks. In *ACM SenSys'03*, pages 280–291, Los Angeles, CA, November 2003.

65. Henri Koskinen. Performance Studies of Wireless Multihop Networks, 2006. URL: http://lib.tkk.fi/Diss/2006/isbn9512281376/isbn9512281376.pdf.

66. Sunil Kumar, Vineet S. Raghavan, and Jing Deng. Medium Access Control Protocols for Ad Hoc Wireless Networks: A Survey. *Elsevier Ad Hoc Networks Journal*, 4(3):326–358, May 2006.

67. Duan-Shin Lee. Generalized Longest Queue First: An Adaptive Scheduling Discipline for ATM Networks. In *IEEE INFOCOM*, volume 1, pages 7–11, April 1997.

68. Kelvin K. Lee and Samuel T. Chanson. Packet Loss Probability for Real-Time Wireless Communications. *IEEE Transactions on Vehicular Technology*, 51(6):1569–1575, November 2002.

69. Kelvin K. Lee and Samuel T. Chanson. Packet Loss Probability for Bursty Wireless Real-Time Traffic Through Delay Model. *IEEE Transactions on Vehicular Technology*, 53(3):929–938, May 2004.

70. Chengzhi Li and Edward W. Knightly. Cooridnated Multihop Scheduling: A Framework for End-to-End Services. *IEEE/ACM Transactions on Networking*, 10(6):776–789, December 2002.

71. Feng-Li Lian, James Moyne, and Dawn Tilbury. Time Delay Modeling and Sample Time Selection for Networked COntrol Systems. In *Proceedings of ASME-DSC, 2001 International Mechanical Engineering Congress and Exposition*, November 2001.

72. P. Liu, R. Berry, and M. Honig. Delay-Sensitive Packet Scheduling in Wireless Networks. In *IEEE WCNC 2003*, March 2003.

73. Wei Liu, Yuguang Fang, and Younggoo Kwon. Performance Enhancement in Multi-hop Wireless Ad Hoc Networks. In *VTC 2003*, volume 4, pages 2177 – 2181, October 2003.

74. X. Liu, E. Chong, and N. Shroff. Opportunistic Transmission Scheduling with Resource-Sharing Constraints in Wireless Networks. *IEEE Journal on Selected Areas in Communications*, 19(10):2053–2064, October 2001.

75. X. Liu, E. Chong, and N. Shroff. Transmission Scheduling for Efficient Wireless Utilization. In *IEEE INFOCOM*, pages 776–785, 2001.

76. Xiangheng Liu and Andrea Goldsmith. Wireless Medium Access Control in Networked Control Systems. In *IEEE American Control Conference*, 2004.

77. Xiaowen Liu and Martin Haenggi. Throughput Analysis of Fading Sensor Networks with Regular and Random Topologies. *EURASIP Journal on Wireless Communications and Networking*, 4:554–564, 2005.

78. Xin Liu, Edwin K. P. Chong, and Ness B. Shroff. A Framework for Opportunistic Scheduling in Wireless Networks. *Computer Networks*, 41(4):451–474, 2003.

79. Yonghe Liu and Edward Knightly. Opportunistic Fair Scheduling over Multiple Wireless Channels. In *IEEE INFOCOM*, volume 2, pages 1106–1115, March 2003.

80. Songqwu Lu, Thyagarajan Nandagopal, and Vaduvur Bharghavan. A Wireless Fair Service Algorithm for Pakcet Cellular Networks. In *ACM/IEEE MobiCom*, Dallas, TX, October 1998.

81. Songwu Lu, Vaduvur Bharghavan, and R. Srikant. Fair Scheduling in Wireless Packet Networks. *IEEE/ACM Transactions on Networking*, 7(4):473–489, August 1999.

82. Michael G. Luby, Michael Mitzenmacher, M. Amin Shokrollahi, and Daniel A. Spielman. Efficient Erasure Correcting Codes. *IEEE Transactions on Information Theory*, 47(2):569–584, February 2001.

83. H. Luo and S. Lu. A topology-independent fair queueing model in ad hoc wireless networks. In *IEEE ICNP (International Conference on Network Protocols)*, November 2000.

84. H. Luo, S. Lu, and V. Bharghavan. A New Model for Packet Scheduling in Multihop Wireless Networks. In *ACM MobiCom*, pages 76–86, Boston, MA, 2000.

85. H. Luo, P. Medvedev, J. Cheng, and S. Lu. A Self-Coordinating Approach to Distributed Fair Queueing in Ad Hoc Wireless Networks. In *IEEE INFOCOM*, April 2001.

86. Haiyun Luo, Songwu Lu, Vaduvur Bharghavan, Jerry Cheng, and Gary Zhong. A Packet Scheduling Approach to QoS Support in Multihop Wireless Networks. *Mobile Networks and Applications*, 9(3):193–206, June 2004.

87. G. F. Marias, P. Georgiadis, D. Flitzanis, and K. Mandalas. Cooperation Enforcement Schemes for MANETs: A Survey. *Wireless Communications and Mobile Computing*, 6(3):319–332, May 2006.

88. Rudolf Mathar and Jurgen Mattfeldt. On the Distribution of Cumulated Interference Power in Rayleigh Fading Channels. *Wireless Networks*, 1(1):31–36, February 1995.

89. James Miller. *Game Theory At Work*. McGraw-Hill, 2003. ISBN 0-07-140020-6.

90. I. Mitrani and R. Chakka. Spectral Expansion Solution for A Class of Markov Models: Application and Comparison with the Matrix-geometric Method. *Performance Evaluation*, 23(3):241–260, September 1995.

91. John A. Morrison. Two Discrete-Time Queues in Tandem. *IEEE Transactions on Communications*, 27(3):563–573, March 1979.

92. T. Nandagopal, S. Lu, and V. Bharghavan. A Unified Architecture for the Design and Evaluation of Wireless Fair Queueing Algorithms. *Wireless Networks*, 8(2/3):231–247, March–May 2002.

93. Michael J. Neely. Exact Queueing Analysis of Discrete Time Tandems with Arbitrary Arrival Processes. In *IEEE International Conference on Communications (ICC'03)*, volume 4, pages 2221 – 2225, 2003.

94. R. Nelson and L. Kleinrock. Spatial TDMA: A Collision-Free Multihop Channel Access Protocol. *IEEE Transactions on Communications*, 33(9):934–944, September 1985.

95. M. F. Neuts. Matrix-Geometric Solutions in Stochastic Models. *Johns Hopkins University Press*, 1981.

96. T. S. E. Ng, I. Stoica, and H. Zhang. Packet Fair Queueing Algorithms for Wireless Networks with Location-Dependent Errors. In *INFOCOM*, volume 3, pages 1103–1111, April 1998.

97. J. Nilsson. Real-time control systems with delays, 1998. Ph.D Thesis, Lund Institute of Technology.

98. OPNET Architecture OPNET Users' Manual. http://forums.opnet.com.

99. Daeyoung Park, Hanbyul Seo, Hojoong Kwon, and Byeong Gi Lee. A New Wireless Packet Scheduling ALgorithm based on the CDF of User Transmission Rates. In *IEEE GLOBECOM*, volume 1, pages 528–532, December 2003.

100. J. D. Parsons. *Mobile Radio Propagation Channel*. John Wiley & Sons, November 2000. ISBN: 047198857.

101. Malcolm C. H. Peh, Stephen V. Hanly, and Philip Whiting. Random Access with Multipacket Reception over Fading Channels, 2003. Whitepaper can be found in http://www.cubinlab.ee.mu.oz.au/∼mchp/whitepaper/.

102. R. R. Pillai. A Distributed Overload Control Algorithm for Delay-Bounded Call Setup. *IEEE/ACM Transactions on Networking*, 9:780–789, December 2001.

103. Balaji Prabhakar, Elif Uysal Biyikoglu, and Abbas El Gamal. Energy-Efficient Transmission over a Wireless Link via Lazy Packet Scheduling. In *IEEE INFOCOM*, pages 386–394, 2001.

104. Balaji Prabhakar and Robert Gallager. Entropy and the Timing Capacity of Discrete Queues. *IEEE Transactions on Information Theory*, 49(2):357–370, February 2003.

105. D. Puccinelli and M. Haenggi. Wireless Sensor Networks-Applications and Challenges of Ubiquitous Sensing. *IEEE Circuits and Systems Magazine*, 5:19–29, August 2005.

106. H. Qi, S. S. Iyengar, and K. Chakrabarty. Distributed Sensor Networks – A Review of Recent Research. *Journal of the Franklin Institute*, 338:655–668, 2001.

107. X. Qin and R. Berry. Exploiting Multiuser Diveristy for Medium Access Control in Wireless Networks. In *IEEE INFOCOM*, San Francisco, CA, March 2003.

108. V. Raghunathan, S. Ganeriwal, and M. B. Srivastava. Energy Efficient Wireless Packet Scheduling and Fair Queueing. *ACM Transactions on Embedded Comupting Systems*, 3(1):3–23, February 2004.

109. Parameswaran Ramanathan and Prathima Agrawal. Adapting Packet Fair Queueing Algorithms to Wireless Networks. In *ACM MOBICOM*, pages 1–9, 1998.

110. Theodore S. Rappaport. *Wireless Communications: Principles and Practice*. Prentice Hall PTR, January 1996. ISBN: 0133755363.

111. T. Bheemarjuna Reddy, I. Karthigeyan, B. S. Manoj, and C. Siva Ram Murthy. Quality of Service Provisioning in Ad Hoc Wireless Networks: A Survey of Issues and Solutions. *Ad Hoc Networks*, 4(1):83–124, January 2006.

112. L. G. Roberts. ALOHA Packet System With and Without Slots and Capture. *ACM Sigcomm Computer Communication Review*, 5(2):28–42, April 1975.

113. Elizabeth M. Royer and C-K. Toh. A Review of Current Routing Protocols for Ad-Hoc Mobile Wireless Networks. *IEEE Personal Communications*, 6(2):46–55, April 1999.

114. Nobuo Ryoki, Kenji Kawahara, Takeshi Ikenaga, and Yuji Oie. Performance Analysis of Queue Length Distribution of Tandem Routers for QoS Measurement. In *2002 Symposium on Applications and the Internet (SAINT) Workshops*, page 82, 2002.

115. T. Sheu S. Sheu. DBASE: A Distributed Bandwidth Allocation/Sharing/Extension Protocol for Multimedia over IEEE802.11 Ad Hoc Wireless LAN. In *IEEE INFOCOM 2001*, volume 3, pages 1558–1567, April 2001.

116. B. Sadeghi, V. Kanodia, A. Sabharwal, and E. Knightly. Opportunistic Media Access for Multirate Ad Hoc Networks. In *ACM MOBICOM*, pages 23–28, Atlanta, GA, September 2002.

117. V. Saligrama and D. Starobinski. On the Macroscopic Effects of Local Interactions in Multi-hop Wireless Networks. In *Wi-opt 2006*, 2006.

118. Cesar Santivanez and Ioannis Stavrakakis. Study of Various TDMA Schemes for Wireless Networks in the Presence of Deadlines and Overhead. *IEEE Journal on Selected Areas in Communications*, 17(7):1284–1304, July 1999.

119. C. Schurgers and M. Srivastava. Energy Optimal Scheduling under Average Throughput Constraint. In *IEEE ICC*, pages 1648–1652, Anchorage, AK, May 2003.

120. S. Shakkottai and A. Stolyar. Scheduling for Multiple Flows Sharing a Time-Varying Channel: the Exponential Rule. *American Mathematical Society Translations*, 207(2), 2002.

121. Sanjay Shakkottai, Theodore S. Rappaport, and Peter C. Karlsson. Cross-Layer Design For Wireless Networks. *IEEE Communication Magazine*, October 2003.

122. Sanjay Shakkottai and R. Srikant. Scheduling Real-Time Traffic with Deadlines over a Wireless Channel. *ACM/Baltzer Wireless Networks Journal*, 8(1):13–26, January 2002.

123. B. Shrader, M. Sanchez, and T. C. Giles. Throughput-Delay Analysis of Conflict-Free Scheduling in Multihop Ad-Hoc Networks. In *Proceedings of the 3rd Swedish Workshop on Wireless Ad-hoc Networks*, May 2003.

124. Moshe Sidi. Tandem Packet-Radio Queueing Systems. *IEEE Transactions on Communications*, 35(2):246–248, February 1987.

125. John A. Silvester and Leonard Kleinrock. On the Capacity of Multihop Slotted ALOHA Networks with Regular Structures. *IEEE Transactions on Communications*, 31(8):974–982, August 1983.

126. M. Srivastava, C. Fragouli, and V. Sivaraman. Controlled Multimedia Wireless Link Sharing via Enhanced Class-based Queueing with Channel-State-Dependent Packet Scheduling. In *IEEE INFOCOM*, March 1998.

127. Vineet Srivastava and Mehul Motani. Cross-Layer Design: A Survey and the Road Ahead. *IEEE Communication Magazine*, pages 112–119, December 2005.

128. William Stallings. *Wireless Communications and Networks*. Prentice Hall, August 2001. ISBN: 0130408646.

129. Gordon L. Stuber. *Principles of Mobile Communication*. Kluwer Academic Pub, November 2000. ISBN 0792379985.

130. L. Tassiulas and A. Ephremides. Jointly Optimal Routing and Scheduling in Packet Radio Networks. *IEEE Transactions on Information Theory*, 38(1):165–168, January 1992.

131. Leandros Tassiulas and Anthony Ephremides. Dynamic Server Allocation to Parallel Queues with Randomly Varying Connecticity. *IEEE Transactions on Information Theory*, 39(2):466–478, March 1993.

132. I. Emre Telatar and Robert G. Gallager. Combining Queueing Theory with Information Theory for Multiaccess. *IEEE Journal on Selected Areas in Communications*, 13(6):963–969, August 1995.

133. S. Tilak and W. Heinzelman N. B. Abu-Ghazaleh. A Taxonomy of Wireless Micro-Sensor Network Models. *Mobile Computing and Communications Review*, 6(2):28–36, 2002.

134. S. Toumpis and A. Goldsmith. Performance, Optimization, and Cross-Layer Design of Media Access Protocols for Wireless Ad Hoc Networks. In *IEEE ICC'03*, volume 3, pages 2234 – 2240, May 2003.

135. Kishor R. Trivedi. *Probability and Statistics with Reliability, Queueing and Computer Science Applications*. Wiley, John and Sons, 2001. ISBN 0471333417.

136. B. S. Tsybakov. File Transmission over Wireless Fast Fading Downlink. *IEEE Transactions on Information Theory*, 48(8):2323–2337, August 2002.

137. E. Uysal-Biyikogly, B. Prabhakar, and A. El Gamal. Energy-Efficient Packet Transmission over a Wireless Link. *IEEE/ACM Transactions on Networking*, 10(4):487–499, August 2002.

138. Nitin H. Vaidya, Paramvir Bahl, and Seema Gupta. Distributed Fair Scheduling in a Wireless LAN. In *ACM MobiCom*, Boston, MA, August 2002.

139. Hong Shen Wang and Pao-Chi Chang. On Verifying the First-Order Markovian Assumption for a Rayleigh Fading Channel Model. *IEEE Transactions on Vehicular Technology*, 45(2):353–357, May 1996.

140. Alec Woo and David E. Culler. A Transmission Control Scheme for Media Access in Sensor Networks. In *ACM SIGMOBILE*, pages 221–235, Rome, Italy, 2001.

141. Min Xie and Martin Haenggi. Performance Analysis of a Priority Queueing System over Rayleigh Fading Channels. In *41th Allerton conference on Communication, Control, and Computing*, October 2003.

142. Min Xie and Martin Haenggi. Delay Performance of Different MAC Schemes for Multihop Wireless Networks. In *GLOBECOM'05*, November 2005.

143. Min Xie and Martin Haenggi. A Study of the Correlations between Channel and Traffic Statistics in Multihop Networks, 2006. accepted by IEEE Transactions on Vehicular Technology.

144. Min Xie and Martin Haenggi. Delay-Reliability Tradeoffs in Wireless Networked Control Systems. In *Networked Embedded Sensing and Control, Lecture Notes in Control and Information Sciences series*. Springer, ISBN: 3-540-32794-0, 2006.

145. Min Xie and Martin Haenggi. Queueing Analysis of Discrete-time D/Geom/1 Systems with Non-integer Interarrival Times, 2006. submitted to Queueing Systems.

146. Min Xie and Martin Haenggi. Statistical Delay Analysis of TDMA and ALOHA in Wireless Multihop Networks, 2006. submit to IEEE Transactions on Networking.

147. Shugong Xu and Tarek Saadawi. Does the IEEE 802.11 MAC Protocol Work Well in Multihop Wireless Ac Hoc Networks? *IEEE Communications Magazine*, 39(6):130–137, June 2001.

148. Shugong Xu and Tarek Saadawi. Revealing the Problems with 802.11 Medium Access Control Protocol in Multi-hop Wireless Ad Hoc Networks. *Computer Networks*, 38(4):531–548, March 2002.

149. Yang Yang and Tak-Shing Peter Yum. Delay Distributions of Slotted ALOHA and CSMA. *IEEE Transactions on Communications*, 51(11):1846–1857, November 2003.

150. Wei Ye, John Heidemann, and Deborah Estrin. An Energy-Efficient MAC Protocols for Wireless Sensor Networks. In *IEEE INFOCOM*, volume 3, pages 1567–1576, June 2002.

151. Xiang Zeng, Rajive Bagrodia, and Mario Gerla. GloMoSim: A Library for Parallel Simulation of Large-Scale Wireless Networks. In *PADS 98*, May 1998.

152. Hongqiang Zhai, Jianfeng Wang, and Yuguang Fang. Distributed Packet Scheduling for Multihop Flows in Ad Hoc Networks. In *IEEE Wireless Communications and Networking Conference (WCNC)*, volume 2, pages 1081 – 1086, March 2004.

153. Hua Zhu, Ming Li, and Imrich Chlamtac. A Survey of Quality of Service in IEEE802.11 Networks. *IEEE Wireless Communications*, pages 6–14, August 2004.

154. M. Zorzi, R. R. Rao, and L. B. Milstein. On the Accuracy of the First-order Markovian Assumption for Data Block Transmission on Fading Channels. In *ICUPC'95*, pages 211–215, November 1995.

155. Michele Zorzi. On the Analytical Computation of the Interference Statistics with Applications to the Performance Evaluation of Mobile Radio Systems. *IEEE Transactions on Communications*, 45(1):103–109, January 1997.

156. Michele Zorzi. Data-Link Packet Dropping Models for Wireless Local Communications. *IEEE Transactions on Vehicular Technology*, 51(4):710–719, July 2002.

157. Michele Zorzi and Silvano Pupolin. Slotted ALOHA for High-Capacity Voice Cellular Communications. *IEEE Transactions on Vehicular Technology*, 43(4):1011–1021, November 1994.

158. Michele Zorzi and Ramesh R. Rao. Energy Constrained Error Control for Wireless Channels. *IEEE Personal Communication Magazine*, 4:27–33, December 1997.

This document was prepared & typeset with LaTeX 2$_\varepsilon$*, and formatted with* NDdiss2$_\varepsilon$ *classfile (v3.0[2005/07/27]) provided by Sameer Vijay.*